OXIDATIVE DECARBOXYLATION OF RETINOIC ACID IN VITRO

By

NATALIE LARSEN ROCKLEY

Bachelor of Arts
Hope College
Holland, Michigan
1971

Master of Public Health
University of Minnesota
Minneapolis, Minnesota
1974

Submitted to the Faculty of the Graduate College
of Oklahoma State University
in partial fulfillment of the requirements
for the Degree of
Doctor of Philosophy
December, 1979

OXIDATIVE DECARBOXYLATION OF

RETINOIC ACID IN VITRO

Thesis Approved:

Eldon E Nelson
Thesis Adviser

F. N. Owens

Carl D Mitchell Jr

Margaret K. Essenberg

Roger E. Koeppe

Norman N Durham
Dean of the Graduate College

PREFACE

The primary objective of this study was to characterize and identify oxidation and decarboxylation products of retinoic acid formed *in vitro*.

The author wishes to express her appreciation to her major adviser, Dr. E. C. Nelson and to Dr. B. A. Halley for their guidance and assistance throughout this study. Appreciation is also expressed to members of the advisory committee, Dr. M. K. Essenberg and Dr. E. D. Mitchell, for valuable advice concerning the manuscript for Chapter III and to Dr. R. E. Koeppe and Dr. F. N. Owens for their assistance in the preparation of the final manuscript.

A note of thanks is given to Dr. K. D. Berlin for his suggestions on the interpretation of the nuclear magnetic resonance spectra and to Dr. J. P. Devlin and Mr. G. L. Ritzhaupt for help and guidance in obtaining infrared spectral data. Appreciation is also extended to Dr. E. J. Eisenbraun for providing the diazomethane and to Dr. J. Toth for the LAOCN3 program.

To Dr. R. H. Thayer and the Poultry Science Department, the author expresses her appreciation for provision and care of the chicks.

Sincere thanks are extended to Dr. R. M. McKenzie for numerous discussions, to W. Dobson, M. Corcoran, K. Ahern, C. Hintz, K. Bachle and S. O. Sigle for technical assistance and to S. Heil for typing this manuscript.

Special gratitude is expressed to my husband, Mark, for many

helpful discussions, for his encouragement and understanding and to my parents for their concern.

Finally the author is indebted to the Biochemistry Department and the Oklahoma Agricultural Experiment Station for facilities and financial support. This investigation was supported in part by NIH Research Grant AM-09191 from the National Institute of Arthritis, Metabolism and Digestive Diseases.

TABLE OF CONTENTS

Chapter		Page
I.	INTRODUCTION	1
	Formation, Function and Transport of Retinoic Acid	1
	Cellular Retinoic Acid-Binding Protein	4
	Retinoic Acid and Carcinogenesis	6
	Metabolism of Retinoic Acid	9
II.	OXIDATION AND DECARBOXYLATION OF RETINOIC ACID IN VITRO	13
	Materials	14
	Retinoic Acid, Catalysts and Coreactants	14
	Buffers and Solvents	15
	Chicks	15
	Methods	16
	Incubation Conditions	16
	Extraction of Incubation Products	19
	Liquid Chromatography	19
	High Performance Liquid Chromatography	21
	Preparation of Chick Liver Microsomal Fraction	23
	Results	25
	Optimum Concentrations of Retinoic Acid, $FeCl_2$, H_2O_2 and Horseradish Peroxidase in the Incubations	25
	Time Course of the Horseradish Peroxidase Catalyzed Incubation	27
	pH of the Horseradish Peroxidase Catalyzed Incubation	30
	Effect of Buffer on the Horseradish Peroxidase Catalyzed Incubation	30
	Catalysts Other Than Horseradish Peroxidase in the Incubation	34
	Extraction Controls	36
	Liver Microsomal Fraction Incubations	38
	Liquid Chromatography of the Incubation Mixtures	38
	High Performance Liquid Chromatography of the Extracts from the Incubation Mixtures	42
	Discussion	50
III.	ISOLATION AND CHARACTERIZATION OF OXIDATION PRODUCTS OF RETINOIC ACID	56

Chapter Page

Experimental 56
Materials 56
Methods 57
Incubation Conditions 57
High Performance Liquid Chromatography 58
Mass Spectroscopy 58
Nuclear Magnetic Resonance Spectroscopy . . . 58
Infrared Analyses 59
Results 59
Separation of Incubation Extracts by HPLC 59
Purification and Identification of Peak 1 60
Purification and Identification of Peak 2 74
Purification of Peaks 4 and 5 83
Purification and Identification of Peak 6 86
Discussion 86

IV. INFRARED SPECTROSCOPY OF RETINOIDS 96

Experimental 97
Materials 97
Retinoids 97
Solvents 98
Methods 98
Purification of Retinoids by High Performance Liquid Chromatography 98
Infrared Analyses 98
Results and Discussion 99
Purification of Retinoids by High Performance Liquid Chromatography 99
Infrared Analyses 101

V. SUMMARY 119

BIBLIOGRAPHY 122

LIST OF TABLES

Table		Page
I.	Effect of pH on the Decarboxylation of Retinoic Acid	32
II.	Effect of Buffer on the Decarboxylation of Retinoic Acid	33
III.	Effect of Catalyst on the Decarboxylation of Retinoic Acid	35
IV.	Effect of Diet on the Decarboxylase Activity of Chick Liver Microsomal Fraction	39
V.	Summary of Abs_{max}, Mass Ion, $^{3}H/^{14}C$ Ratio and Extinction Coefficient Data of Oxidation and Decarboxylation Products Isolated from Peaks 1, 2, 4, 5	95
VI.	Infrared Frequencies of Retinoids	114

LIST OF FIGURES

Figure		Page
1.	Oxidation of Retinol to Retinoic Acid	3
2.	Purification of All-trans-[11,12-$^{3}H_2$]- and [15-^{14}C]-Retinoic Acid by HPLC	17
3.	HPLC Profile of Isomers of Retinoic Acid	22
4.	Scheme for the Isolation of Chick Liver Microsomal Fraction	24
5.	Effect of Retinoic Acid Concentration on the Decarboxylation of Retinoic Acid and on the Amount of Product Obtained in the Fe^{+2} Reaction (Top) and in the H_2O_2 Reaction (Bottom)	26
6.	Effect of H_2O_2 Concentration on the Decarboxylation of Retinoic Acid	28
7.	Effect of Oxygen and Fe^{+2} Concentration on the Decarboxylation of Retinoic Acid	28
8.	Effect of HRP Concentration on Decarboxylation of Retinoic Acid	29
9.	Time Course of the Fe^{+2} Reaction and of the H_2O_2 Reaction	31
10.	Extraction of ^{14}C-Labeled (A) and ^{3}H-Labeled (B) Oxidation and Decarboxylation Products of Retinoic Acid	37
11.	Effect of Retinoic Acid Concentration (Top) and Microsomal Concentration (Bottom) on Decarboxylation of Retinoic Acid in the Chick Liver Microsomal Incubations	40
12.	Chromatography of Fe^{+2} Incubations on Sephadex LH-20 (Top) and on LIPIDEX-1000 and LIPIDEX-5000 (Bottom)	41
13.	HPLC of HRP and Hemoglobin Catalyzed Incubation Mixtures	43

Figure Page

14. HPLC of HRP and Microsomal Incubation Mixtures 45

15. HPLC Profile of Products of Fe^{+2} Reactions Lacking Retinoic Acid, HRP or Phosphate Buffer 46

16. HPLC Profile of Products of H_2O_2 Reactions Lacking Retinoic Acid, H_2O_2, HRP or Phosphate Buffer 47

17. HPLC Profile of Products of Fe^{+2} Reactions After 0, 10, 30, 45, 90 Minutes of Incubation 48

18. HPLC Profile of Products of H_2O_2 Reactions After 0, 6, 20 and 30 Minutes of Incubation 49

19. HPLC and $^3H/^{14}C$ Profiles of Products Generated from ^3H- and ^{14}C-Labeled Retinoic Acid in the Presence of H_2O_2 and HRP (A) or Microsomal Fractions (B) 51

20. HPLC Profile of Products Generated from Incubations Containing Retinoic Acid, H_2O_2 and HRP on a Partisil M9 Column (70% methanol, 30% water at 1.4 ml per minute) . . . 61

21. HPLC Profile of the Oxidative Decarboxylation Product Present in Peak 1 62

22. Structure of the Retinoid Purified from Peak 1 64

23. Absorption Spectrum of the Retinoid Purified from Peak 1 65

24. Mass Spectrum of the Retinoid from Peak 1 66

25. Fragmentation Pattern of the Retinoid from Peak 1 67

26. Fragmentation of Ring Nucleus of the Retinoid Purified from Peak 1 69

27. NMR Spectrum of the Retinoid from Peak 1 71

28. Vinyl Region of NMR Spectrum of the Retinoid from Peak 1 73

29. Infrared Spectrum of the Retinoid from Peak 1 75

30. HPLC Profile (A) and Absorption Spectrum (B) of the Retinoid Isolated from Peak 2 76

31. Mass Spectrum of the Retinoid from Peak 2 78

32. NMR Spectrum of the Retinoid from Peak 2 79

Figure Page

33. Vinyl Region of NMR Spectrum of the Retinoid from Peak 2 81

34. Proposed Structures for the Retinoid Isolated from Peak 2 84

35. HPLC Profile (A) and Absorption Spectrum (B) of the Retinoid Isolated from Peak 4 85

36. Mass Spectrum of the Retinoid from Peak 4 87

37. HPLC Profile (A) and Absorption Spectrum (B) of the Retinoid from Peak 5 88

38. Mass Spectrum of the Retinoid from Peak 5 89

39. HPLC Profile (A) and Absorption Spectrum (B) of the Retinoid from Peak 6 90

40. Mass Spectrum of the Retinoid from Peak 6 91

41. Postulated Pathway for the Formation of the Major Oxidative Decarboxylation Product 93

42. Structures of Nine Retinoids 100

43. Infrared Spectrum of Retinoic Acid (Top), 5,6-Epoxyretinoic Acid (Middle) and 5,8-Epoxyretinoic Acid (Bottom) from 4000 to 600 cm^{-1} 102

44. Infrared Spectra of Retinal (Top), 9-*cis*-Retinal (Middle) and 13-*cis*-Retinal (Bottom) from 4000 to 600 cm^{-1} 103

45. Infrared Spectra of 4-Oxoretinoic Acid (Top), C_{19}-Aldehyde (Middle) and 4-Oxo-9-hydroxy-C_{19}-Aldehyde (Bottom) from 4000 to 600 cm^{-1} 104

46. Infrared Spectrum of Retinoic Acid from 2000 to 600 cm^{-1} . . . 105

47. Infrared Spectrum of 5,6-Epoxyretinoic Acid from 2000 to 600 cm^{-1} 106

48. Infrared Spectrum of 5,8-Epoxyretinoic Acid from 2000 to 600 cm^{-1} 107

49. Infrared Spectrum of Retinal from 2000 to 600 cm^{-1} 108

50. Infrared Spectrum of 9-*cis*-Retinal from 2000 to 600 cm^{-1} 109

Figure Page

51. Infrared Spectrum of 13-cis-Retinal from 2000 to 600 cm^{-1} 110

52. Infrared Spectrum of 4-Oxoretinoic Acid from 2000 to 600 cm^{-1} 111

53. Infrared Spectrum of C_{19}-Aldehyde from 2000 to 600 cm^{-1} 112

54. Infrared Spectrum of 4-Oxo-9-Hydroxy-C_{19}-Aldehyde from 2000 to 600 cm^{-1} 113

NOMENCLATURE

BSA	Bovine serum albumin
cyt c	Cytochrome c
ε	Extinction coefficient
Hb	Hemoglobin
HEPES	N-2-hydroxyethylpiperazine-N'-2-ethanesulfonic acid
HPLC	High performance liquid chromatography
HRP	Horseradish peroxidase
IR	Infrared
LAOCN3	Computer program for analysis of NMR spectra
MES	2-(N-morpholino)ethanesulfonic acid
NMR	Nuclear magnetic resonance
ODS	Octadecylsilane
Pi	Phosphate
PIPES	Piperazine-N,N'-bis(2-ethanesulfonic acid)
Porph	Protoporphyrin IX
TES	N-tris(hydroxymethyl)-methyl-2-aminomethanesulfonic acid
TMS	Tetramethylsilane
Tris	Tris(hydroxymethyl)aminomethane
Tricine	N-tris(hydroxymethyl)methylglycine
UV	Ultraviolet

CHAPTER I

INTRODUCTION

The existence of a "fat-soluble A factor" which is essential for life was first demonstrated by McCollum and Davis (1, 2) at the University of Wisconsin in 1913 and by Osborne and Mendel (3) at Yale University. The structures of this vitamin A and of β-carotene, the provitamin A form, were determined by Karrer et al. (4, 5) in the 1930's, while the syntheses of these two compounds were accomplished some fifteen years later. The term "vitamins A" includes retinol as well as compounds similar to retinol in structure and function while natural and synthetic analogs of vitamin A are referred to as "retinoids" (6). Vitamin A is involved in many biological processes including vision, growth, reproduction, and maintenance of epithelial tissues (7, 8, 9, 10, 11, 12). The function of vitamin A in the visual cycle was elucidated by George Wald (13) who was awarded the Nobel Prize for Medicine in 1967. Vitamin A compounds involved in the visual system include all-*trans*- and 11-*cis*-retinal (both vitamin A aldehydes). The role of vitamin A in biological processes other than vision is not well understood.

Formation, Function and Transport of Retinoic Acid

Retinol (vitamin A alcohol) is reversibly oxidized *in vivo* to

retinal (vitamin A aldehyde) which is then irreversibly oxidized to retinoic acid (vitamin A acid) (12) as shown in Figure 1.

Retinoic acid was synthesized from β-ionone by Arens and Van Dorp (14) more than thirty years ago. When given orally to vitamin A deficient rats, retinoic acid had a growth promoting activity equal to that of the alcohol (15). Arens and Van Dorp (16) first suggested that retinoic acid was not converted to retinol in vivo. After retinoic acid was injected or fed, retinol could not be detected in the liver (16). These findings were later substantiated by Dowling and Wald (17, 18) who reported that rats maintained on retinoic acid, though growing normally, became blind. In addition, retinoic acid was unable to maintain normal fertility in female rats or spermatogenesis in male rats (19, 20).

The growth promoting activity of retinoic acid has been confirmed by other investigators who have reported it to be as active as retinol (21, 22). Retinoic acid was as effective as the alcohol in reducing elevated cerebrospinal fluid pressures of vitamin A deficient pigs, suggesting that these two compounds have similar biological activities (23). Cerebrospinal fluid pressure has proven to be an adequate criterion for assessing the vitamin A status of the pig. In addition, retinoic acid had a sparing effect on liver vitamin A in the pig (23).

The presence of retinoic acid in blood plasma was first detected quantitatively by Nelson et al. (24). When [6,7-^{14}C]retinoic acid was fed to pigs, retinoic acid concentration in blood plasma reached a maximum in 1.5 to 3 hours then decreased until none could be detected after 12 hours.

The formation of retinoic acid in tissues was demonstrated through

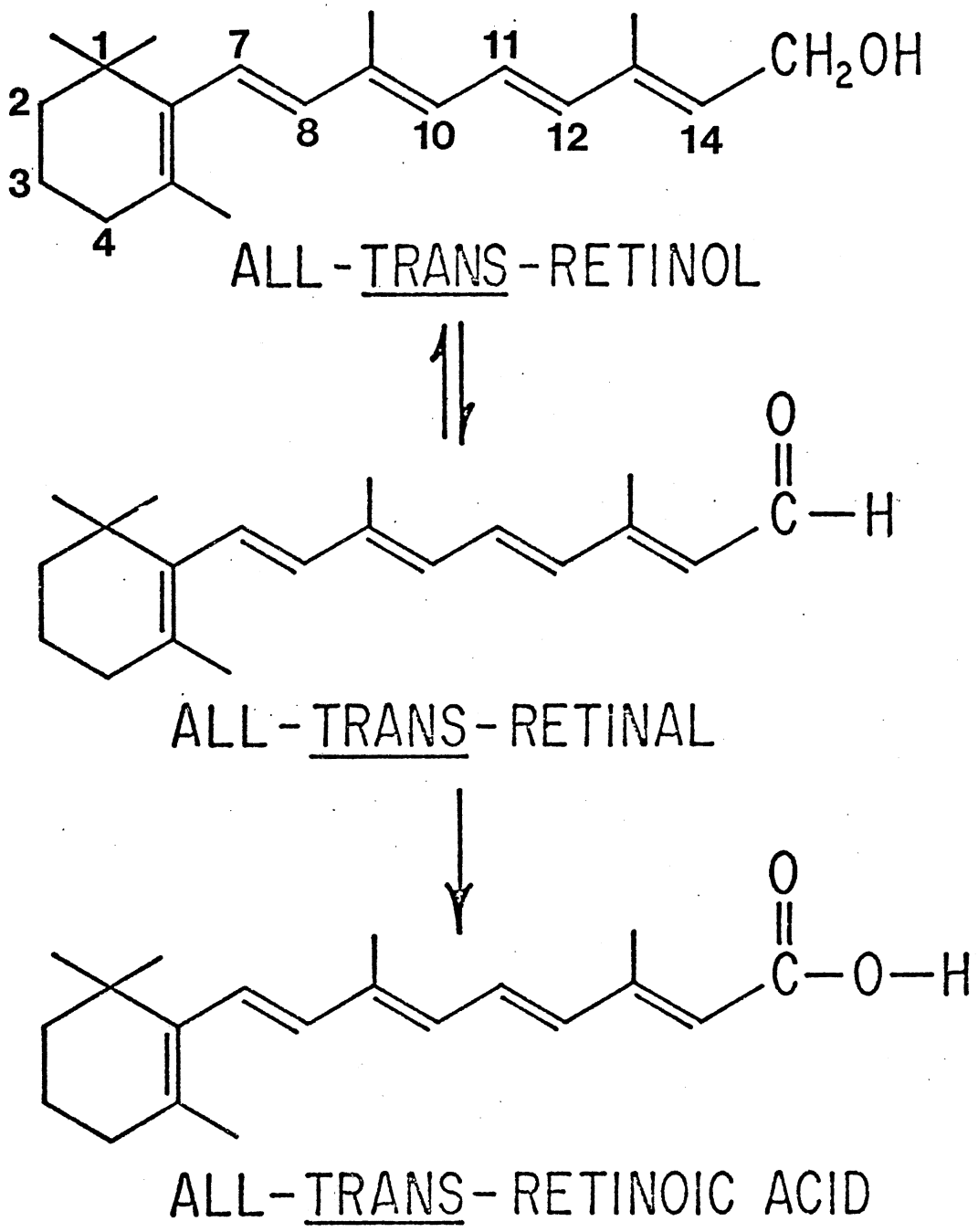

Figure 1. Oxidation of Retinol to Retinoic Acid

the use of radioactive precursors. Small amounts of intravenously injected retinal could be recovered as retinoic acid in bile (25), liver and intestine (26). Retinoic acid was also formed in the intestine following the administration of β-carotene (27) or retinol (28). More recently, the administration of a physiological dose of retinyl acetate led to the detection of retinoic acid in blood plasma (29) and in rat liver, intestine and testes (30). After the intravenous administration of physiological doses of [6,7-^{14}C]retinoic acid to vitamin A deficient rats, the radioactivity was distributed among all tissues, with highest levels in the liver and small intestine (31).

The transport of retinoic acid in the blood of the rat has recently been examined (32, 33). Retinoic acid is transported in rat serum bound to serum albumin, and not to retinol-binding protein, the specific transport protein for retinol in blood plasma. Analogs of retinoic acid also bind serum albumin but no correlation has been found between binding affinity for albumin and the biological potency of these analogs (34).

Cellular Retinoic Acid-Binding Protein

The discovery of a cellular retinoic acid-binding protein, distinct from cellular retinol-binding protein, has given added impetus to the idea that retinoic acid acts as a distinct physiological compound, separate from retinol (35). Cellular retinoic acid-binding protein (CRABP) was first isolated from rat testes (35) and from chick embryo skin (36). Whereas cellular retinol-binding protein was found in all organs with the exception of serum and muscle, cellular retinoic acid-

binding protein was only detected in brain, skin, eye, ovary, uterus and testes. CRABP was presented in smaller amounts in bladder, prostate, heart muscle, trachea and mammary glands but was not detected in small intestine, kidney, colon, liver, lung, serum, muscle and spleen (35, 37-40). In addition, cellular retinoic acid-binding protein has been found in the nuclei of chick embryo skin and in the nuclei isolated from a transplantable colon tumor and Lewis lung carcinoma (41, 42). When intact retinoblastoma cells were preincubated with retinoic acid, cellular retinoic acid-binding protein was detected in the nuclear extract (43). This preliminary result may point to a possible involvement of retinoic acid at the gene level.

Different and changing requirements for retinoic acid in rat organ development and maturation have been suggested (44). During perinatal development of lung, the level of cellular retinoic acid-binding protein increased at parturition, peaking at day ten, and fell rapidly to an undetectable level at day 21. Liver levels of the protein were not detectable after day 5. These observed changes in concentration suggest a higher requirement of retinoic acid during embryogenesis than in later life (44).

A fuller characterization of CRABP has been possible through its purification from rat testes (45) and from chick embryo skin (46, 47). The binding was saturatable and specific, with retinol, retinal and long chain fatty acids unable to bind (35, 36). Several analogs of retinoic acid were tested for binding affinity. The binding affinity of these analogs correlated with biological activity in the differentiation of epithelial tissues and in the control of tumorigenesis (34, 47-49). This correlation suggests that the action of retinoic

acid and its analogs in carcinogenesis could be mediated by cellular retinoic acid-binding protein (34, 48).

Retinoic Acid and Carcinogenesis

Vitamin A plays an essential role in controlling normal differentiation of many epithelial tissues *in vivo* (7, 11, 50-53). This has also been demonstrated *in vitro* in recent years in both tracheal organ cultures (54, 55) and in prostate gland organ cultures (56-58). In vitamin A deficiency, the mucus-secreting lining of epithelial tissues was replaced by a squamous metaplastic epithelium with an increased production of keratin. This is thought to represent the first phase in the transformation process from a normal tissue to a neoplastic tissue. When vitamin A or a structural analog (retinoid) was added to the organ culture, a reversal of the keratinization process was seen along with a replacement of the abnormal squamous cells by columnar ciliated and mucous cells.

Several studies have indicated that lower levels of vitamin A predispose epithelial tissues to carcinogenesis. For example, the induction of colon tumors by aflatoxin B_1 and dimethylhydrazine is greater and faster in vitamin A deficient rats (59, 60). This increased susceptibility to chemical carcinogens in vitamin A deficiency has been reviewed by Sporn et al. (6, 61). Carcinogenesis involves a de-differentiation in epithelia and since the vitamins A are involved in the regulation of normal cell differentiation, they have been used as chemopreventive agents, interfering with tumor induction by carcinogens.

Natural retinoids have been shown to prevent the development of

epithelial cancer during its preneoplastic period in several tissues. Saffioti et al. (62) demonstrated that vitamin A given to hamsters inhibited benzo(a)pyrene induction of respiratory tract tumors. In studies by Bollag (63-65), treatment with retinyl palmitate or with retinoic acid led to the regression of skin papillomas in mice induced by dimethylbenzanthracene and croton oil. Retinoic acid had a prophylactic effect, in that its administration led to a delay in appearance of the papillomas, as well as a therapeutic effect, accounting for a retardation of the growth and induction of the regression of papillomas (65). An increased survival time and a decreased rate of mammary tumor growth was observed in mice fed retinyl palmitate (66) while administration of retinyl acetate to rats one week following the intragastric installation of dimethylbenz(a)anthracene resulted in reduction both in the incidence of benign and malignant mammary tumors and in the number of tumors (67).

Several effects of natural vitamin A compounds greatly reduce their usefulness in cancer prevention. These include the likelihood of liver injury due to excessive deposition of high doses of vitamin A and the inadequate tissue distribution of natural retinoids (6, 61, 68). For these reasons, synthetic retinoids have been developed and used as chemopreventive agents. The nature of the terminal polar group of retinoids is an important determinant in modifying activity, toxicity, metabolism and tissue distribution of this class of molecules (69).

Synthetic retinoids were highly active in mouse prostate organ culture in inhibiting the effects of methylcholanthrene (58) and of N-methyl-N'-nitro-N-nitrosoguanidine (56). Sporn et al. (55, 70, 71) used synthetic retinoids in organ cultures of hamster trachea in order

to assay their anticarcinogenic activities, while Wilkoff et al. (49) tested vitamin A analogs for activity in altering epithelial differentiation of chick embryo metatarsal skin explants. In addition to their effect *in vitro*, retinoids also reduced the growth or the incidence of chemically induced tumors in skin, lung, bladder and mammary tissues *in vivo*. The first such studies utilizing a synthetic retinoid involved chemically induced skin papillomas and carcinomas of mice. Bollag (68, 72-74) demonstrated that an aromatic retinoic acid derivative with a modified polar end group exerted a prophylactic as well as a therapeutic effect on the tumors and was more effective than all-*trans*-retinoic acid. Two compounds were successfully used to inhibit mammary cancer in the rat. Retinyl methyl ether inhibited the incidence and decreased the number of mammary tumors induced by 7,12-dimethylbenz(a)-anthracene (75, 76) while N-(4-hydroxyphenyl)-all-*trans*-retinamide inhibited the development of mammary cancer induced by N-nitroso-N-methylurea (77).

13-*cis*-Retinoic acid was an effective anticarcinogen in the lung as well as in the bladder. It prevented tracheobronchial cancer in hamsters after malignancy had been induced by benzo(a)pyrene (78). Whether rat bladder carcinogenesis was induced by N-methyl-N-nitroso-urea (39) or by N-butyl-N-(4-hydroxybutyl)nitrosamine (80, 81), 13-*cis*-retinoic acid was equally effective in reducing the incidence, number and severity of the resultant carcinomas. This was found to be true even after a nine-week delay in starting the retinoid feeding (81).

Since epithelial cancers account for a large proportion of new cancer cases and of cancer deaths in humans, this chemopreventive

approach to the control of cancer offers great promise for the future. However, the mechanism of action of these retinoids remains to be determined. It has been suggested by De Luca et al. (7, 51-53) that retinoids function by an action on cell membranes, specifically in the synthesis of glycoproteins.

Metabolism of Retinoic Acid

The metabolism of retinoic acid has been investigated in the hope of determining the biologically active form(s) of vitamin A. Knowledge of the chemical structure of the metabolites of retinoic acid would greatly aid in the search for the metabolic role of vitamin A in processes other than vision.

The major metabolite of retinoic acid in bile has been identified as retinoyl β-glucuronide (25, 82). Several other excretory products of retinoic acid metabolism have been proposed. Sundaresan and Bhagavan (83) reported the presence of at least six metabolites of retinoic acid in the urine of rats. The major metabolite lacked both C-14 and C-15 of retinoic acid. A specific loss of tritium at C-11 and C-12 was also observed (84). Rietz et al. (85), on the basis of spectroscopic data, proposed a 4-oxo metabolite of retinoic acid with a carboxyl function in place of the methyl group at C-1 and a nonconjugated carboxyl group at C-15. Hanni et al. (86) isolated three major urinary metabolites following intraperitoneal administration of retinoic acid. In these metabolites the tetraene side chain at carbons 9-12 was converted to a furanone, the cyclohexene ring was oxidized at C-4 and one of the methyl groups at C-1 was oxidized to a primary alcohol. The physiological importance of these metabolites, generated when very high doses

(grams) of retinoic acid were administered to rats, is still to be determined.

Three major metabolites as well as intact retinoic acid were isolated and identified from rat feces, following intraperitoneal administration of the parent compound (87). Hydroxylation of the methyl group at C-5, oxidation of the ring at C-4 and cis-trans isomerization of the side chain produced these metabolites. It was proposed that metabolites with a shortened side chain are mainly eliminated by the kidney while metabolites with an intact side chain and retinoic acid are eliminated in feces by the liver and bile. The glucuronides of retinoic acid and its metabolites may be hydrolyzed in the intestine before excretion.

While retinoic acid seems to undergo glucuronic acid conjugation in the formation of biliary retinoyl β-glucuronide (25, 82, 88, 89) and hydroxylation and cleavage in the formation of the urinary and fecal metabolites (86, 87), several other possible fates for retinoic acid have been proposed. Isomerization to 13-cis-retinoic acid has been reported in rat liver (90), but since extensive isomerization occurs during routine handling of all-trans-retinoic acid, the physiological significance of this finding is questionable (90). 5,8-Epoxyretinoic acid has been reported as a metabolite of retinoic acid (91), although it has also been identified as a major impurity of samples of ^{3}H- and ^{14}C-labeled all-trans-retinoic acid (92). Sundaresan and Sundaresan (84) have discussed the metabolism of the side chain of retinoic acid with specific loss of tritium at positions 11 and 12. This could occur through hydroxylation at the 11,12 double bond. More recently, evidence has been presented indicating that the

major pathway of retinoic acid metabolism in hamster liver microsomes and in hamster intestine involves hydroxylation at C-4 in the ring followed by the formation of a keto group at the same position (93-95). 4-Oxoretinoic acid is then converted to more polar metabolites. Retinoic acid is also metabolized to 4-hydroxyretinoic acid and 4-oxoretinoic acid in a hamster tracheal organ culture system (96, 97). These compounds displayed one tenth the biological activity of all-trans-retinoic acid when tested in a vitamin A deficient hamster tracheal organ culture assay. Retinoic acid also may be metabolized to a hydroxylated derivative (98) which becomes phosphorylated, forms a mannosyl phosphate derivative and subsequently leads to the formation of a mannoglycoprotein (51).

The decarboxylation of retinoic acid has been under study since the discovery of a decarboxylation product that was biologically active (99). The breakdown of ^{14}C-retinoic acid labeled either at C-6, C-14 or C-15 was studied by several investigators by analysis of the radioactivity in urine, carbon dioxide and feces following intravenous injections of the substrate into retinol deficient rats (100-102). These studies indicated that retinoic acid was metabolized quite rapidly. With the 15-^{14}C- and 14-^{14}C-labeled compounds, a significant amount of radioactivity was recovered as $^{14}CO_2$ (10-20%).

The decarboxylation of retinoic acid in vitro was demonstrated with tissue slices of rat liver and kidney (103, 104). When run in the presence of microsomes, the reaction required NADPH and Fe^{+2} and was further stimulated by pyrophosphate. A maximum of 50% decarboxylation was achieved (104). The decarboxylation could also occur nonenzymatically in the presence of ascorbate, Fe^{+2} and boiled micro-

somes. This NADPH reaction resembled lipid peroxidation in the cofactor requirements and the response to inhibitors. N,N'-Diphenyl-p-phenylenediamine (DPPD), an antioxidant, inhibited the decarboxylation in the rat liver or kidney microsomal fractions and in the tissue slices, whether the inhibitor had been injected into the animal prior to the isolation of the tissues or had been added *in vitro* (105).

Similar results were obtained by Lin (102) and Nelson et al. (106). Lin observed a requirement for O_2 and Fe^{+2} in order for a partially purified preparation of microsomal enzyme to decarboxylate retinoic acid (102). When retinoic acid was incubated in phosphate buffer and Fe^{+2} with horseradish peroxidase or with an acetone-butanol-ether dried liver powder, decarboxylation was 48% and 40%, respectively (106). The decarboxylation of retinoic acid by horseradish peroxidase has been further investigated by McKenzie and Nelson (107). They demonstrated that the requirements for phosphate, oxygen and ferrous ion could be eliminated when hydrogen peroxide was present in the incubation medium. Hemoglobin could be substituted for horseradish peroxidase in the decarboxylation reaction, provided that hydrogen peroxide was present.

Therefore, the objective of the present study was to isolate and identify the products formed in the decarboxylation of retinoic acid *in vitro*. Once the structures of these metabolites have been determined, it should be easier to identify metabolites formed *in vivo* and to elucidate the molecular function of vitamin A in growth, reproduction and maintenance of epithelial tissues.

CHAPTER II

OXIDATION AND DECARBOXYLATION OF RETINOIC ACID *IN VITRO*

The search for metabolites of retinoic acid has been in progress for two decades. Several compounds have been characterized including retinoyl β-glucuronide (25) and 5,8-epoxyretinoic acid (91). In addition, all-*trans*-4-oxoretinoic acid, 9-*cis*-5'-hydroxyretinoic acid and all-*trans*-5'-hydroxyretinoic acid have been isolated from rat feces (87) while three retinoic acid metabolites obtained from rat urine have an oxidized cyclohexene ring and a shortened side chain (86). With the exception of the glucuronide, neither the physiological importance of these compounds nor their modes of production *in vivo* have been ascertained.

The metabolism of retinoic acid *in vitro*, and specifically its decarboxylation has also been under study (102, 104, 106, 107) since the discovery of a decarboxylation product that was biologically active (99). Nelson et al. (106) developed a model system for the study of the decarboxylation of retinoic acid. The incubation which consists of retinoic acid, horseradish peroxidase and ferrous chloride resulted in 48% decarboxylation (106). McKenzie and Nelson (107) demonstrated that the requirements for phosphate, oxygen and ferrous ion could be eliminated when hydrogen peroxide was present in the incubation medium. The horseradish peroxidase requirement could be eliminated by the

substitution of hemoglobin when hydrogen peroxide was present in the decarboxylation reaction. The use of horseradish peroxidase preparations as the decarboxylating agent was based on their low levels of contaminating lipids and on the observation that liver and kidney microsomes seem to decarboxylate retinoic acid *in vitro* by a free radical mechanism resembling that in peroxidation (104). In addition, thin-layer chromatography of ^{14}C-labeled products, isolated from incubations containing retinoic acid and either liver microsomes, crude liver powders or horseradish peroxidase revealed products with similar migration rates (106, 108).

The objective of the work presented in this chapter was twofold: to optimize the production of decarboxylated products generated from retinoic acid and to further characterize the model system developed by Nelson et al. (102, 106, 107).

Materials

Retinoic Acid, Catalysts and Coreactants

All-*trans*-retinoic acid, all-*trans*-[11,12-$^{3}H_2$]retinoic acid (4.85 μCi/mg or 2.9 mCi/mM stored in toluene) and all-*trans*-[15-^{14}C]retinoic acid (59 μCi/mg or 0.16 mCi/mM when methanol was added) were obtained as gifts from Dr. W. E. Scott, Hoffman-La Roche Inc. (Nutley, NJ). These radiochemicals were stored under nitrogen and in the dark at 4° or -20°C.

Horseradish peroxidase (type VI), hemoglobin (type I, from beef blood), cytochrome c (from horse heart), hemin (type I, bovine), protoporphyrin IX (grade I, dimethyl ether from ox hemin) and bovine serum

albumin were all obtained from Sigma Chemical Co. (St. Louis, MO).

Coreactants in the incubations consisted of $FeCl_2$ from Matheson Coleman and Bell (Norwood, OH) and hydrogen peroxide (H_2O_2) 30% from Fisher (Fair Lawn, NJ).

Buffers and Solvents

Incubations were usually in phosphate buffer from Fisher Scientific Co. (Fair Lawn, NJ). Other buffers included piperazine-N,N'-bis(2-ethanesulfonic acid)(PIPES), glycylglycine, Tris (hydroxymethyl)amino-methane (Tris) and N-tris(hydroxymethyl)methylglycine (Tricine) from Sigma Chemical Co. (St. Louis, MO), 2-(N-Morpholino)ethanesulfonic acid (MES), N-2-hydroxyethylpiperazine-N'-2-ethanesulfonic acid (HEPES) and N-tris(hydroxymethyl)-methyl-2-aminoethanesulfonic acid (TES) were purchased from Cal Biochem (La Jolla, CA). Boric acid was obtained from Mallinckrodt Chemical Works (St. Louis, MO). Glass-distilled residue-free solvents (Burdick and Jackson Labs, Muskegon, MI) were used for extractions as well as liquid and high performance liquid chromatography (HPLC). The water was deionized and redistilled in glass.

Chicks

Chicks, 2-5 weeks of age, were obtained from Dr. R. H. Thayer, Animal Science Department, Oklahoma State University (Stillwater, OK). Day old chicks were divided into three groups and fed one of three rations. Group A was fed a vitamin A deficient diet; group B was fed a diet which was deficient in vitamin A until 24 hours prior to the experiment when retinoic acid was added to the ration; group C was fed a diet containing retinoic acid from the time of hatching. The retinoic acid

was stabilized in gelatin beadlets (Hoffman-La Roche Inc.) added to the ration at a level of 1.1 mg of retinoic acid per kg of feed.

Methods

Incubation Conditions

Incubations as described by Nelson et al. (106) were carried out either in 18 x 150 mm stoppered test tubes, or in 125 ml stoppered erlenmeyer flasks. The test tube racks and flasks containing the incubations were placed in a reciprocating waterbath (Eberbach Corp., Ann Arbor, MI), at a temperature of 37°C, for two hours in the dark. The stoppers supported a small glass rod to which a glass cup, containing a filter-paper wick and ethanolamine with 2-methoxyethanol (1:2, v/v), was attached. The stoppered test tubes held 0.3 ml of the CO_2 trapping solution in the glass cups while the stoppered flasks held 3 ml.

Before use, both the ^{3}H- and the ^{14}C-labeled retinoic acid were routinely purified by high performance liquid chromatography and eluted at 50 minutes, as indicated by the arrows in Figure 2. The labeled and unlabeled retinoic acid, dissolved in methanol, were added first in all incubation procedures so as to obtain a uniform distribution of the label prior to addition of the aqueous assay reagents. The retinoic acid was present at a final concentration of 133 μM, while approximately 2×10^4 dpm of each label were added per test tube or 2×10^5 dpm per stoppered flask. The coreactant was either $FeCl_2$ (2 mM) or hydrogen peroxide (1 mM), and the reactions are referred to as the Fe^{+2} reaction and the H_2O_2 reaction. The catalyst was added last and was one of the following: horseradish peroxidase (4 μM), hemoglobin (13 μM), cyto-

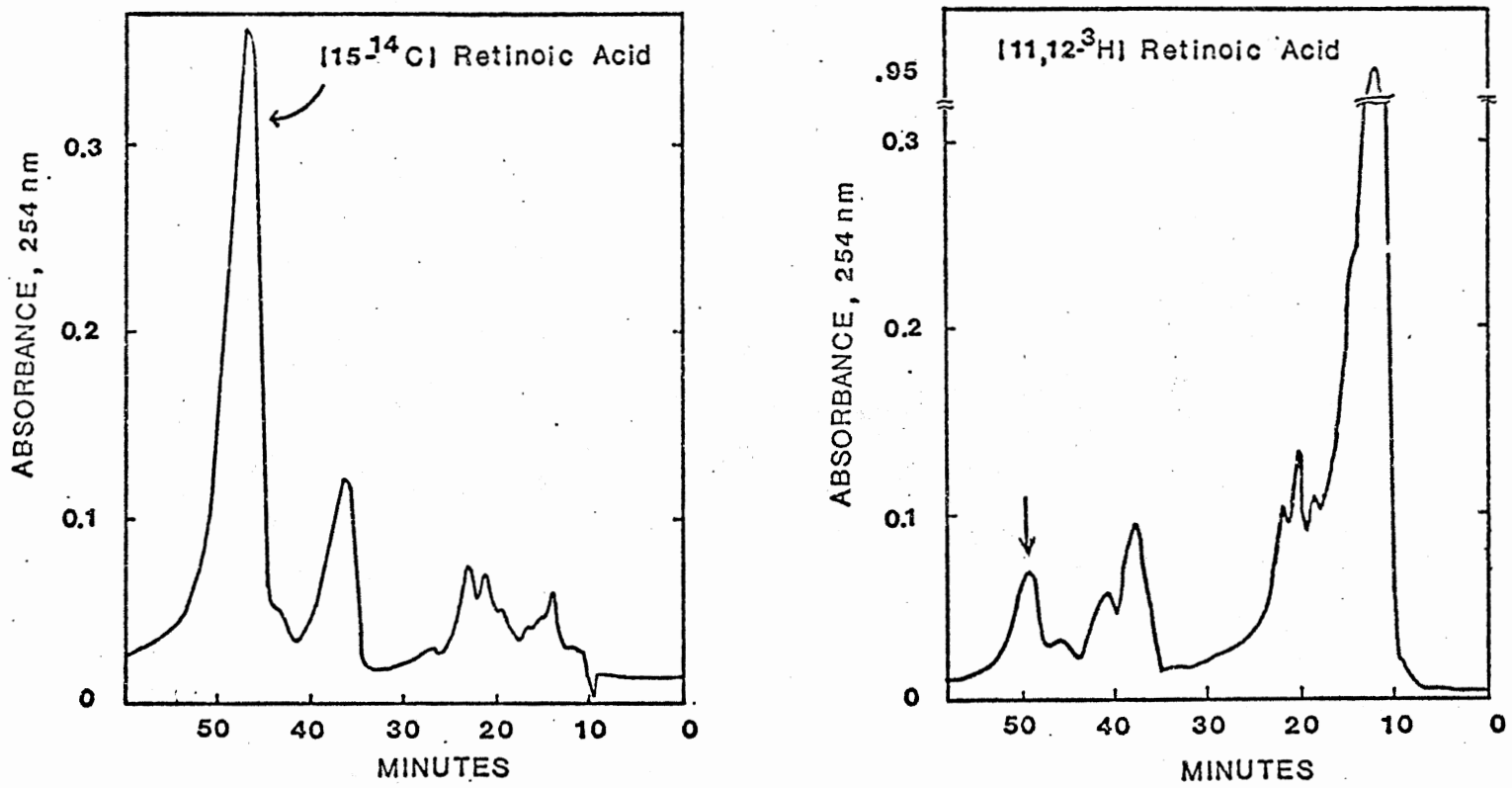

Figure 2. Purification of All-trans-[11,12-$^{3}H_2$]- and [15-^{14}C]Retinoic Acid by HPLC. Chromatography was performed with 68% methanol, 32% water at 0.5 ml per minute, on two Partisil 10-ODS columns in series.

chrome c (12.9 μM), hemin (3.7 μM), protoporphyrin IX (4.1 μM), and bovine serum albumin (3.5 μM). Microsomal incubations contained retinoic acid (13.3 μM), $FeCl_2$ (1 mM) and 50 mg freshly prepared microsomal fraction per 2.5 ml incubation or 0.5-1.0 g microsomal fraction per 25 ml incubation. The substrate, coreactant and catalyst were diluted to a final volume of 2.5 ml (stoppered test tubes) or 25 ml (stoppered flasks) with 200 mM potassium phosphate buffer, pH 6.4. Where indicated, other buffers were used at a concentration of 100 mM including: borate (pH 9.0), PIPES (pH 6.4), Tris (pH 7.0), glycylglycine (pH 7.4), MES (pH 6.5), HEPES (pH 7.0), TES (pH 7.0), or Tricine (pH 7.0). Reaction vessels containing $FeCl_2$ were purged with a gentle stream of oxygen prior to being placed in the waterbath.

At the end of the incubation period, 0.2 ml of 2N HCl and 0.1 ml of 200 mM $NaHCO_3$ were added to the test tubes unless products were later to be isolated from the reaction vessels. The acid was added to stop the reaction and to release $^{14}CO_2$. The addition of the $NaHCO_3$ reduced the variability in the counts of ^{14}C among the triplicate test tubes (107).

After 1 hour at 37°C, the glass cups were removed from the reaction vessels and were rinsed with 5 ml of Insta-Gel (Packard Instrument Co. Inc., Downers Grove, IL). Their contents were transferred to a counting vial along with the filter-paper wick. Radioactivity was counted with a PRIAS liquid scintillation counter (Model PL from Packard Instrument Co. Inc., Downers Grove, IL). The standard deviation of the triplicate measurements is shown as a vertical error bar in the figures where percent $^{14}CO_2$ is plotted.

When products were to be isolated, the flasks and test tubes

were set aside for extraction of the incubation products, while the CO_2 traps were removed and their contents assayed for radioactivity. No additions of HCl or $NaHCO_3$ were made.

Extraction of Incubation Products

Incubation mixtures were routinely extracted six times with equal volumes of chloroform. Where indicated, hexane was used instead of chloroform. The extracts were concentrated by evaporation on a rotary evaporator (Rotovapor-R, by Buchi/Brinkmann Instruments, Westbury, NY) at a setting of 4-5 and a temperature of 37°C. The residue was dissolved in methanol and filtered through a 0.5 μm filter (filter type FH, from Millipore Corp., Bedford, MA) prior to chromatographic analysis. Filtering removed any large molecules, such as HRP, which tend to adhere to the high performance liquid chromatography columns.

Liquid Chromatography

Three different types of lipophilic gels were used as packing material for an analytical column (1.2 x 60 cm) and included Sephadex LH-20 (Pharmacia Fine Chemicals Inc., Piscataway, NJ) which is a hydroxypropyl derivative of Sephadex G-25, LIPIDEX-1000 and LIPIDEX-5000 (Packard Instrument Co. Inc., Downers Grove, IL), both hydroxy-alkoxypropyl derivatives of Sephadex G-25. While LIPIDEX-1000 was 10% substituted, LIPIDEX-5000 was 50% substituted. All liquid chromatography was at room temperature (22-32°C), in the dark. The gels were slurried in the various solvents used for elution, and left to equilibrate for approximately 24 hrs prior to pouring into the columns to a height of 0.5 m. Procedures followed were those of

Ito et al. (30).

Sephadex LH-20 (20 g, particle size 25-100 μm) was slurried with 100 ml of chloroform-hexane-methanol (65:35:1). Extracts from incubations containing retinoic acid, $FeCl_2$ and horseradish peroxidase were chromatographed at a flow rate of 0.5 ml per min and collected in 2 ml fractions. In order to remove any remaining material from the column, methanol-acetone (1:1) was substituted as the solvent and 5 ml fractions were collected. The contents of each fraction were analyzed for absorbance at 350 nm.

LIPIDEX-1000 or LIPIDEX-5000 (20 g) were slurried with 100 ml of hexane-acetone (92:8). Extracts from incubations containing retinoic acid, $FeCl_2$ and horseradish peroxidase were methylated prior to chromatography by the procedure described by Schlenk and Gellerman (109). The products were extracted with diethylether, concentrated by evaporation and dissolved in 10 ml of 10% methanol and 90% diethylether, prior to the addition of diazomethane (obtained from Dr. E. J. Eisenbraun, Chemistry Department, Oklahoma State University, Stillwater, OK). After 10 to 15 min, the sample was dried under a gentle stream of nitrogen to remove excess diazomethane, and redissolved in the solvent used for chromatography. Hexane-acetone was eluted from the column at a flow rate of 0.5 ml per min, and 2 ml fractions were collected from the two LIPIDEX columns for the first 60 min, after which 5 ml fractions were collected.

A 0.2 ml aliquot of each fraction obtained from the three different columns was transferred to a vial containing 10 ml of scintillation fluid consisting of toluene (60%), 2-methoxyethanol (36%), ethanolamine (2%), and Permablend I or III (Packard Instrument Co., Downers Grove,

IL), 5.5 g/l. These vials were counted in a liquid scintillation counter.

High Performance Liquid Chromatography

High performance liquid chromatography was performed with two 0.46 x 25 cm bonded octadecylsilane (ODS) columns (Partisil 10-ODS, Whatman, Clifton, NJ) in series. When larger quantities of materials were to be separated, a 0.94 x 50 cm ODS column (Partisil M9, 10/50 ODS, Whatman) was used. The Partisil M9 column was connected to a DuPont Model 830 (E. I. DuPont de Nemours and Co., Wilmington, DE) high pressure pumping system equipped with a single-beam 254 nm photometer. The Partisil 10 columns were operated through a Model 314 pump (Isco, Lincoln, NE) connected to a DuPont gradient-elution accessory. The spectrophotometer was a Model 25 (Beckman, Fullerton, CA) fitted with a set of Model LC-25 microcells (Waters Assoc., Milford, MA). Solvents used were methanol-water. Prior to injection, the samples were dried under a gentle stream of nitrogen with the aid of a waterbath (25-35°C), and redissolved in the same solvent concentration as that used on the column. Where indicated, 1 min fractions were collected in scintillation vials containing 5 ml of Insta-Gel and counted in a liquid scintillation counter. Column performance was checked at least once per week by injecting a standard solution of 2.5 µg retinoic acid which had been isomerized by exposure to light for a period of approximately 24 hrs in methanol (Figure 3). The eluting solvent was 68% methanol, 32% water. By adjusting the high pressure pumping system so as to obtain the same flow rate, the resolution and retention times of the retinoic acid isomers could be compared from one

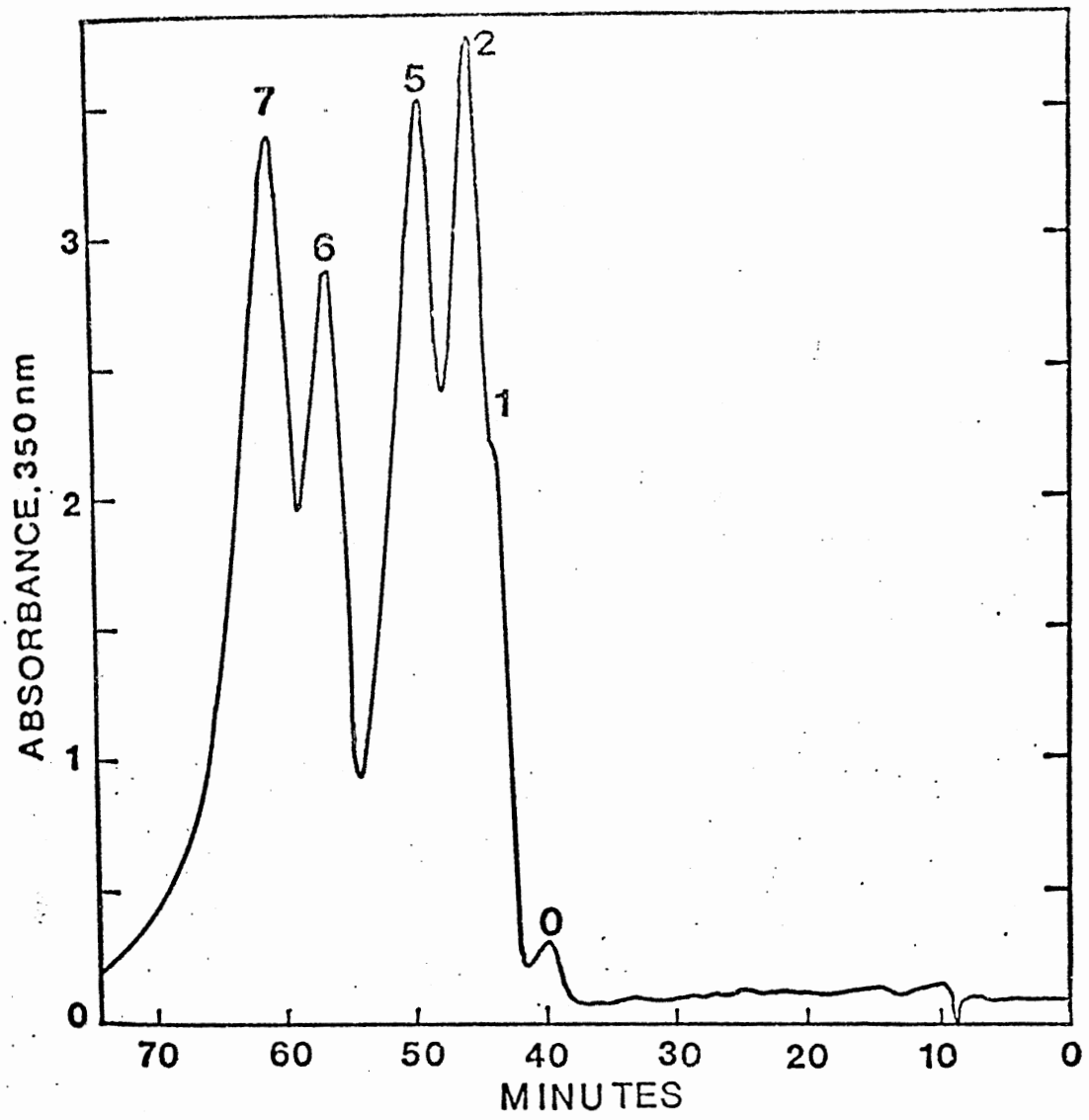

Figure 3. HPLC Profile of Isomers of Retinoic Acid

week to the next. These isomers are numbered in Figure 3 as follows: peak 0 = 13-cis(5→10) photocyclized isomer; peak 1 = 9,11,13-tri-cis-retinoic acid; peak 2 = 11,13-di-cis-retinoic acid; peak 5 = 11-cis-retinoic acid; peak 6 = 9-cis-retinoic acid; peak 7 = all-trans-retinoic acid (110, 111). When the resolution was unsatisfactory, the column was regenerated overnight by pumping 250 ml of 0.5 M acetic acid in water through the column at a flow rate of approximately 0.2 ml per min.

Preparation of Chick Liver Microsomal Fraction

Following cervical dislocation, the livers were removed from the chicks and placed in 0.25 M sucrose at 4°C. Liver tissue was homogenized by expulsion through a 1 mm stainless steel screen by means of a screw press (Harvard Apparatus, Inc., Cambridge, MA) to remove connective tissue. A 10% solution (w/v) of 0.25 M sucrose was then added to the livers as they were homogenized in a Potter-Elvejhem glass tissue grinder with a motor driven grooved teflon pestle. The procedure of Schneider and Hogeboom (110) was modified for the preparation of the microsomal fraction. The 10% homogenate was centrifuged at 10,000 x g for 20 min (Figure 4). The supernatant solution was decanted and centrifuged for 1 hr at 4°C and 105,000 x g. The 105,000 x g pellet was suspended in a 10% solution of phosphate buffer (250 mM, pH 6.4) and kept refrigerated at 4°C until use.

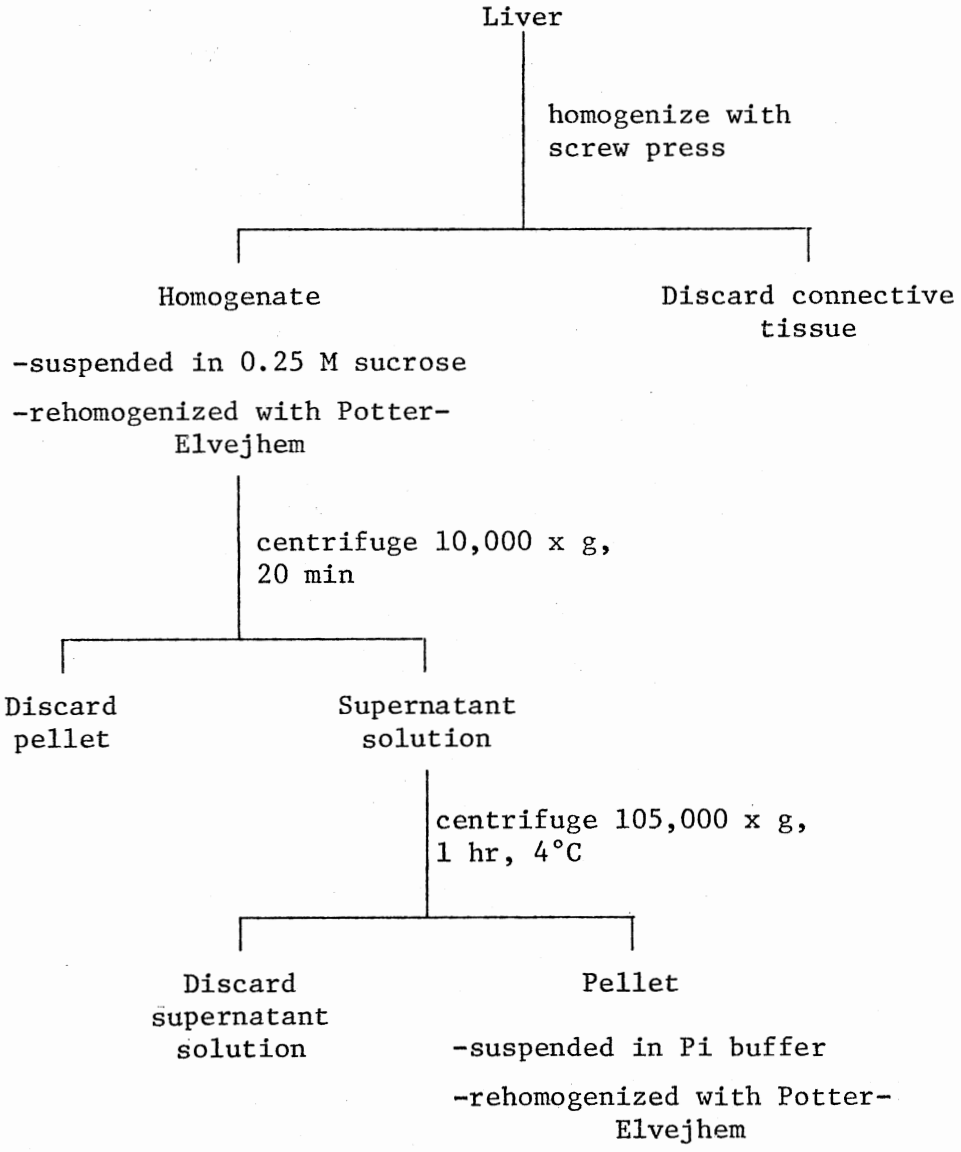

Figure 4. Scheme for the Isolation of Chick Liver Microsomal Fraction

Results

Optimum Concentrations of Retinoic Acid, $FeCl_2$, H_2O_2 and Horseradish Peroxidase in the Incubations

The incubations were run in stoppered test tubes and contained all-trans-retinoic acid and all-trans-[15-^{14}C]retinoic acid as substrates, $FeCl_2$ or hydrogen peroxide as coreactants and horseradish peroxidase as catalyst. Percent $^{14}CO_2$ release following each incubation was measured as described under "Experimental". Each value reported as a percent decarboxylation of retinoic acid was determined using the average of triplicate incubations.

The effect of retinoic acid concentration on the amount of product produced is shown in Figure 5. Horseradish peroxidase was at 4 μM, and concentrations of $FeCl_2$ (top) and H_2O_2 (bottom) were held constant at 2 mM and 1 mM, respectively. Plotted are percent decarboxylation (circles) and micrograms total products formed (triangles) versus micrograms retinoic acid per assay. While the percent $^{14}CO_2$ decreased with increasing retinoic acid, the total amount of decarboxylation and oxidation products increased. The levels of decarboxylation never exceeded 50%. The concentration of retinoic acid which yielded the greatest amount of product in the Fe^{+2} reaction was 50-100 μg per assay and in the H_2O_2 reaction was 80-100 μg per assay. The upper limit of 100 μg per assay (133 μM) was chosen as the optimum concentration of retinoic acid in all succeeding incubations.

When incubations contained 133 μM retinoic acid and 4 μM horseradish peroxidase (HRP), maximum percent decarboxylation of retinoic

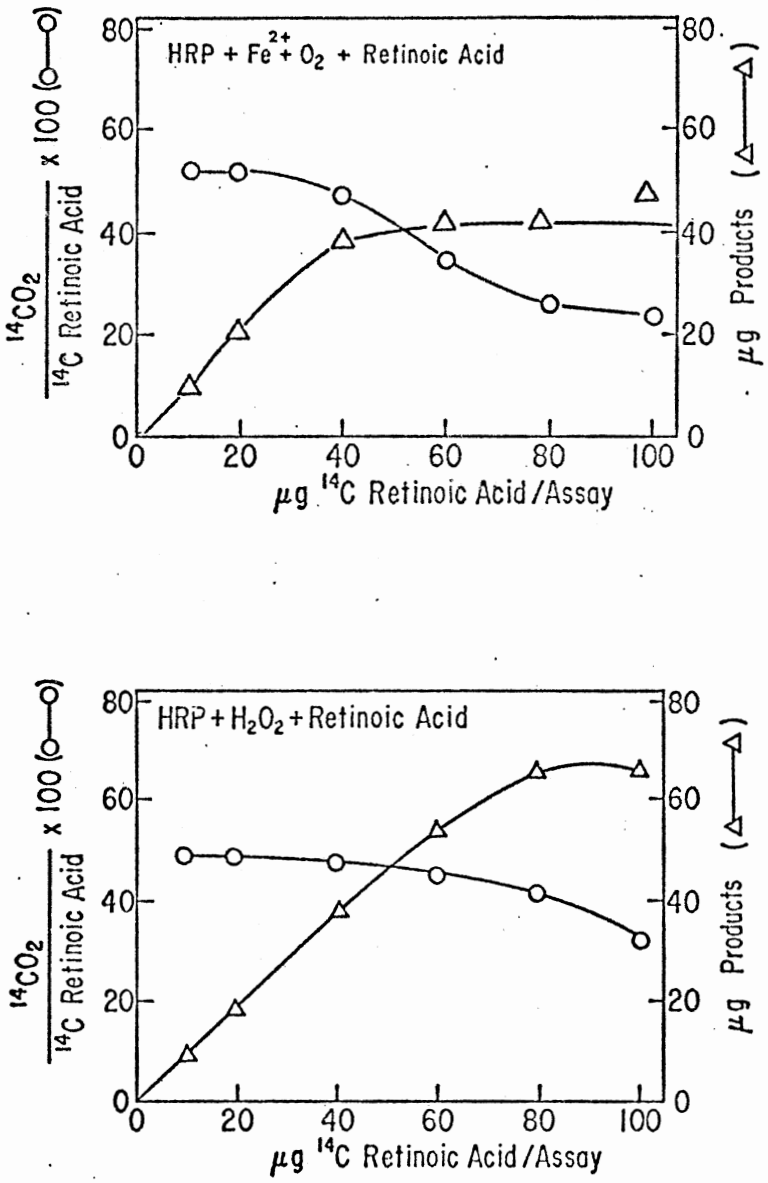

Figure 5. Effect of Retinoic Acid Concentration on the Decarboxylation of Retinoic Acid and on the Amount of Product Obtained in the Fe^{+2} Reaction (Top) and in the H_2O_2 Reaction (Bottom)

acid was obtained with levels of 0.5 to 2 mM H_2O_2 as shown in Figure 6. A concentration of 1 mM H_2O_2 was used in all subsequent incubations.

In Figure 7 the percent $^{14}CO_2$ produced versus time are plotted for incubations containing [15-^{14}C]retinoic acid (133 μM), HRP (4 μM) and 1 or 2 mM $FeCl_2$, in the presence or absence of oxygen. A gentle stream of oxygen was allowed to flow into the test tubes prior to capping, at zero time of incubation. When concentrations higher than 2 mM $FeCl_2$ were added, an ion salt precipitated. The highest levels of decarboxylation were achieved with 2 mM $FeCl_2$ in the presence of oxygen. In an attempt to increase the amount of $^{14}CO_2$ generated, $FeCl_2$ was added at 1, 2 and 3 hours. The tubes were also purged with oxygen every hour, but neither the additional purging with oxygen nor the hourly addition of $FeCl_2$ led to higher percent decarboxylation.

The optimum concentration of horseradish peroxidase per assay was determined in the two types of incubations as shown in Figure 8. In the iron reaction, 4 to 10 μM HRP were saturating levels (top), while in the H_2O_2 reaction, 2 to 10 μM HRP led to maximum amounts of $^{14}CO_2$ formation (bottom). All subsequent incubations were carried out with 4 μM HRP.

When $FeCl_2$ or H_2O_2 were left out of the incubation medium only 1.5 (± 0.1) percent decarboxylation was observed. The omission of horseradish peroxidase from the mixture led to 0.2 (± 0) percent $^{14}CO_2$ in the Fe^{+2} reaction and 0.2 (± 0.1) percent $^{14}CO_2$ in the H_2O_2 reaction.

Time Course of the Horseradish Peroxidase Catalyzed Incubation

The decarboxylation of retinoic acid, as determined by percent

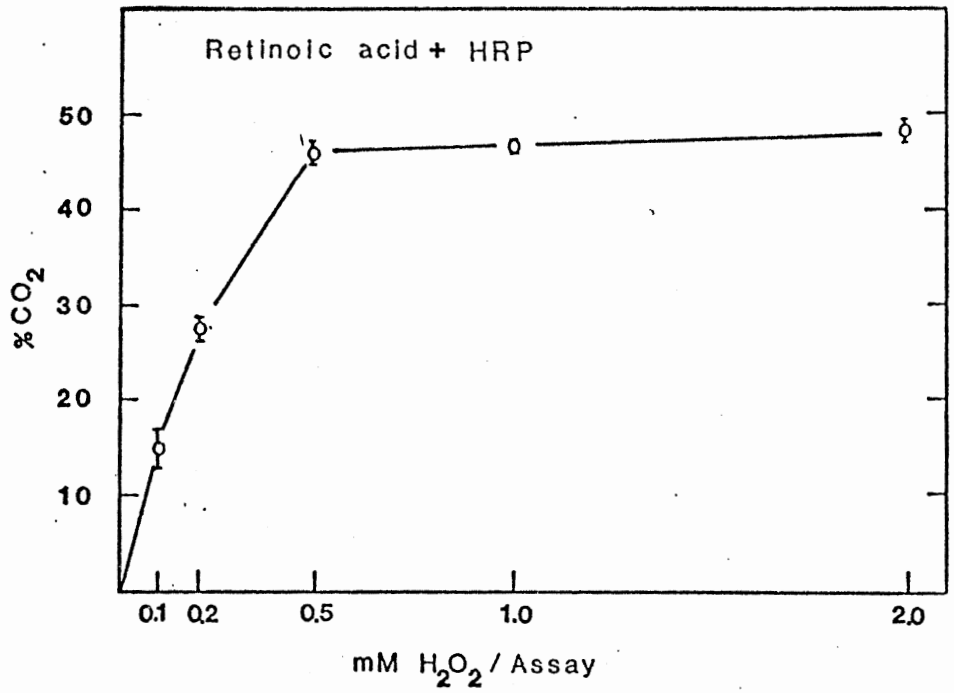

Figure 6. Effect of H_2O_2 Concentration on the Decarboxylation of Retinoic Acid

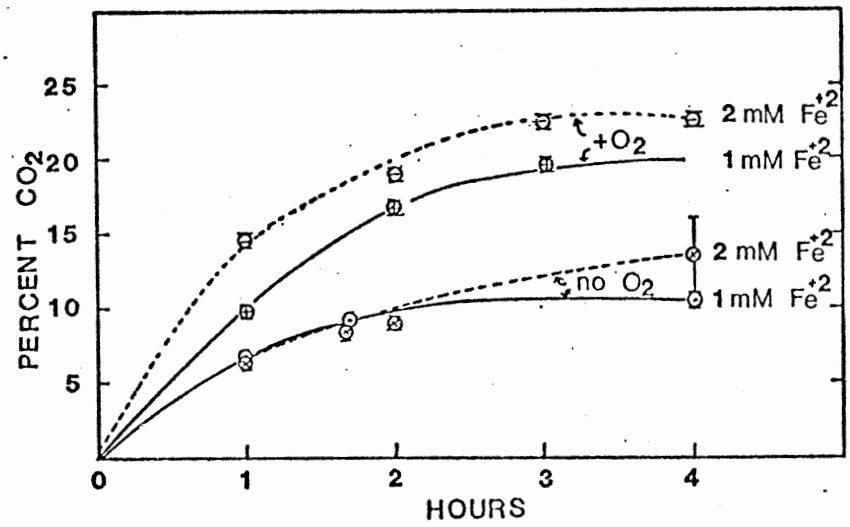

Figure 7. Effect of Oxygen and Fe^{+2} Concentration on the Decarboxylation of Retinoic Acid

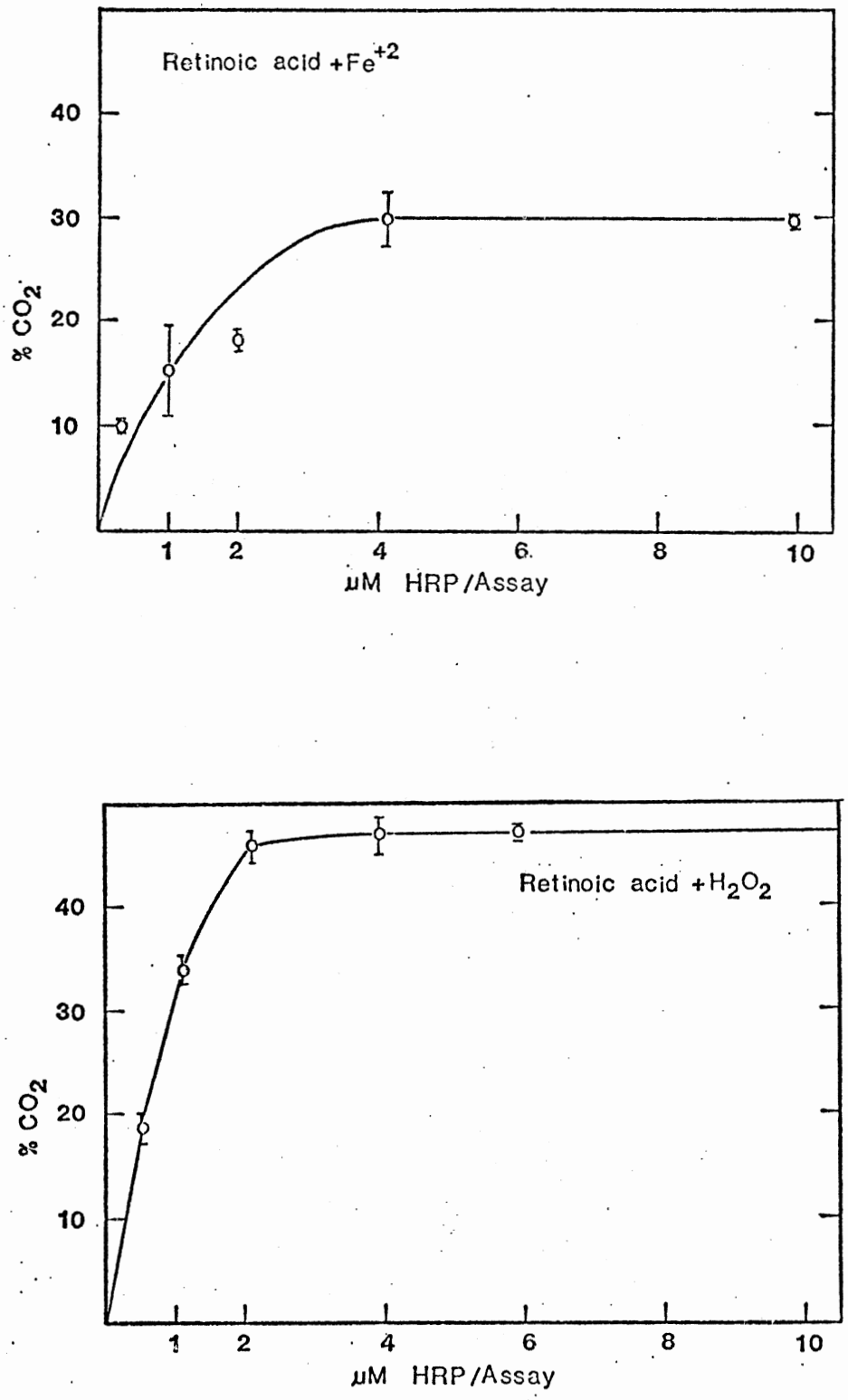

Figure 8. Effect of HRP Concentration on Decarboxylation of Retinoic Acid

$^{14}CO_2$ release, was essentially complete at the end of two hours of incubation (Figure 9). Therefore, all incubations were routinely run for a period of at least two hours in order to obtain maximum decarboxylation.

pH of the Horseradish Peroxidase Catalyzed Incubation

In an attempt to determine the pH optimum of the incubations containing $FeCl_2$ or H_2O_2, phosphate buffers (pK_a = 7.2, buffering range: 6.2 to 8.2) were prepared at the pH values indicated in Table I. Each percent decarboxylation value in the table represents the average of nine phosphate containing incubations for the Fe^{+2} reaction and six phosphate containing incubations for the H_2O_2 reaction. While the H_2O_2 reaction led to similar levels of decarboxylation from pH 6 to 8.5, the $FeCl_2$ reaction appeared to have a pH optimum well above the previously reported value of 6.4 (106). In order to determine what this pH optimum was, borate buffer was selected since its buffering capacity was higher than that of phosphate. However, as indicated in Table I, only 3.7% $^{14}CO_2$ could be achieved for the Fe^{+2} incubation in borate at pH 7.9. The H_2O_2 incubation led to decarboxylation of retinoic acid equally well in phosphate or in borate buffer.

Effect of Buffer on the Horseradish Peroxidase Catalyzed Incubation

Following the observation that retinoic acid was decarboxylated in the Fe^{+2} containing reaction in the presence of phosphate but not borate, other buffers were selected for the incubations (Table II).

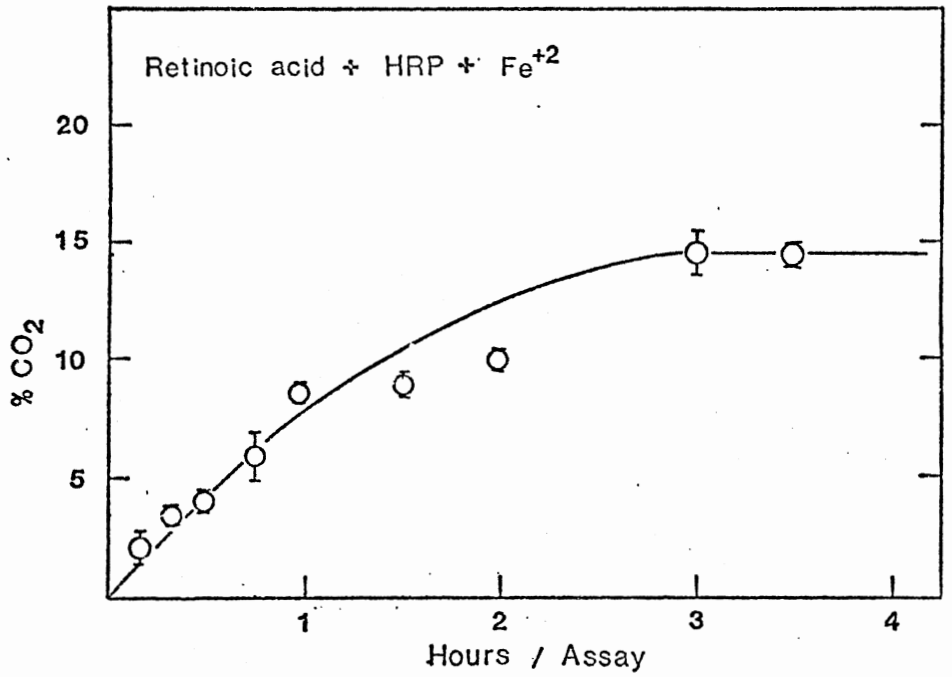

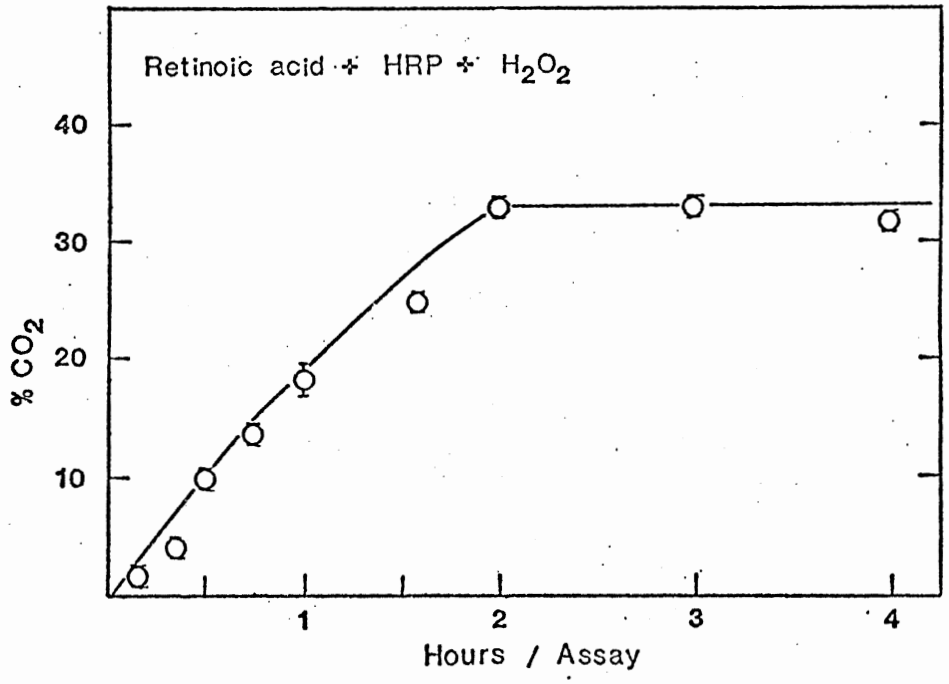

Figure 9. Time Course of the Fe^{+2} Reaction and of the H_2O_2 Reaction

TABLE I

EFFECT OF pH ON THE DECARBOXYLATION OF RETINOIC ACID

pH	Buffer	Percent Decarboxylation	
		H_2O_2 (1 mM)	Fe^{+2} (2 mM)
5.9	Pi (200 mM)	30.2 ± 6.5	11.6 ± 1.9
6.6		30.0 ± 2.7	13.5 ± 2.2
7.2		30.5 ± 4.2	14.7 ± 0.1
7.7		27.2 ± 1.2	17.6 ± 0.7
8.2		22.8 ± 1.7	19.2 ± 1.8
7.9	Borate (100 mM)	34.0 ± 1.7	3.7 ± 0.3
8.5		32.6 ± 3.8	
9.0		27.3 ± 1.9	
9.5		25.9	
10.0		23.3 ± 1.5	

TABLE II

EFFECT OF BUFFER ON THE DECARBOXYLATION OF RETINOIC ACID

Buffer	pH	Percent Decarboxylation	
		Fe^{+2} (2 mM)	H_2O_2 (1 mM)
Pi (200 mM)	6.4	33.6 ± 1.0	49 ± 1.0
PIPES (100 mM)	6.4	6.7 ± 0.4	40.4 ± 0.2
Tris (100 mM)	7	33.6 ± 1.0	50 ± 0.4
Glycyl-Glycine (100 mM)	7.4	6.2 ± 0.1	42.5 ± 2.5
MES (100 mM)	6.5	5.2 ± 0.3	37.6 ± 0.8
HEPES (100 mM)	7	5.6 ± 0.1	33.3 ± 0.3
TES (100 mM)	7	17.9 ± 0.2	40
Tricine (100 mM)	7	4.6 ± 0.2	38.5 ± 0.8
Borate (100 mM)	8	3.7 ± 0.3	34 ± 1.7

The pH value chosen for each buffer was within its buffer zone except for Tricine where it was slightly lower. The buffers included PIPES, pH 6.4 (buffer zone 6.1-7.5); Tris, pH 7.0 (buffer zone 7-9); Glycylglycine, pH 7.4 (buffer zone 7.4-9.4); MES, pH 6.5 (buffer zone 5.5-7.0); HEPES, pH 7.0 (buffer zone 6.8-8.2); TES, pH 7.0 (buffer zone 6.8-8.2); and Tricine, pH 7.0 (buffer zone 7.4-8.8). Retinoic acid was decarboxylated in all incubations containing H_2O_2, regardless of the buffer used. Phosphate and Tris buffered assays led to maximum decarboxylation (50%), at the pH values selected. When Fe^{+2} was present in the incubations, only three buffers, phosphate, Tris or TES supported substantial decarboxylation of the substrate. In the case of phosphate or Tris buffered incubations, 33.6 (± 1.0) percent $^{14}CO_2$ was released with approximately half as much $^{14}CO_2$ released in incubations in TES.

Catalysts Other Than Horseradish Peroxidase in the Incubation

It had been reported (107) that hemoglobin and horseradish peroxidase decarboxylated retinoic acid with equal facility in the presence of hydrogen peroxide. Hemoglobin was not effective as a catalyst for decarboxylation in the Fe^{+2} reaction. It was suggested that the H_2O_2 reaction was a nonenzymatic, heme catalyzed peroxidation. In order to check the validity of this hypothesis and to ensure that the reaction was not being catalyzed by the protein part of these heme containing compounds, the Fe^{+2} and H_2O_2 incubations were carried out in the presence of a variety of catalysts (Table III). Mixtures containing retinoic acid and $FeCl_2$ showed an absolute requirement for horseradish

TABLE III

EFFECT OF CATALYST ON THE DECARBOXYLATION OF RETINOIC ACID

Coreactant	PERCENT DECARBOXYLATION Catalyst					
	HRP (4 μM)	Hb (13 μM)	Hemin (3.7 μM)	Porph (4.1 μM)	Cyt_c (12.9 μM)	BSA (3.5 μM)
Fe^{+2} (2 mM)	19	1	4	-	0.7	1
H_2O_2 (1 mM)	35	21	28	2	22	1

peroxidase. Hemoglobin, hemin and cytochrome c were effective catalysts for the decarboxylation of retinoic acid in the H_2O_2 reaction. These three compounds and HRP all have an iron porphyrin moiety in common. Protoporphyrin IX, containing no metal, and bovine serum albumin were unable to catalyze the decarboxylation reaction.

Extraction Controls

Freshly distilled diethyl ether had been routinely used in this laboratory for extraction of incubation mixtures (102, 108). Due to the potential presence of peroxides in the ether, other solvents were investigated for extraction, including chloroform and hexane (Figure 10). Duplicate incubations were run in stoppered flasks containing either all-*trans*-[15-^{14}C]retinoic acid (Figure 10-A) or all-*trans*-[11,12-$^{3}H_2$]retinoic acid (Figure 10-B) in the presence of $FeCl_2$ and horseradish peroxidase. The mixture from each flask was extracted with an equal volume of chloroform 6 to 9 times, then with an equal volume of hexane 3 to 6 times (solid lines in Figure 10). The mixture from the duplicate incubation was extracted with hexane 6 to 7 times, then with chloroform 3 to 6 times (dashed lines). An aliquot of each extraction was counted on the liquid scintillation counter in order to determine efficiency of extraction of labeled products from the aqueous medium. The results indicated that chloroform and hexane were equally useful solvents for extraction of ^{14}C-labeled products. ^{3}H-labeled decarboxylation products, however, were more readily removed from the aqueous incubation mixture by chloroform.

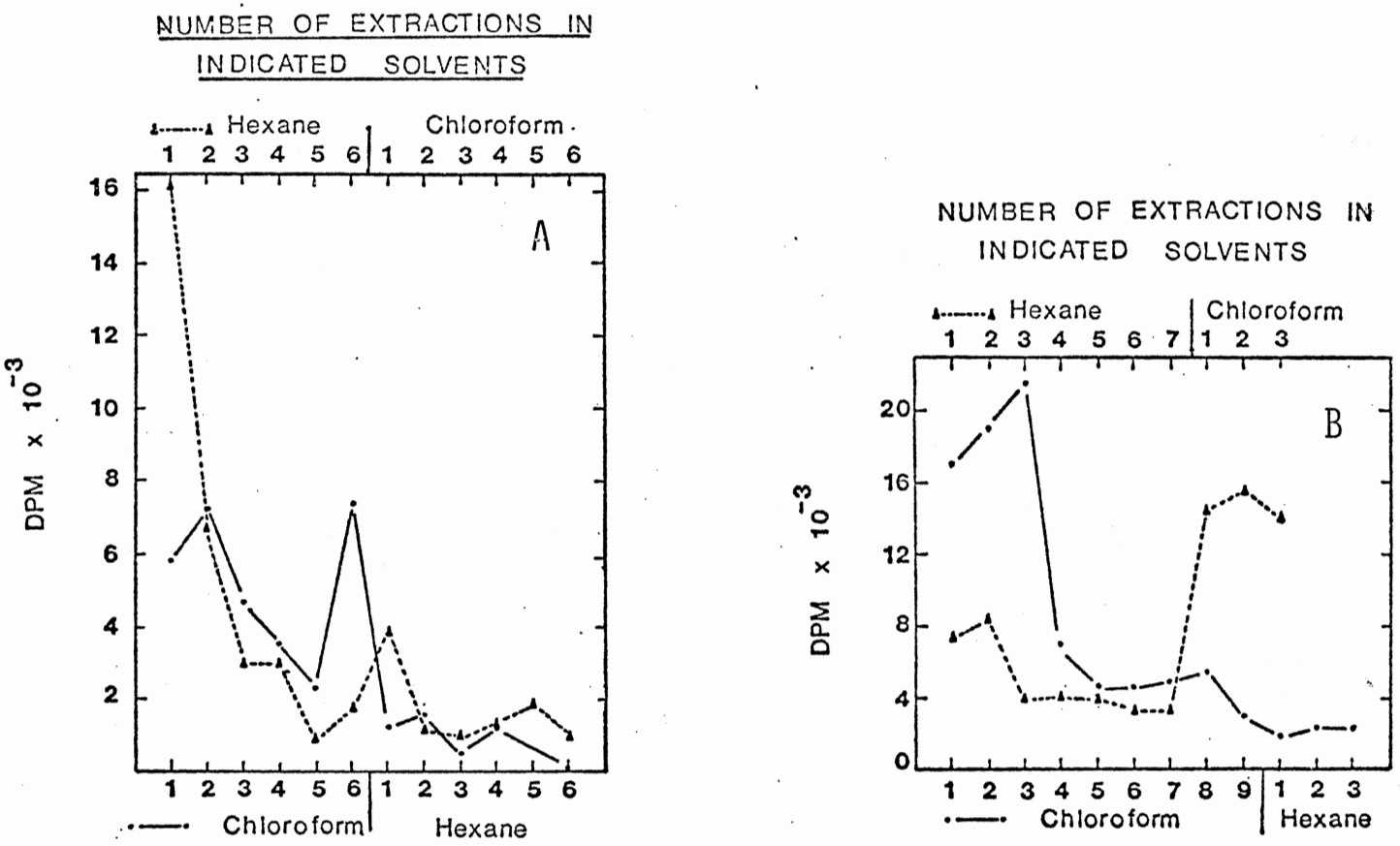

Figure 10. Extraction of ^{14}C-Labeled (A) and ^{3}H-Labeled (B) Oxidation and Decarboxylation Products of Retinoic Acid

Liver Microsomal Fraction Incubations

Chicks were divided into three groups based on the presence or absence of retinoic acid in their diets, as described in "Experimental". Liver microsomal fractions decarboxylated retinoic acid *in vitro* to the same extent, regardless of the diet of the chicks. In contrast with previous reports, no Fe^{+2} was required in these incubations (Table IV).

Optimum concentrations of retinoic acid and liver microsomal fraction were determined as shown in Figure 11 and found to be consistent with those of other investigations (102, 108). When retinoic acid was incubated at 13.3 to 133 μM concentrations in the presence of 50 mg of the liver microsomal fraction, the percent $^{14}CO_2$ released dropped from 31% to 22% (Figure 11, top). In incubations containing 6.6 μM retinoic acid, saturation of the microsomal fraction was reached between 30-100 mg of liver (Figure 11, bottom).

Liquid Chromatography of the Incubation Mixtures

Extracts from incubations containing ^{3}H-labeled retinoic acid, $FeCl_2$ and horseradish peroxidase were chromatographed on a Sephadex LH-20 column, as described under "Experimental" and as shown in Figure 12 (top). Sephadex LH-20 is a polar gel so as the number of milliliters of column effluent increases, the polarity of the compounds eluting from the column increases. The single peak eluting at 80 ml of column effluent was all-*trans*-retinoic acid. This was demonstrated by applying a pure sample of retinoic acid to the column under identical conditions, and observing that it eluted in the same tube

TABLE IV

EFFECT OF DIET ON THE DECARBOXYLASE ACTIVITY OF CHICK LIVER MICROSOMAL FRACTION

Retinoic Acid in Diet		Percent Decarboxylation	
Hatch to -24 hrs	-24 hr to test	No Fe^{+2}	Fe^{+2}
no	no	22.3 ± 0.5	15.0 ± 2.4
no	yes	24.7 ± 0.9	17.0 ± 1.0
yes	yes	24.7 ± 0.2	21.0 ± 1.3

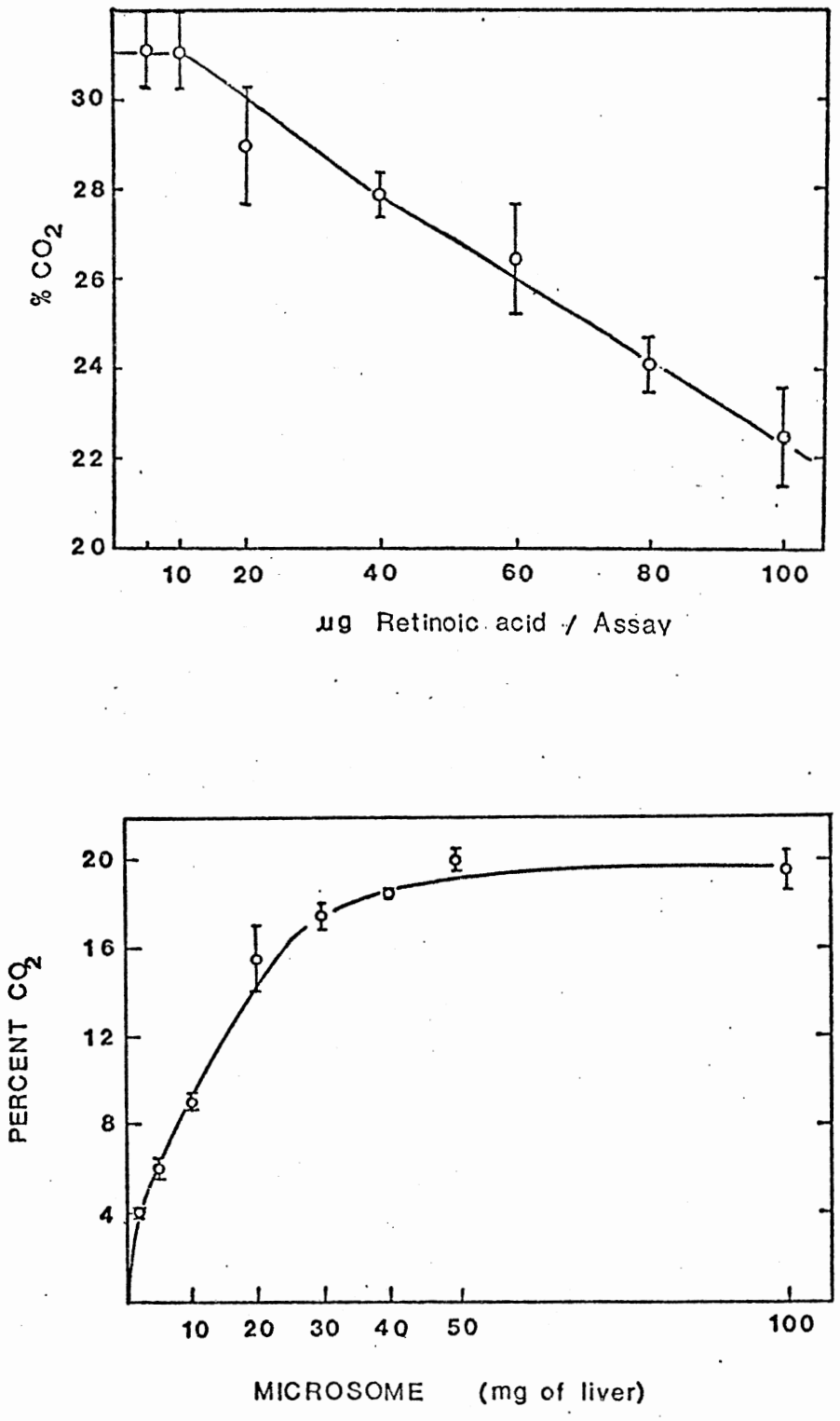

Figure 11. Effect of Retinoic Acid Concentration (Top) and Microsomal Concentration (Bottom) on Decarboxylation of Retinoic Acid in the Chick Liver Microsomal Incubations

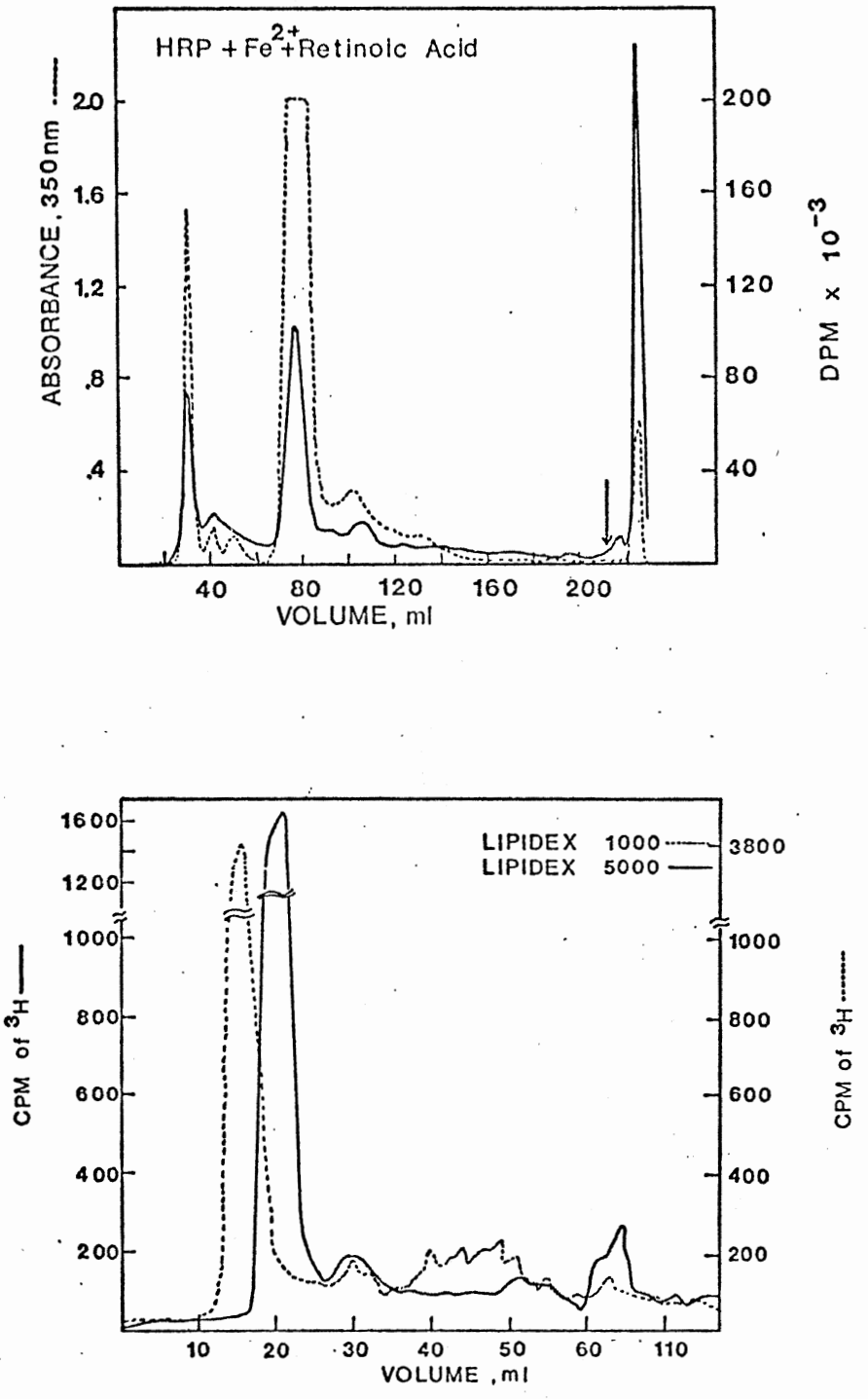

Figure 12. Chromatography of Fe^{+2} Incubations on Sephadex LH-20 (Top) and on LIPIDEX-1000 and LIPIDEX-5000 (Bottom)

number. A large percentage of the ^{3}H-labeled derivatives of retinoic acid appeared in the more polar fractions after 200 ml of column effluent, and were not resolved on this column. Attempts to separate decarboxylation products generated from the microsomal incubations failed due to this lack of resolution.

Extracts from incubations containing ^{3}H-labeled retinoic acid, $FeCl_2$ and horseradish peroxidase were methylated with diazomethane and chromatographed on two types of reverse phase columns, LIPIDEX-5000 and the more polar LIPIDEX-1000 (Figure 12, bottom). Despite the fact that the incubation mixtures were methylated and therefore less polar, these mixtures were not well resolved on either of the two columns and eluted close to the void volumes.

High Performance Liquid Chromatography of the Extracts from the Incubation Mixtures

Incubation mixtures containing microsomal fractions or horseradish peroxidase as catalysts for the decarboxylation of retinoic acid were successfully separated by high performance liquid chromatography performed on reverse phase columns as described under "Experimental".

In Figure 13 the product profiles of three different incubation mixtures were compared when they were chromatographed on the Partisil 10-ODS columns using 60% methanol and 40% water at a flow rate of 0.5 ml per min. The peak at 58 minutes was eluted from the column upon injection of 100% methanol and contained retinoic acid. The retention times of the oxidation and decarboxylation products obtained from incubations containing retinoic acid + H_2O_2 + HRP, retinoic acid + $FeCl_2$ +

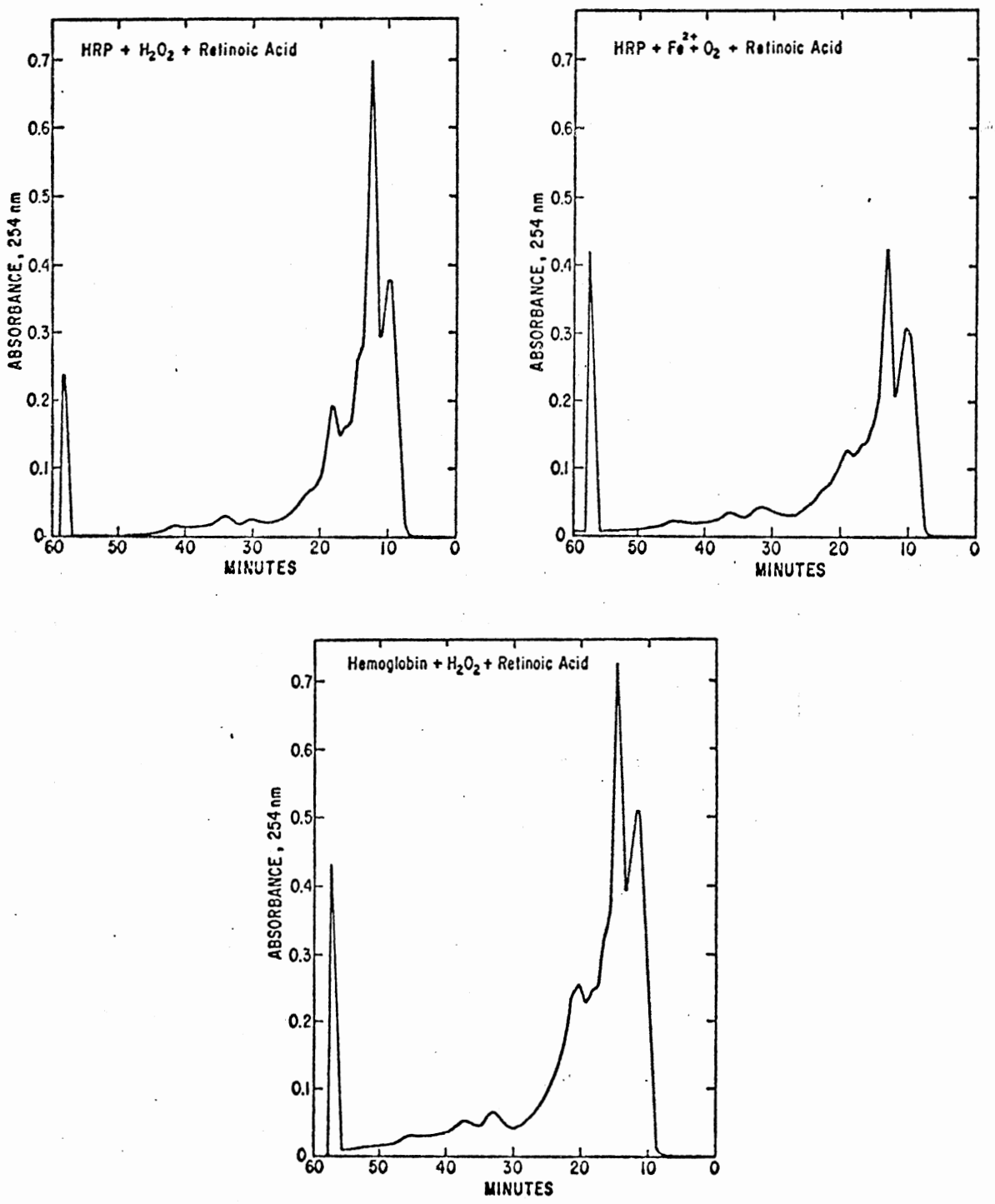

Figure 13. HPLC of HRP and Hemoglobin Catalyzed Incubation Mixtures. Chromatography was performed with two Partisil 10-ODS columns in series, with 60% methanol and 40% water at 0.5 ml per minute.

HRP and retinoic acid + H_2O_2 + hemoglobin were found to be practically identical.

The retention time and absorbance of products resulting from incubations containing either the microsomal fraction with retinoic acid (dashed line) or HRP + H_2O_2 + retinoic acid (dotted line) are shown in Figure 14. The two Partisil 10-ODS columns were used in 60% methanol, 40% H_2O at 0.67 ml per min. These product profiles were not as similar as those from the heme catalyzed reactions (Figure 13).

To ensure that artifacts were not being generated on the column, controls were performed by deleting components individually. Either retinoic acid, the coreactant H_2O_2 or $FeCl_2$, the catalyst HRP, or phosphate were left out of the incubations. The mixtures were then chromatographed in 60% CH_3OH, 40% H_2O at 0.5 ml per min, as shown in Figures 15 and 16. The peak at 60-75 min in each chromatogram resulted from a gradient of 60-100% CH_3OH. When incubations included retinoic acid, the substrate was detected in the gradient elution. The small peak at approximately 15 min corresponds to a change in refractive index when the solvent in the void volume passed through the detector. The product profiles of the incubations in the absence of phosphate buffer confirmed the absolute requirement for phosphate in the Fe^{+2} reaction but not in the H_2O_2 reaction.

In Figures 17 and 18, the HPLC product profiles of the Fe^{+2} and H_2O_2 reactions are shown after varying the time of incubation. As the time of incubation increased, the percent decarboxylation of retinoic acid increased and this was accompanied by the formation of oxidation and decarboxylation products. Particularly noteworthy was the increasing absorbance of the polar fractions eluting from the column

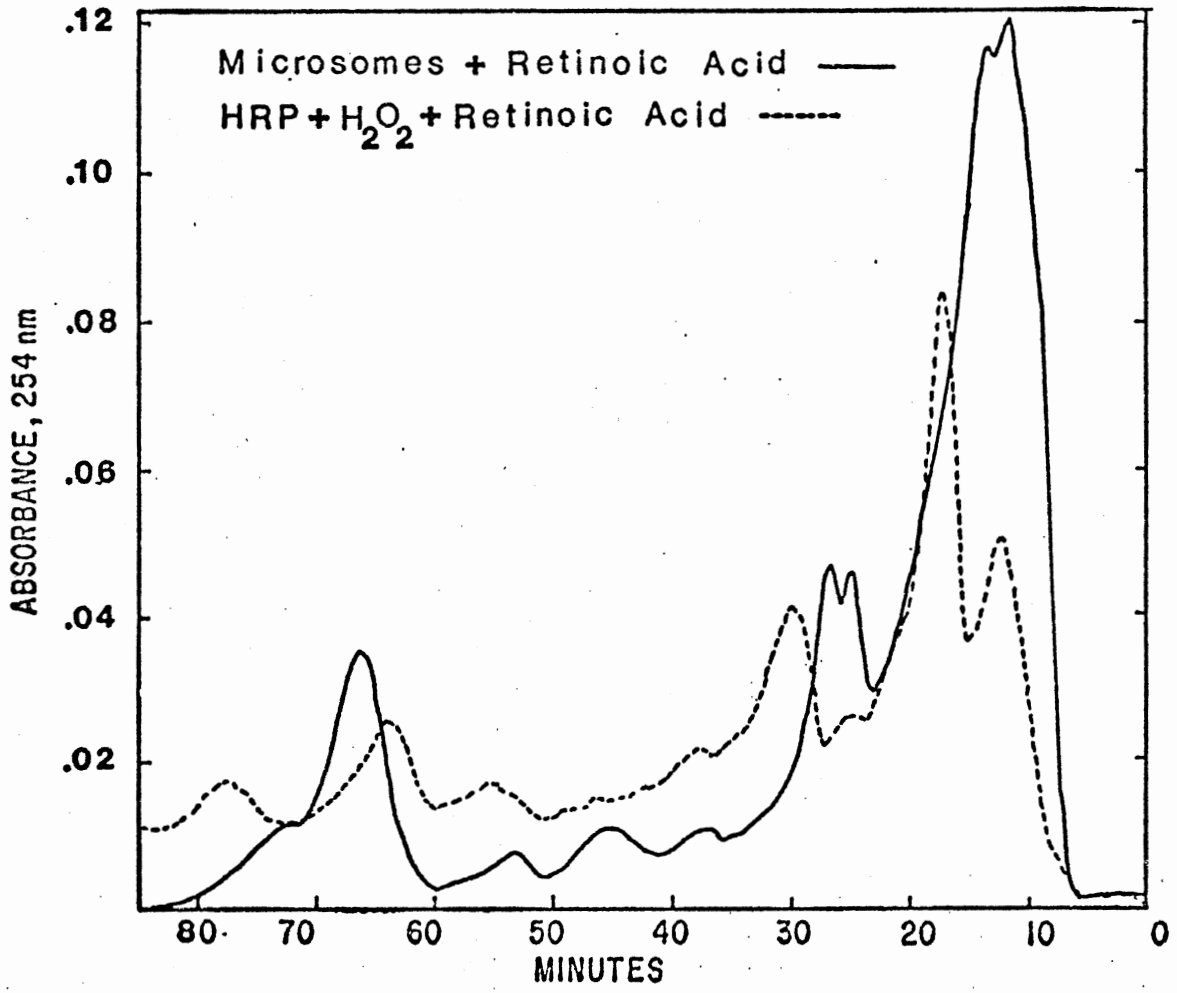

Figure 14. HPLC of HRP and Microsomal Incubation Mixtures. Chromatography was performed with two Partisil 10-ODS columns in series, with 60% methanol and 40% water at 0.67 ml per minute.

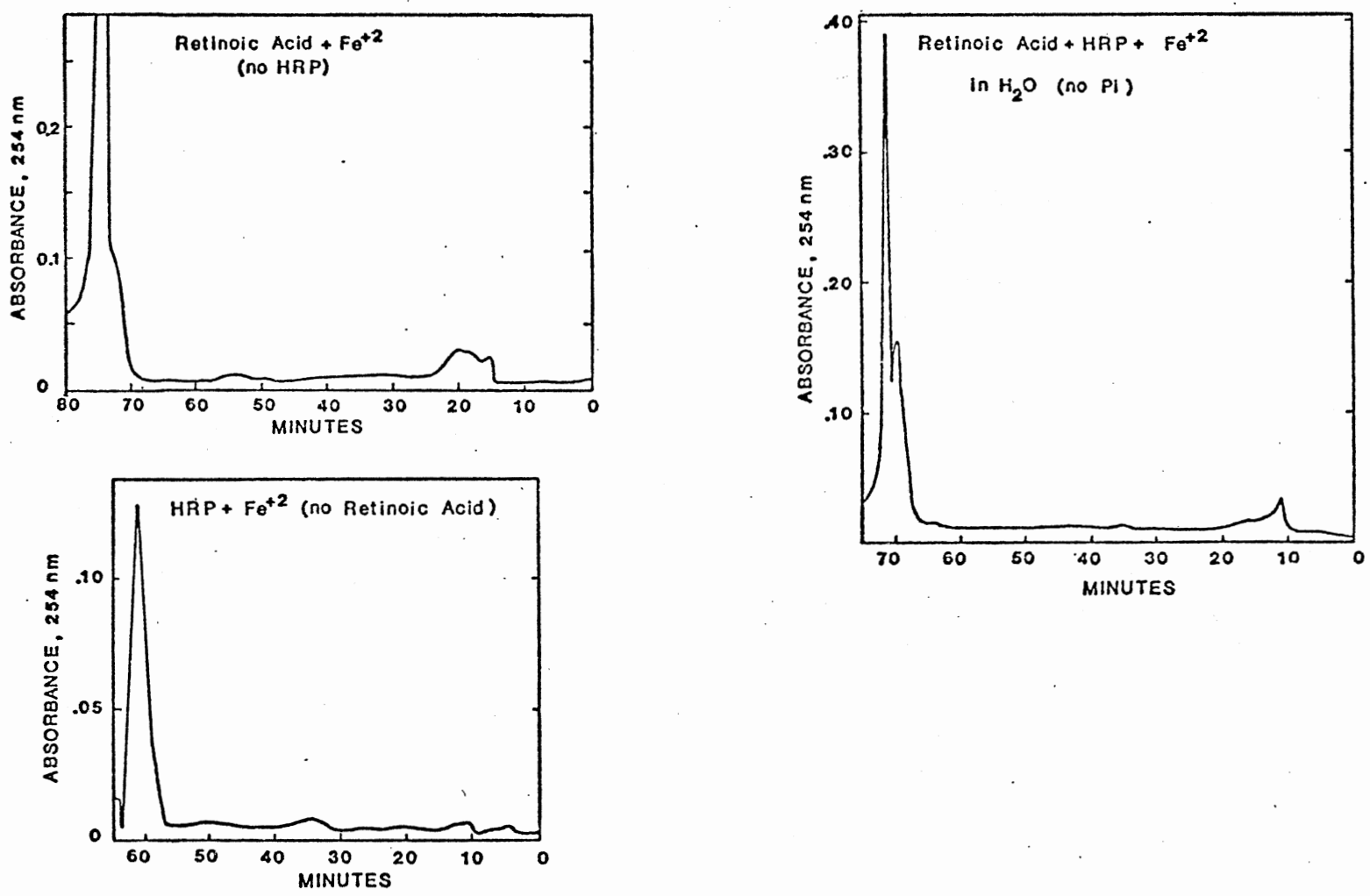

Figure 15. HPLC Profile of Products of Fe^{+2} Reactions Lacking Retinoic Acid, HRP or Phosphate Buffer. Chromatography was performed with two Partisil 10-ODS columns in series, in 60% methanol and 40% water at 0.5 ml per minute.

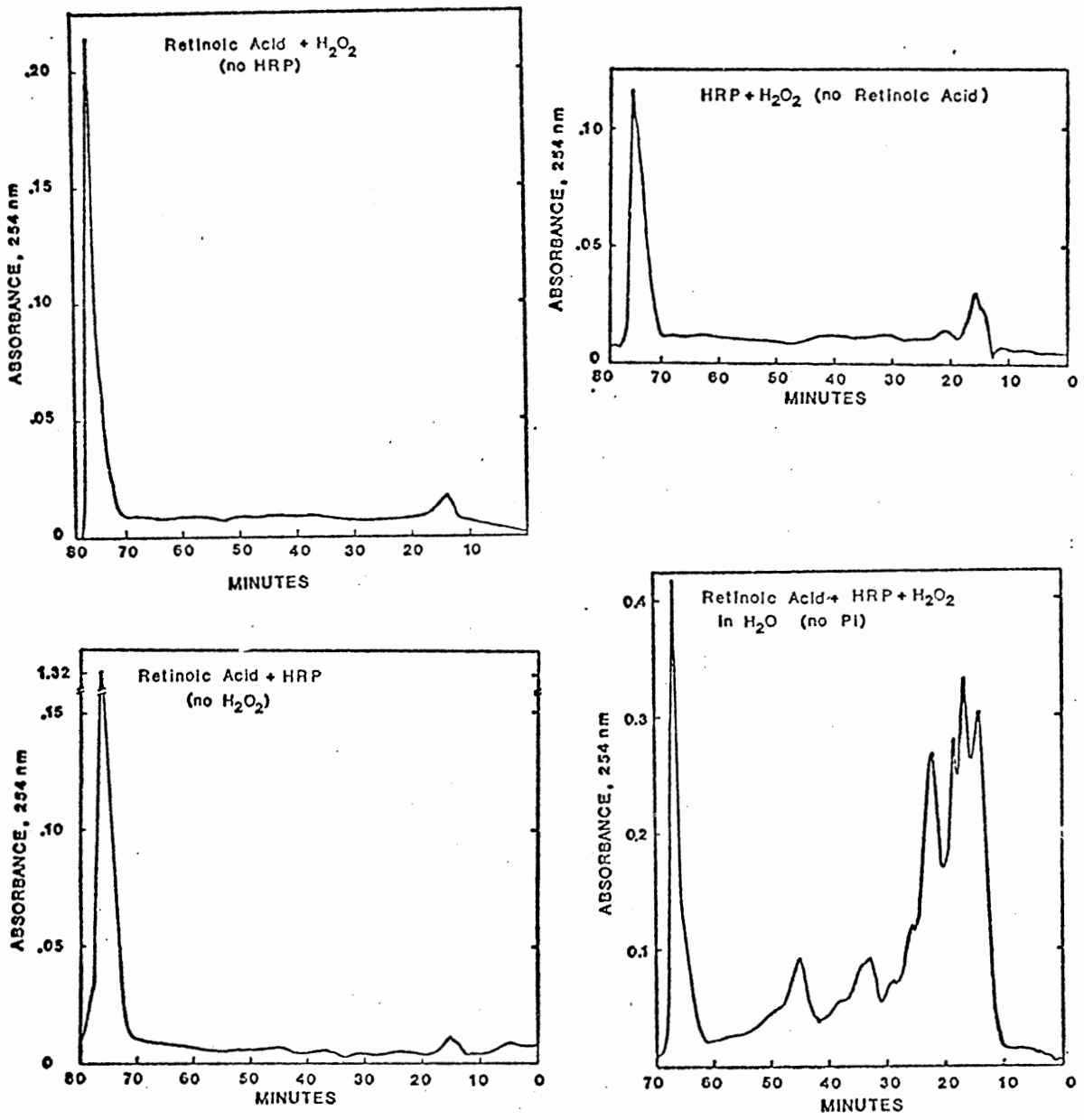

Figure 16. HPLC Profile of Products of H_2O_2 Reactions Lacking Retinoic Acid, H_2O_2, HRP or Phosphate Buffer. Chromatography was performed with two Partisil 10-ODS columns in series, in 60% methanol, 40% water at 0.5 ml per minute.

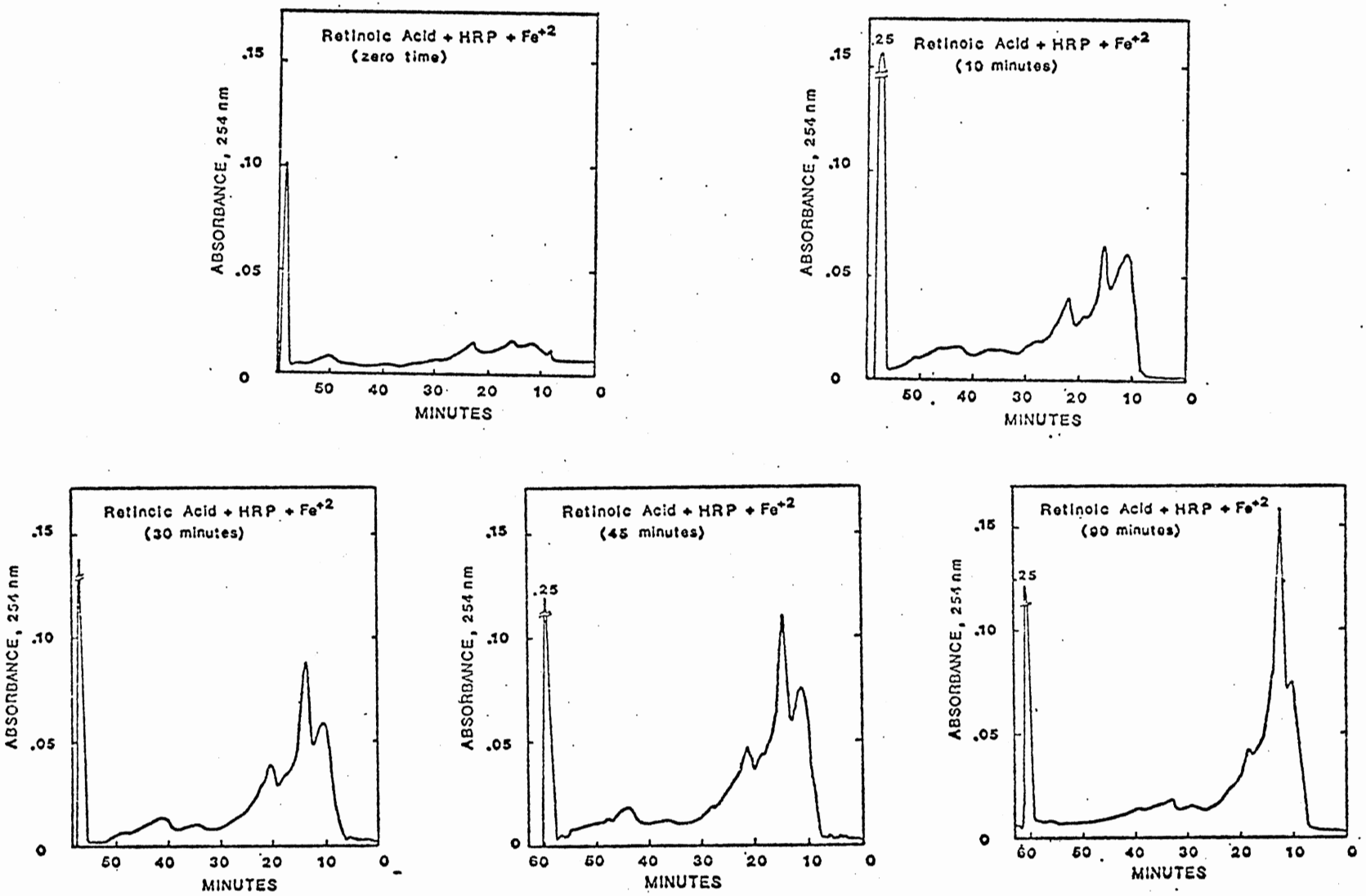

Figure 17. HPLC Profile of Products of Fe^{+2} Reactions After 0, 10, 30, 45, 90 Minutes of Incubation

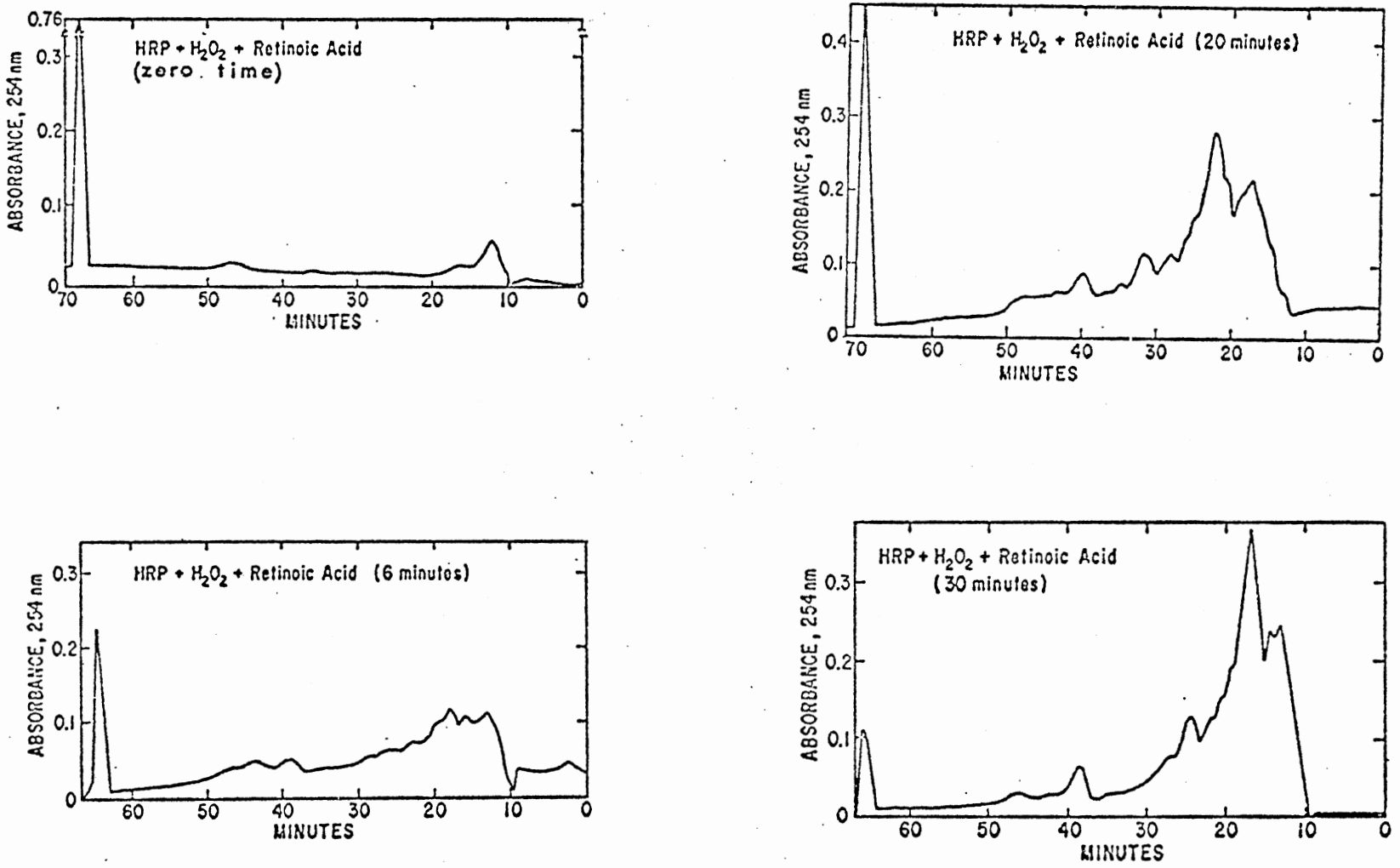

Figure 18. HPLC Profile of Products of H_2O_2 Reactions After 0, 6, 20 and 30 Minutes of Incubation. Chromatography was performed with two Partisil 10-ODS columns in series, in 60% methanol, 40% water at 0.5 ml per minute.

between 8 and 25 minutes. These polar fractions contained the decarboxylation products of retinoic acid.

HPLC of the extracts from incubations containing all-trans-[11,12-$^{3}H_2$]retinoic acid and all-trans-[15-^{14}C]retinoic acid with horseradish peroxidase and H_2O_2 or with microsomal fractions are shown in Figure 19-A and 19-B, respectively. Although the ^{3}H to ^{14}C ratio of the retinoic acid was 1:1, the polar fractions eluting from the column had ^{3}H to ^{14}C ratios greater than 1, indicating that some of these ill-resolved early eluting compounds did not contain the ^{14}C label, present on the carboxyl group of the substrate. The less polar compounds in the HRP reaction had ^{3}H to ^{14}C ratios closer to 1.

Discussion

The optimum concentrations of retinoic acid and horseradish peroxidase for incubation were much higher than values previously reported. Retinoic acid was present at a concentration of 133 μM in the horseradish peroxidase catalyzed incubations as compared with 10 μM reported by Reid and Nelson et al. (106, 108) and 8.3 μM reported by McKenzie and Nelson (107). While the latter used 0.21 μM HRP, the former used 2.6 μM HRP and our results indicated a catalyst optimum of 4 μM. The coreactant concentrations were approximately the same in all incubations. The explanation for these wide divergences in concentrations of substrate and catalyst lies in the fact that the previous investigators sought to maximize the percent decarboxylation of retinoic acid while our efforts were to maximize the amount of product formed. This was a necessary prerequisite for the subsequent isolation of sufficient quantities of purified product to permit

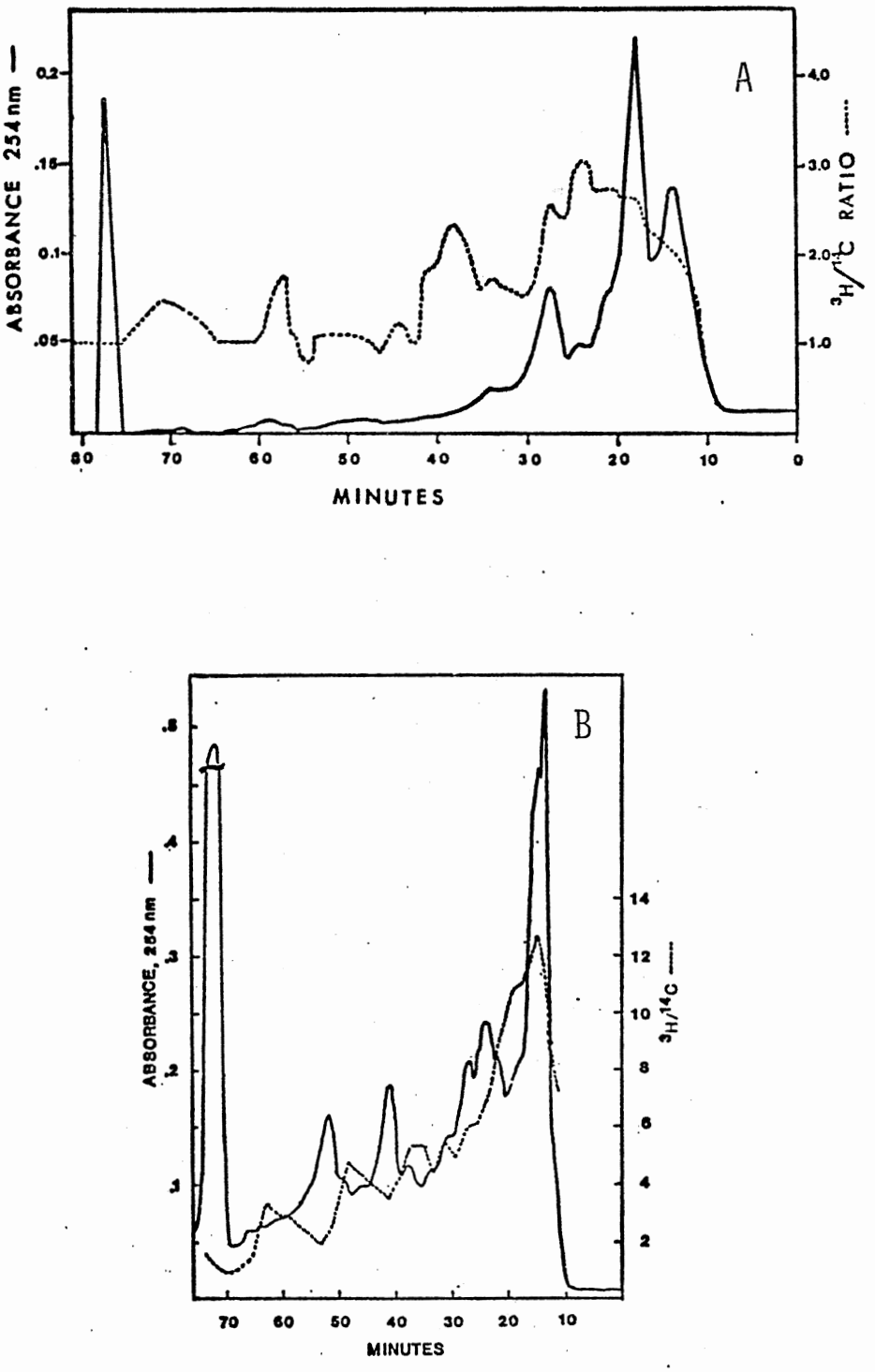

Figure 19. HPLC and $^3H/^{14}C$ Profiles of Products Generated from ^3H- and ^{14}C-Labeled Retinoic Acid in the Presence of H_2O_2 and HRP (A) or Microsomal Fractions (B). Chromatography was performed with two Partisil 10-ODS columns in series, in 60% methanol, 40% water at 0.5 ml per minute.

spectroscopic analysis.

The requirement for $FeCl_2$ and O_2 could be met by the presence of H_2O_2 in the horseradish catalyzed incubations. This confirms data presented by other investigators (106, 108). The H_2O_2 reaction led to decarboxylation of retinoic acid regardless of the choice of buffer in a pH range of 6.4 to 8.0. The $FeCl_2$ reaction led to decarboxylation of retinoic acid only in a limited number of buffers including phosphate, Tris and TES. If one postulates that H_2O_2 is being produced in the Fe^{+2} reaction as follows:

$$2Fe^{+2} + O_2 + 2H^+ \rightarrow 2Fe^{+3} + H_2O_2$$

then it is reasonable to assume that by forming a stable complex with Fe^{+3}, phosphate prevents the reaction from reversing. Tris contains a primary aliphatic amine of considerable reactivity which could form a coordinate bond with Fe^{+3} (111). TES is synthesized from Tris and could contain enough Tris as a contaminant to account for the 18% $^{14}CO_2$ obtained in the TES buffered Fe^{+2} reaction. If the reaction to generate H_2O_2 does take place as postulated, this would explain the requirement for O_2 demonstrated by the $FeCl_2$ reaction as well as the absence of decarboxylation of retinoic acid in the presence of Fe^{+3} observed by Nelson et al. (106).

The studies on the pH optimum of the Fe^{+2} reaction were inconclusive. They indicated a pH optimum higher than the previously reported value of 6.4 (106). The pH optimum could not be determined since the pH buffering zone for phosphate is 6.2 to 8.2 and the decarboxylation values increased from 11.6 at pH 5.9 to 19.2% at pH 8.2. The H_2O_2 reaction led to optimum decarboxylation at pH values

of 6.0 to 8.5. Since phosphate has a poorer buffering capacity above pH 7.5 (111), a pH of 6.4 was chosen as an optimum value for subsequent incubations.

The only catalyst which successfully decarboxylated retinoic acid in the Fe^{+2} reaction was HRP. The H_2O_2 reaction could be performed with a wide variety of catalysts which contained a heme or hemin group. BSA which has no heme group and protoporphyrin IX which contains no metal did not catalyze the decarboxylation reaction. These results support the hypothesis by McKenzie and Nelson (107) that the reaction is a nonenzymatic, heme catalyzed peroxidation.

The amount of labeled $^{14}CO_2$ never exceeded 50% even though no retinoic acid remained at the end of the incubation. This is consistent with the results of other investigators (104, 106). Although the mechanism of the heme catalyzed reactions remains to be determined, these levels of decarboxylation suggest that two molecules of retinoic acid could be required in order to generate one molecule which was decarboxylated by a free radical reaction. Radiochemical analyses of the products found in the incubation demonstrated the presence of several ^{14}C-labeled non-decarboxylated oxidation products. Therefore, mechanisms of this reaction seem to involve oxidation as well as decarboxylation of retinoic acid.

High performance liquid chromatography on reverse phase columns resulted in much better separation of the polar oxidation and decarboxylation products of retinoic acid than did liquid chromatography on Sephadex LH-20, LIPIDEX-1000 and LIPIDEX-5000. The advantages of the HPLC system over these traditional liquid chromatographic methods include an increased resolution of the products, much more rapid

separation, a higher sensitivity of detection and greater reproducibility. We were also able to show that ODS columns produce no artifacts from retinoic acid during the separations. Incubations containing retinoic acid + Fe^{+2} + HRP, retinoic acid + H_2O_2 + HRP, and retinoic acid + H_2O_2 + hemoglobin had very similar product profiles. The products formed in these incubations may well be identical.

Chick liver microsomes decarboxylated retinoic acid to the same extent, regardless of the presence or absence of vitamin A in the diet of the chicks. This indicates that the microsomal enzymes are not inducible and confirms data in the literature (103). The incubations containing retinoic acid and microsomes did not require the addition of $FeCl_2$ in contrast to previous reports by Lin (102). A possible explanation for this is the fact that these microsomal fractions were not as pure as those used by Lin and probably contained both free and protein bound Fe^{+2} as contaminants. The optimal concentrations of retinoic acid and of microsomal fractions were found to be consistent with literature values (102, 108). When the extracts from microsomal incubations were chromatographed by HPLC on ODS columns, the product profiles were similar to those generated from heme containing incubations. In both the microsome and the heme catalyzed incubations the decarboxylation products eluted in the polar fractions.

In summary, by varying the nature and pH of the buffer, the concentrations of retinoic acid, H_2O_2 or $FeCl_2$, and horseradish peroxidase, the amounts of products generated from the incubations have been optimized. Further evidence has been provided in support of the hypothesis by McKenzie and Nelson (107) that the reaction under study is a nonenzymatic, heme catalyzed peroxidation. HPLC was demonstrated to be the

method of choice for separation of oxidation and decarboxylation products of retinoic acid.

CHAPTER III

ISOLATION AND CHARACTERIZATION OF OXIDATION PRODUCTS OF RETINOIC ACID

Horseradish peroxidase (HRP) preparations have been used as a model system for the decarboxylation of retinoic acid for the past decade. The use of horseradish peroxidase preparations as the decarboxylating agent was based on their low levels of lipid contaminants and on the observation that liver and kidney microsomes seem to decarboxylate retinoic acid *in vitro* by a free radical mechanism resembling that in peroxidation (104). In addition, thin-layer chromatography of ^{14}C-labeled products, isolated from incubations containing retinoic acid and either microsomes, crude liver powders or horseradish peroxidase revealed products with similar migration rates (108). In Chapter II the HPLC product profiles of heme and microsome catalyzed incubations also had similarities. Since the incubations containing retinoic acid, H_2O_2 and horseradish peroxidase consistently led to the highest percent decarboxylation, they were used for the isolation and characterization of several oxidation and decarboxylation products of retinoic acid.

Experimental

Materials

All-*trans*-retinoic acid, all-*trans*-[11,12-$^3H_2$]retinoic acid (2.9

mCi/mM in toluene) and all-trans-[15-^{14}C]retinoic acid (0.16 mCi/mM in methanol) were gifts from Dr. W. E. Scott, Hoffmann-La Roche Inc. (Nutley, NJ). Both the ^{3}H- and ^{14}C-labeled retinoic acid were purified by high performance liquid chromatography as described under "Experimental" in Chapter II. Horseradish peroxidase (type VI) was obtained from Sigma Chemical Co. (St. Louis, MO), and hydrogen peroxide (30%) from Fisher (Fair Lawn, NJ).

Glass-distilled residue-free solvents (Burdick and Jackson Labs., Muskegon, MI) were used for extraction and high performance liquid chromatography (HPLC). The water was deionized and redistilled in glass.

Methods

Incubation Conditions. To obtain sufficient quantities of products, approximately 100 incubations were performed in 125 ml stoppered flasks at 37°C for two hours in the dark. The incubations contained all-trans-retinoic acid (133 μM), horseradish peroxidase (4 μM) and hydrogen peroxide (1 mM), in 200 mM potassium phosphate buffer, pH 6.4. In studies where the extinction coefficients as well as the $^{3}H/^{14}C$ ratios of the purified products were determined, 8 incubations contained retinoic acid as well as all-trans-[15-^{14}C]retinoic acid (2 x 10^4 dpm/assay) and all-trans-[11,12-$^{3}H_2$]retinoic acid (2 x 10^4 dpm/assay). At the end of the incubation period, the reaction mixture was extracted six times with equal volumes of chloroform. The chloroform extracts were concentrated by evaporation on a rotary evaporator (Rotovapor-R, by Buchi/Brinkmann Instruments, Westbury, NY) at a setting of 4-5 and a temperature of 37°C. They were dissolved in methanol and filtered

through a 0.5 μm filter (filter type FH from Millipore Corporation, Bedford, MA). Extracts from equivalent incubations were pooled prior to chromatographic analyses.

High Performance Liquid Chromatography. Products from retinoic acid were separated on a 0.94 x 50 cm octadecylsilane column (ODS) Partisil M9, 10/50 (Whatman, Clifton, NJ), and on two 0.46 x 25 cm Partisil 10-ODS columns (Whatman, Clifton, NH) in series. The high pressure pumping systems and the detectors are described under "Experimental" in Chapter II. Incubation extracts were chromatographed initially on the Partisil M9 column. Fractions eluting from the column which were of interest were collected in individual round bottom flasks. These were shielded from the light with the aid of a black cloth and aluminum foil. The fractions were concentrated by evaporation on a rotary evaporator. Each fraction was then injected onto the two Partisil 10-ODS columns in the same concentration of methanol and water as that used for column elution. By adjusting the solvent concentration the products of interest were further purified until baseline resolution was obtained. Column performance was checked routinely by chromatographing a standard solution of retinoic acid isomers, as described under "Experimental" in Chapter II.

Mass Spectroscopy. The mass spectra were obtained using the direct probe of a prototype of the LKB-9000 mass spectrometer (114). The ion source temperature was 270°C, the direct inlet temperature 75°C to 80°C and the impact voltage was 70 eV.

Nuclear Magnetic Resonance Spectroscopy. Proton nuclear magnetic resonance spectra (NMR) were obtained on a Varian XL-100-15 instrument

(Varian, Palo Alto, CA), interfaced to a Nicolet Technology Corp. TT-100A Fourier transform accessory. Due to the small quantities of product obtained, 16-24 hour accumulations were necessary (approximately 1600-2000 scans). The sample was dissolved in 30 µl of deuteroacetone, 100 atoms % D (Sigma Chemical Co., St. Louis, MO) and was placed in a 1.7 x 90 mm capillary tube (Kimble Products, Toledo, OH). Tetramethylsilane, 99.9+%, NMR grade (Aldrich Chemical Co., Milwaukee, WI) was included in trace amounts as the internal standard and chemical shifts (in ppm) were all downfield from the standard. NMR spectra were matched using a version of LAOCN3 program (115, 116) on an IBM 370/158 computer.

Infrared Analyses. The infrared spectrum was obtained on a Digilab FTS-2DC interfaced to a Data general NOVA 3/12 (Digilab Inc., Cambridge, MA). Three hundred scans were collected at a 4 cm^{-1} resolution. A background spectrum of a window without sample was subtracted from the sample spectrum.

Results

Separation of Incubation Extracts by HPLC

The HPLC product profile of extracts generated from three 25 ml incubations containing retinoic acid, H_2O_2 and horseradish peroxidase is shown in Figure 20. The incubation extracts were first chromatographed on a Partisil M9 column in 70% methanol and 30% water at approximately 1.4 ml per minute. This was done in order to partially resolve the extracts. At 128 min 100% methanol was injected to elute any remaining material from the column. The following fractions were

collected in individual round bottom flasks: fraction 1 from 40 to 60 min; fraction 2 from 60 to 70 min; fraction 3 from 70 to 95 min; fraction 4 from 95 to 105 min; fraction 5 from 105 to 118 min; fraction 6 from 133 to 140 min. The retention times of these fractions may be compared with those of incubation extracts chromatographed on two Partisil 10-ODS columns in series. In Figure 19-A fraction 1 eluted between 10 and 20 min, fraction 2 between 20 and 30 min, fraction 3 between 30 and 55 min, fraction 4 between 55 and 65 min, fraction 5 between 65 and 75 min and fraction 6 between 75 and 78 min.

Fractions 1, 2, 4, 5 and 6 collected from the Partisil M9 column were purified further by repeated chromatography on two Partisil 10-ODS columns in series, with a constant flow rate of approximately 0.5 ml per min. Fraction 3 contained many compounds present at low concentrations so that it was not purified further.

Purification and Identification of Peak 1

Fraction 1 eluting from the column (Partisil M9) between 40 and 60 min (Figure 20), contained the highest concentration of products. When they were chromatographed on the Partisil 10-ODS columns in 40% methanol and 60% water, the peak with the highest intensity at 254 nm and at 350 nm was named peak 1. It corresponded to the peak eluting off the same column at 19 min in Figure 19-A where the solvent concentrations were 60% methanol and 40% water. Peak 1 was collected and further purified by HPLC as shown in Figure 21 (40% CH_3OH, 60% H_2O) where it elutes at 38 min. The peak at 62 min corresponded to a gradient of increasing methanol concentration which was initiated at 50 minutes.

Peak 1 was formed by the decarboxylation of retinoic acid. This

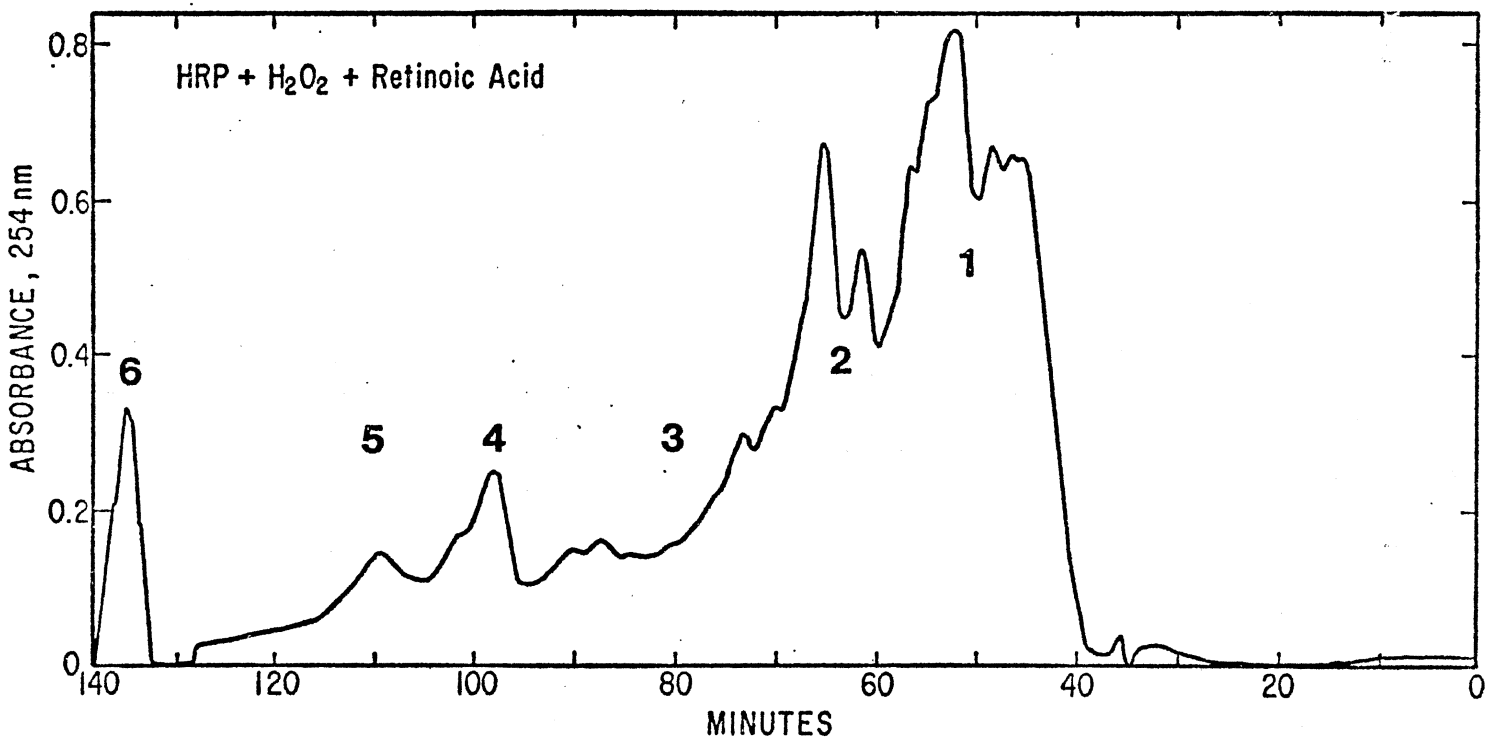

Figure 20. HPLC Profile of Products Generated from Incubations Containing Retinoic Acid, H_2O_2 and HRP on a Partisil M9 Column (70% methanol, 30% water at 1.4 ml per minute).

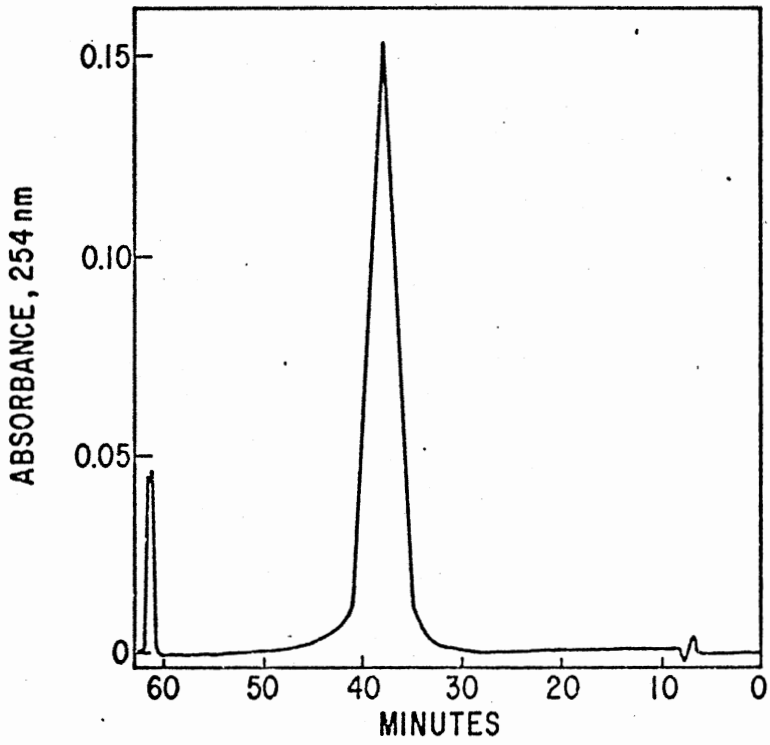

Figure 21. HPLC Profile of the Oxidative Decarboxylation Product Present in Peak 1. Chromatography was performed with two Partisil 10-ODS columns in series, in 40% methanol, 60% water at 0.5 ml per minute.

was shown by including purified all-trans-[15-^{14}C]retinoic acid (carboxyl labeled) and all-trans-[11,12-$^{3}H_2$]retinoic acid in the incubation. Although the ^{14}C to ^{3}H ratio of the retinoic acid was 1:1, the purified product contained ^{3}H but no ^{14}C.

A total of approximately 300 µg of pure peak 1 were obtained from 100 incubations containing 100 mg of retinoic acid. The pure compound was characterized and identified by ultraviolet absorbance, nuclear magnetic resonance, infrared and mass spectroscopy. The structure is shown in Figure 22. This product was identified as a 4-oxo-C_{19}-aldehyde with a hydroxyl group on the side chain at C_9, specifically 8-(2,6,6-trimethyl-3-oxo-cyclohex-1-enyl)-2,6-dimethyl-6-hydroxy-2,4,7-E-octatrienal.

The decarboxylation product had an absorption maximum of 280 nm (Figure 23), which represents a blue shift compared to the λ_{max} of 350 nm observed for retinoic acid. This shift is indicative of a decrease in conjugation. The extinction coefficient at 280 nm was 37,000 ± 4%. When the decarboxylation product was subjected to mass spectral analysis (Figure 24), it yielded a molecular ion of 302 and a base peak of 43, which is also the base peak in the mass spectra of many oxidized derivatives of retinoic acid (117). The ten most intense peaks of the spectrum are, in decreasing order, 43, 41, 95, 55, 69, 57, 259, 121, 109, 107, and are commonly found in the mass spectra of vitamin A analogs (117, 118). The ion at m/z 149 may be a fragment ion formed in the fragmentation of the oxidized compound (117) or it may be formed from a contaminant such as pthalate ester.

The proposed fragmentation pattern of peak 1 is shown in Figure 25. The molecular ion was found to dehydrate forming m/z 284 (M^+-18 (H_2O)),

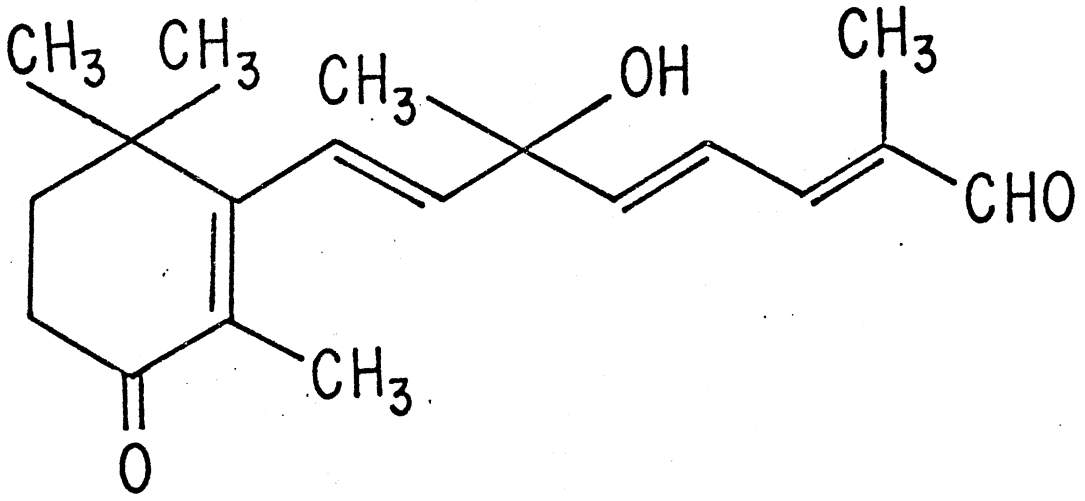

Figure 22. Structure of the Retinoid Purified from Peak 1

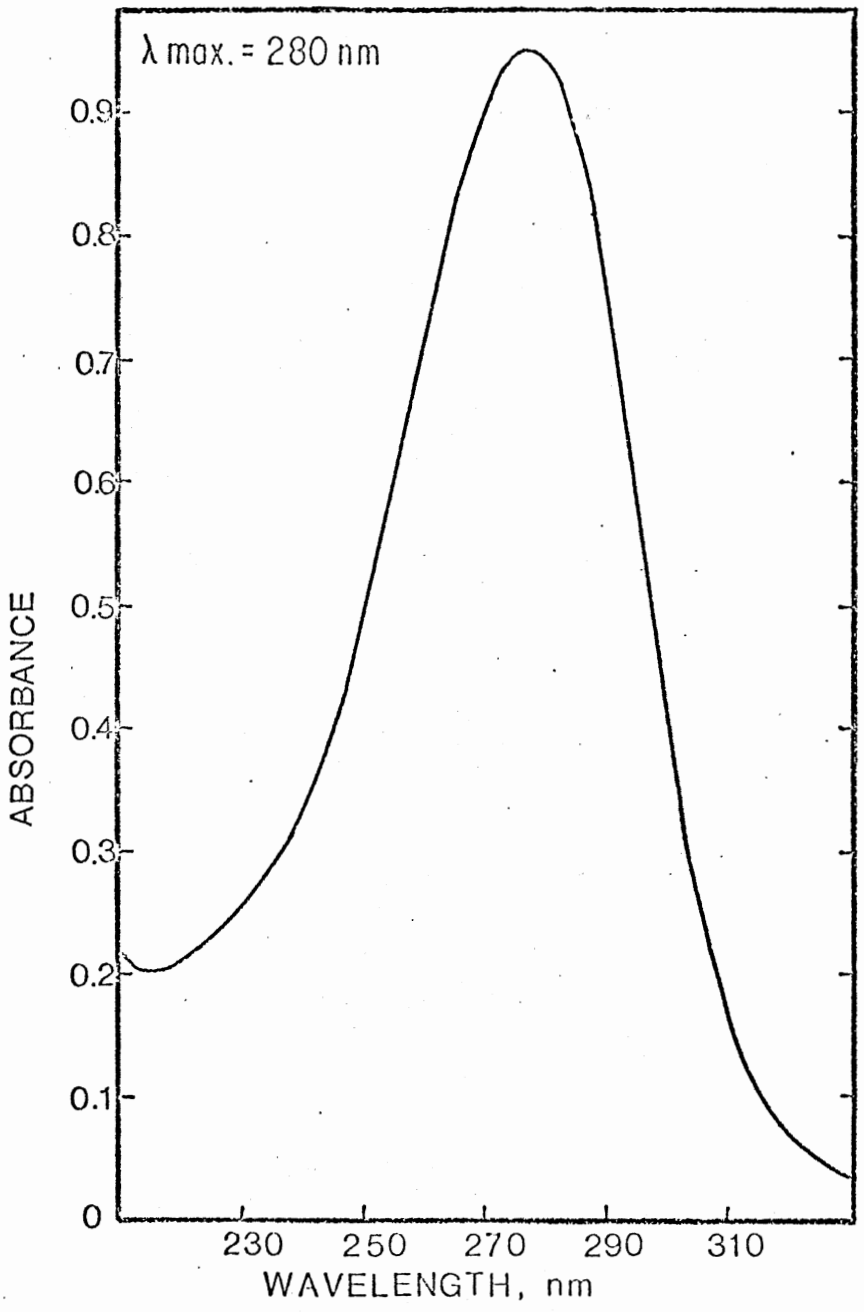

Figure 23. Absorption Spectrum of the Retinoid Purified from Peak 1

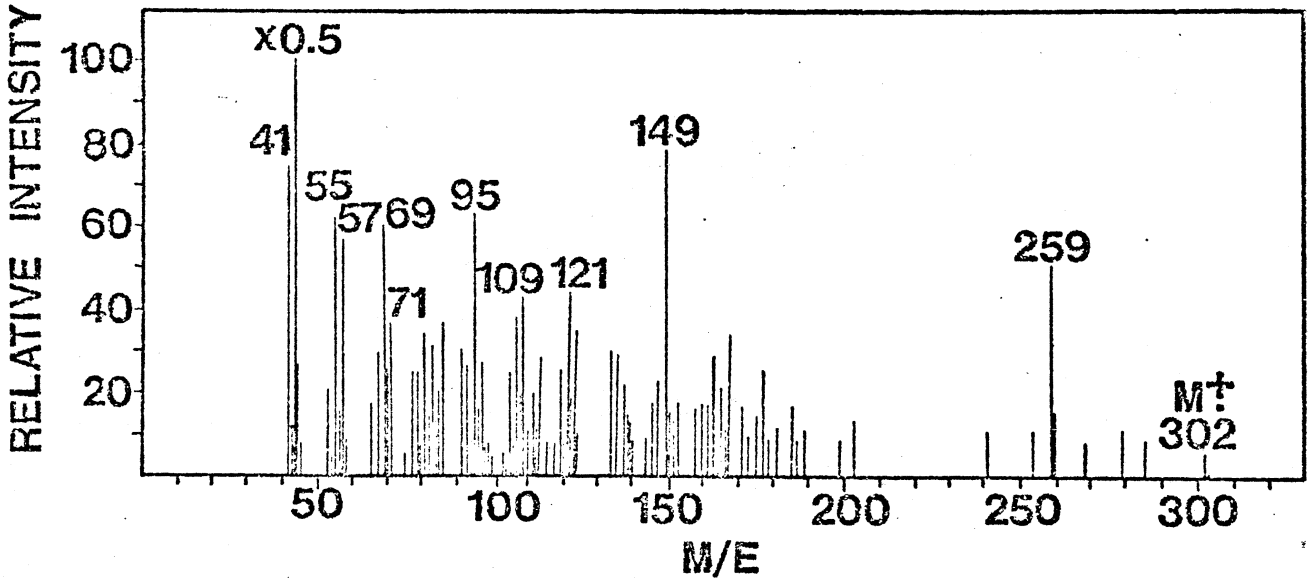

Figure 24. Mass Spectrum of the Retinoid from Peak 1

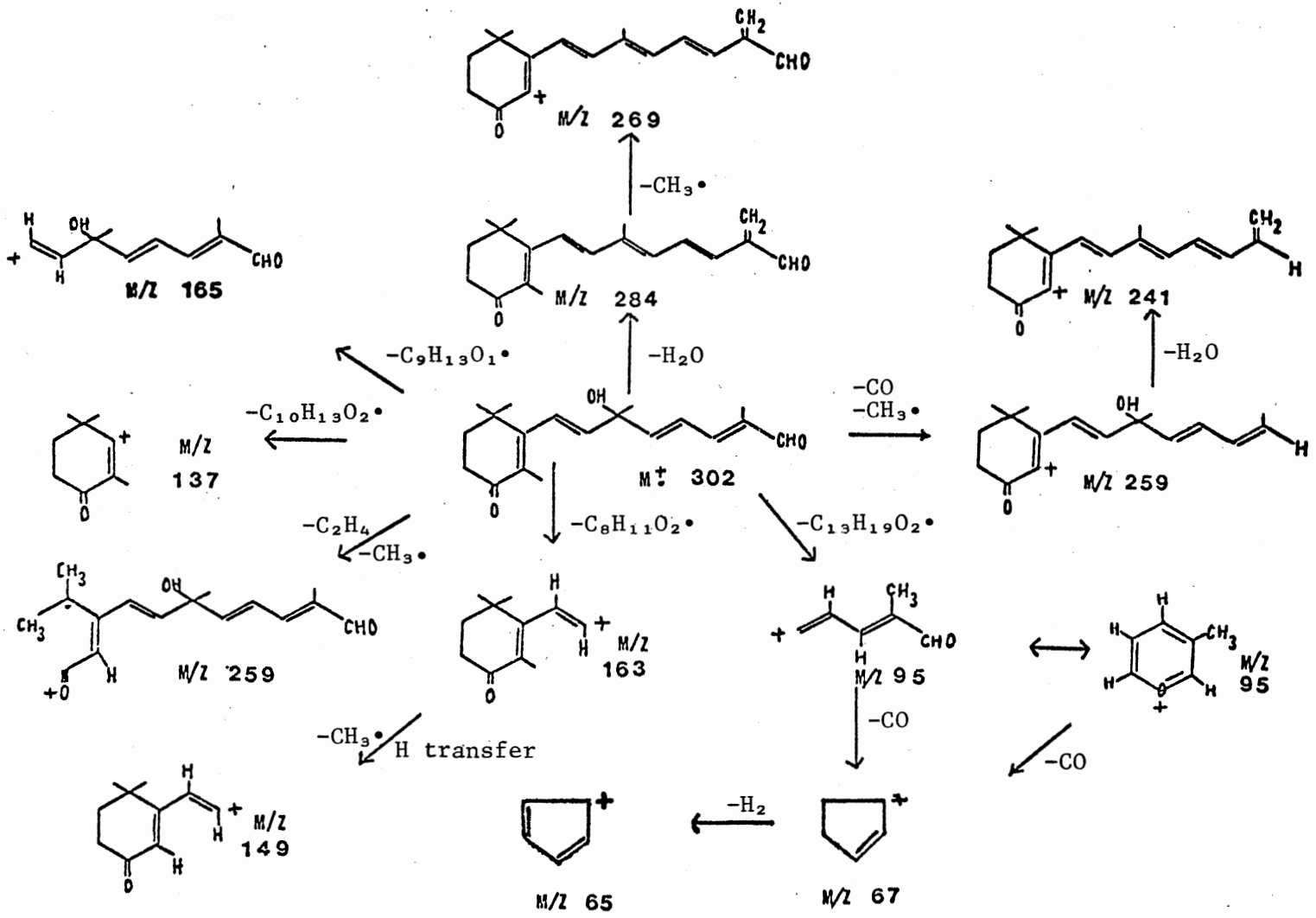

Figure 25. Fragmentation Pattern of the Retinoid from Peak 1

and to lose a functional group as well as a methyl group, m/z 259 (M^+-43 (CH_3, CO)), a pattern which is also found in the fragmentation of retinal (118). The methyl group, which was easily removed, was probably attached to the double bond in the ring at carbon 5, as demonstrated by the mass spectrum of β-ionone which was hexadeuterated at the gem-dimethyls on carbon 1 (119).

According to Enzell and Francis (120) cleavage of the 6,7 bond would be expected to occur with transfer of a hydrogen to the smaller ring fragment, which would then have a m/z of 138 as in canthaxanthin. They also indicated that a prominent M^+-56 peak should be detected and that this would be ascribed to an ion formed by loss of a C_4-C_5 fragment. Although the cyclic portion of canthaxanthin and peak 1 are the same, we did not observe prominent fragments with m/z 138 or M^+-56. Peak 1 seemed to fragment in a manner more analogous to β-ionone or retinoic acid, giving rise to fragment ions m/z 137 and 165. Loss of the $C_{13}O_2H_{19}$ radical led to the formation of m/z 95 which rearranged itself and lost CO to give rise to a furan m/z 67. Loss of H_2 then led to m/z 65 (121). Cleavage of the C_8-C_9 bond gave a fragment of m/z 163 which upon loss of the methyl at C_5 gave rise to m/z 149.

The fragmentation of the ring nucleus is shown in Figure 26. The fragment ion m/z 123 and 109 were both formed by loss of a methyl group followed by a hydrogen transfer, as in the ring nucleus of the β-ionone ring (102). Loss of 2 hydrogen atoms then led to the formation of an ion with m/z 107 (121, 122). As in the fragmentation of β-ionone, retro-Diels-Alder (RDA) reactions could occur resulting in the loss of ethylene to give m/z 137 → m/z 109; m/z 123 → m/z 95; m/z 109 → m/z 81 (102, 123).

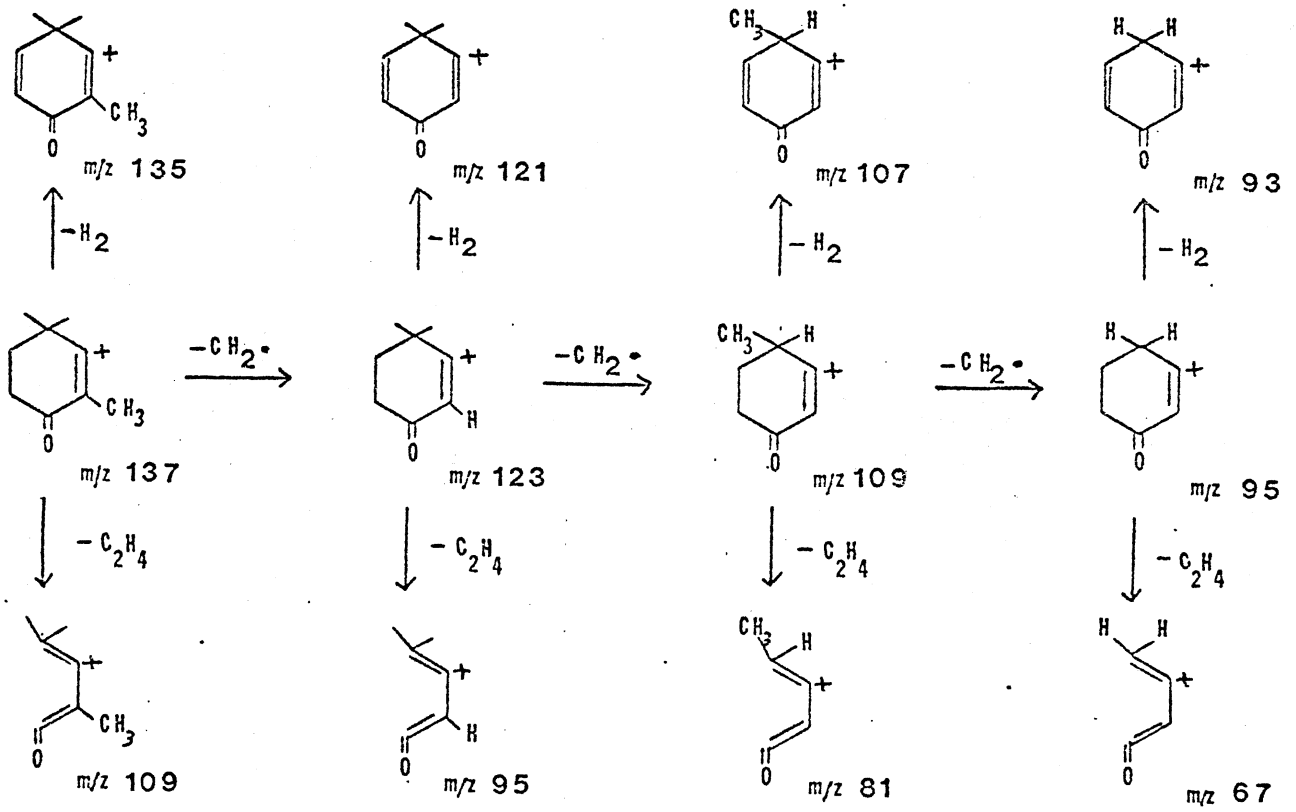

Figure 26. Fragmentation of Ring Nucleus of the Retinoid Purified from Peak 1

The NMR spectrum of the C_{19}-aldehyde is shown in Figure 27. The signal at 9.5 ppm down field from TMS is from an aldehyde proton. This aldehyde is probably trans since the proton signals of conjugated aldehydes with a methyl group at the α carbon usually appear at 9.2 to 9.7 ppm for trans compounds and at 10.0 to 10.3 ppm for cis compounds (124). There are five protons in the vinyl region (between 5.5 and 7.5 ppm), which are located on carbons 7, 8, 10, 11 and 12.

Singlets between 1 and 1.8 ppm were assigned to geminal methyls on carbon 1 and to methyl groups on carbons 5, 9 and 13. The signal at 1.16 ppm was assigned to protons on the gem dimethyls, based on the integration. This assignment is consistent with data in the literature. The chemical shift of the gem dimethyl protons in 4-oxoretinoic acid is 1.2 ppm (125), in 4-oxomethylretinoate is 1.9 ppm (87), in cantha-xanthin is 1.19 ppm (124) and in three urinary metabolites of retinoic acid in the rat, which all contained an oxo group at C_4, the chemical shift varied from 1.08 to 1.13 ppm (86).

The assignment of singlets at 1.50 and 1.74 ppm to methyl groups on carbons 5 and 9 respectively is not certain. There is the possibil-ity that the signal at 1.50 ppm is due to the methyl group at C_5. This is suggested by data from Hanni et al. (86) indicating that in the NMR spectrum of the urinary metabolite isolated from rat, 5-methyl-5-[2-(2,6,6-trimethyl-3-oxo-1-cyclohexen-1-yl)vinyl]-2-tetrahydrofuranone, the signal for CH_3 at C_5 appears at 1.77 ppm while that for CH_3 at C_9 appears at 1.58 ppm in $CDCl_3$. There is also disagreement as to the assignment of chemical shifts to methyl groups on carbons 5 and 9 in 4-oxoretinoic acid. While Surekha Rao et al. (125) assigned the shift at 2.04 ppm to the C_5 methyl group and at 1.8 ppm to the C_9 methyl,

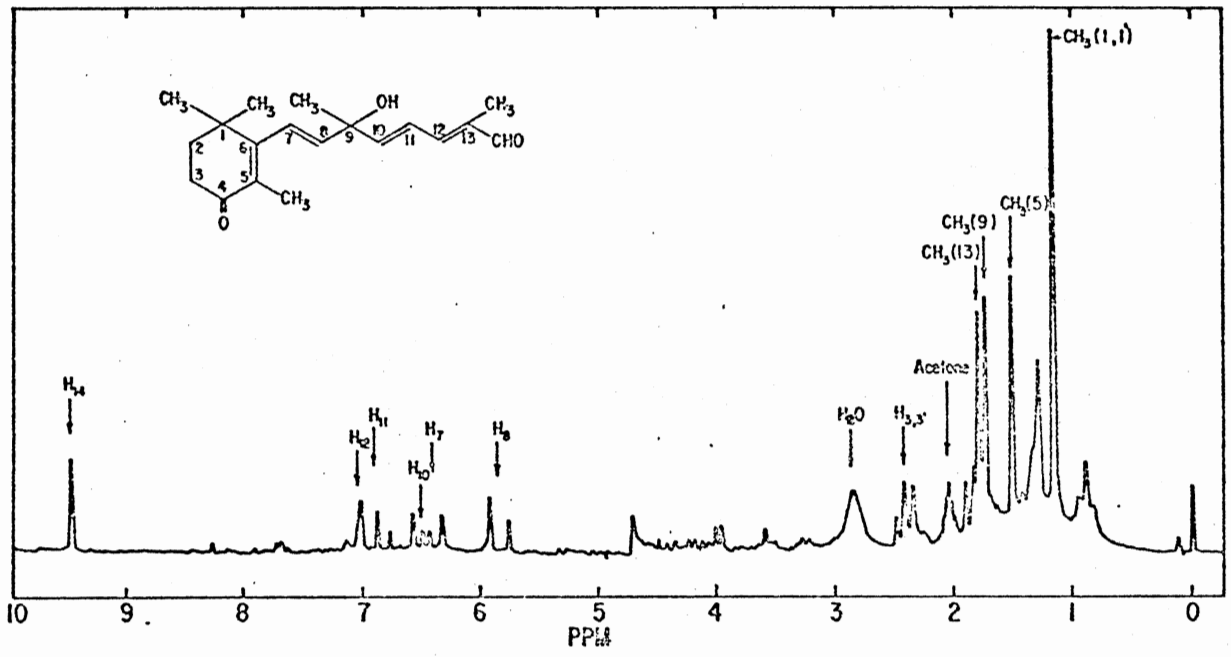

Figure 27. NMR Spectrum of the Retinoid from Peak 1

Hanni et al. (87) assigned them to methyls on C_9 and C_5, respectively.

The signal at 1.80 ppm was assigned to the methyl group at C_{13}. This is slightly upfield of the shift at 2.37 ppm reported for all-trans-methylretinoate (112), 4-oxoretinoate (87) and retinoic acid (113). This shift was probably due to the fact that there is less delocalization caused by a carbonyl two carbons removed from the center than by an acid group three carbons removed. The methyl group at C_{13} experienced greater shielding therefore in the 4-oxo-C_{19}-aldehyde.

The signal at 1.3 ppm is probably due to the methylene protons on carbon 2. The two-proton triplet at 2.4 ppm arises from the protons on carbon 3 adjacent to a keto function at carbon 4 (125, 126). The broad signal at 2.8 ppm arises from the proton on the hydroxyl group attached to carbon 9 as well as to protons on H_2O molecules present as contaminants in the deuteroacetone, or to hydroxyl protons originating from any residual methanol, which was the solvent used for routine storage of the sample. The signal at 0.9 ppm is probably due to the presence of an impurity since all the protons in the compound have been accounted for.

The vinyl region of the NMR spectrum between 5.5 and 7.5 ppm is expanded in the upper part of Figure 28, while a LAOCN3 generated spectrum produced by peak matching is drawn in the lower portion. Interpretation of this portion and of other parts of the NMR spectrum was greatly facilitated by the interpretation of NMR spectra generated from isomers of retinoic acid (112, 113).

The two spin transitions at 5.85 and 6.39 ppm form a pair of doublets with a spin-spin coupling constant of 16.2 Hz, indicative of a trans double bond. These transitions correspond to protons on

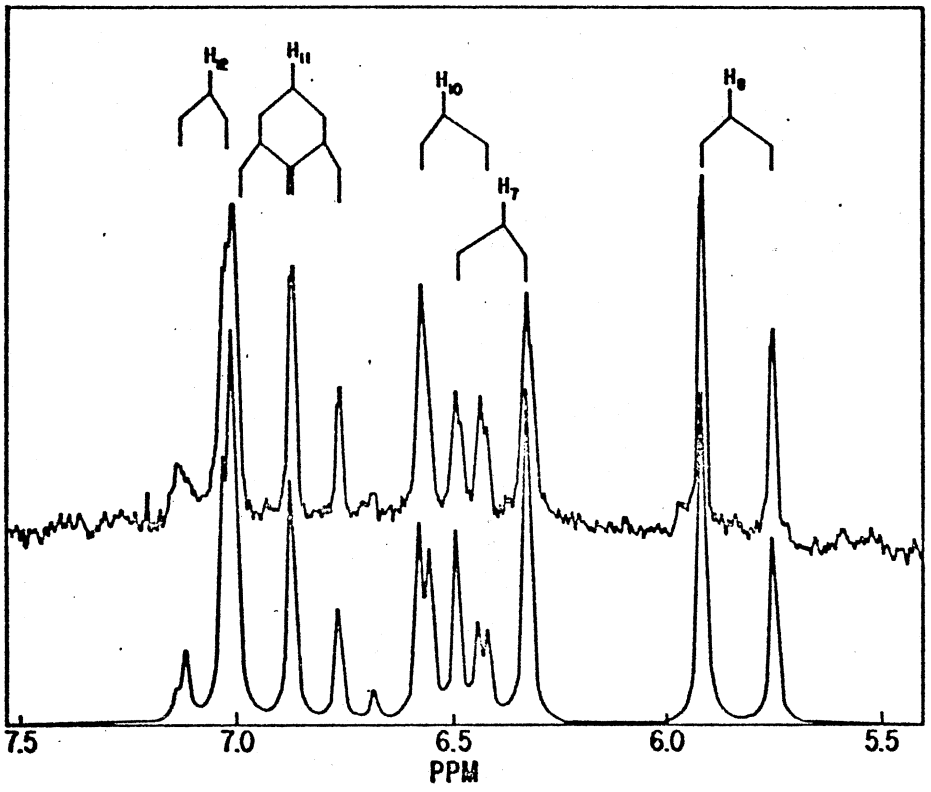

Figure 28. Vinyl Region of NMR Spectrum of the Retinoid from Peak 1

carbons 8 and 7 respectively, with the signals from H_7 being broader than those of H_8 due to long-range coupling. The remaining signals in the vinyl region were solved by LAOCN3 as an isolated system consisting of three protons and indicated that signals at 6.5, 6.88, and 7.03 ppm correspond to protons on carbons 10, 11 and 12 respectively. The coupling constants of 15.4 Hz and 11 Hz are indicative of a trans double bond between carbons 10 and 11 and a single bond between carbons 11 and 12 (113, 124).

The presence of the two carbonyl groups and the hydroxyl group in the decarboxylation product was further confirmed by Fourier transform infrared analysis (Figure 29). The hydroxyl group absorbs in a wide region from 3200 to 3600 cm^{-1}. The peaks at 1730 cm^{-1} and at 2720 cm^{-1} are attributable to the aldehyde on carbon 14 while the peak at 1672 cm^{-1} is consistent with the presence of a conjugated ketone on carbon 4 of the ring (125). The loss of conjugation in the decarboxylated compound is confirmed by a shift to higher wavenumber in the absorbance of the double bonds (at 1600 cm^{-1} and at 1640 cm^{-1}) compared with retinoic acid (at 1578 cm^{-1} and at 1600 cm^{-1}). Further band assignments are made in Chapter IV.

Purification and Identification of Peak 2

Fraction 2, eluting from the Partisil M9 column (Figure 20) between 60 and 70 min, was purified on the Partisil 10-ODS columns at 50% methanol, 50% water (Figure 30-A). A baseline resolved compound, peak 2, eluted at 60 min and corresponds to the peak at 65 min in Figure 20 or at 28 min in Figure 19-A. The absorption spectrum revealed the same λ_{max} as for peak 1, namely 280 nm (Figure 30-B) indicative of a decrease

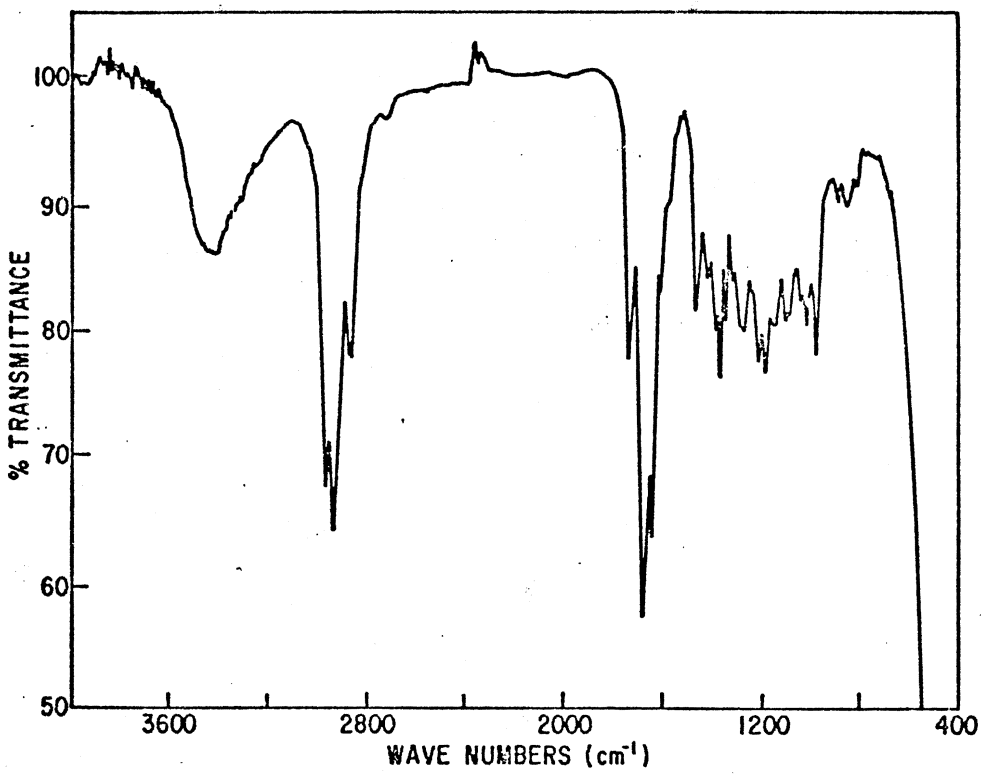

Figure 29. Infrared Spectrum of the Retinoid from Peak 1

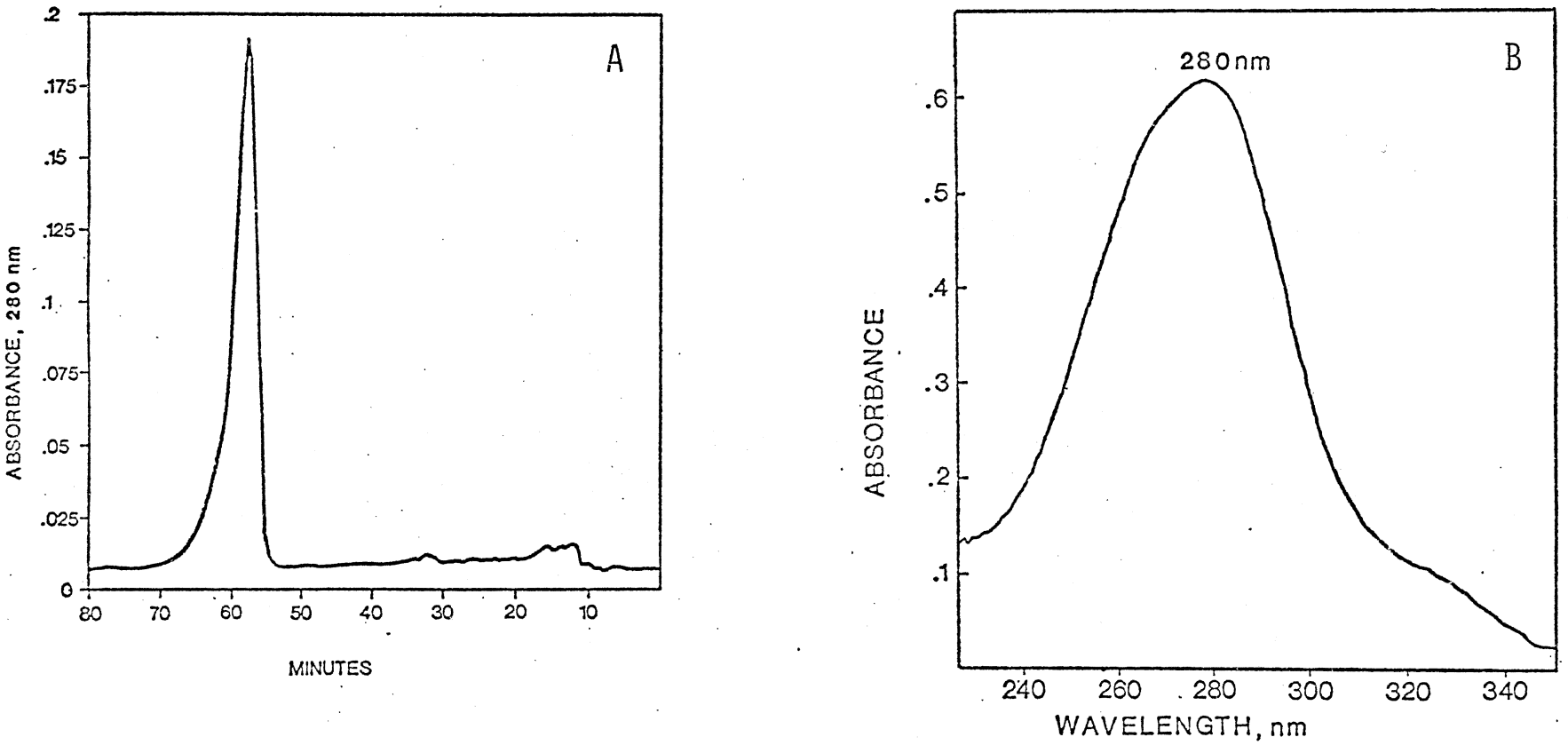

Figure 30. HPLC Profile (A) and Absorption Spectrum (B) of the Retinoid Isolated from Peak 2. Chromatography was performed with two Partisil 10-ODS columns in series, in 50% methanol, 50% water at 0.5 ml per minute.

in conjugation compared with the λ_{max} of 350 nm for retinoic acid. The extinction coefficient was calculated to be 27,000 ± 5%. When incubations contained [11,12-$^{3}H_2$] and [15-^{14}C]retinoic acid (dpm ^{3}H/dpm ^{14}C equal to one), ^{3}H but no ^{14}C was present in peak 2. Thus the carboxyl group of retinoic acid was removed in the formation of this compound.

Approximately 35 µg of purified peak 2 were obtained from 100 incubations containing a total of 100 mg of retinoic acid. This represents one tenth the amount of peak 1, described above. When peak 2 was subjected to mass spectral analysis (Figure 31), it yielded a molecular ion of 316, with a base peak of 43, which is also the base peak of peak 1 and of other oxidized derivatives of retinoic acid (117). The ten most intense peaks of the spectrum are in decreasing order 43, 41, 149, 284, 59, 55, 91, 95, 69 and 77. All but 284 are commonly found in the mass spectra of vitamin A analogs (117, 118). The nuclear magnetic resonance spectrum of peak 2 (Figure 32) showed many similarities with that of peak 1 (Figure 27). There are five protons in the vinyl region between 5.5 and 7.5 ppm. The signal at 9.49 ppm downfield from TMS is from a proton on a trans-α-methyl substituted conjugated aldehyde (124).

The signals between 0 and 2.5 ppm are identical in the spectra of peaks 1 and 2, with the exception of a slight amount of splitting in the singlets attributed to methyl protons on carbon 9 and 13 (at 1.75 and 1.80 ppm). This is due to long-range coupling to protons on carbons 10 and 12 respectively. The fact that these signals are split, while the corresponding ones for peak 1 are not, can be attributed to increased resolution in the NMR spectrum of peak 2 as evidenced by the greater resolution of the deuteroacetone peak at 2.05 ppm. The broad

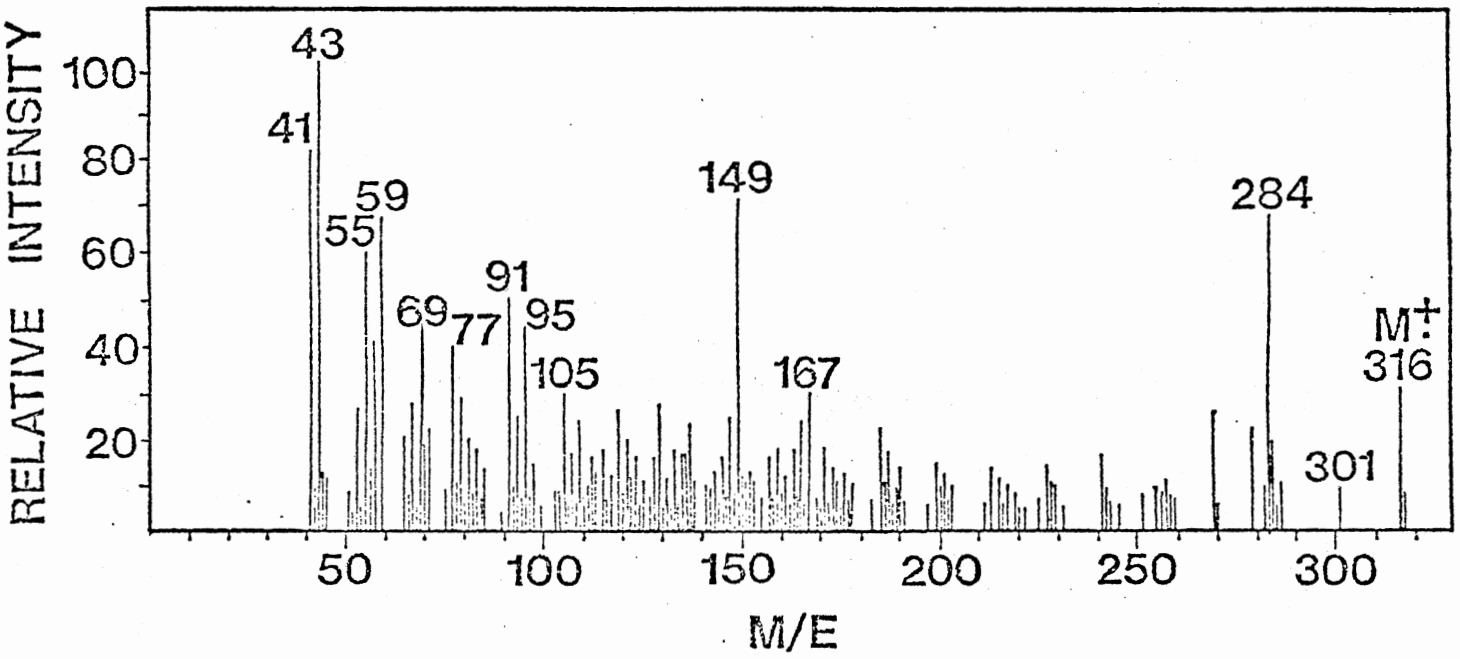

Figure 31. Mass Spectrum of the Retinoid from Peak 2

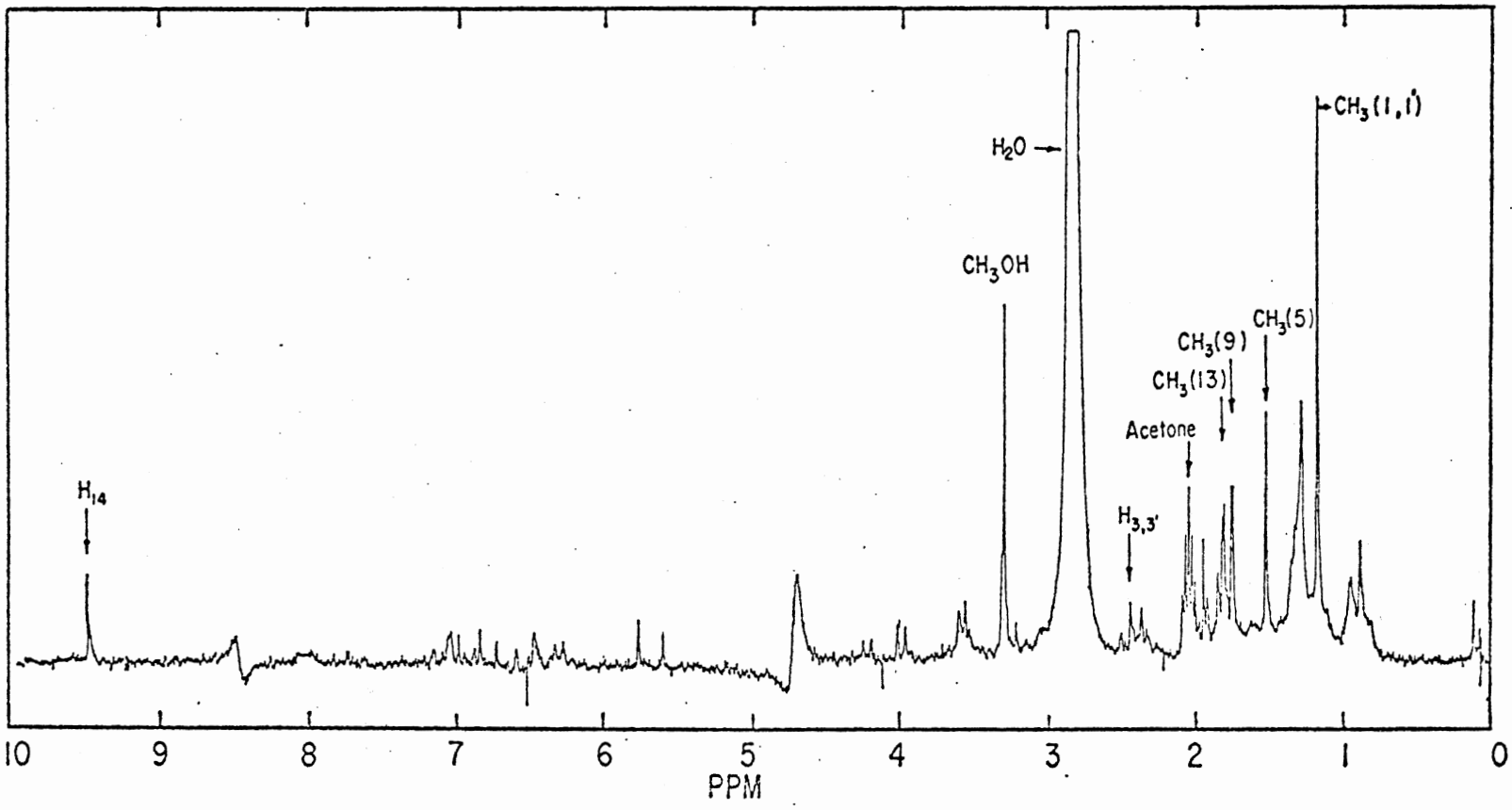

Figure 32. NMR Spectrum of the Retinoid from Peak 2

signal at 2.8 ppm arose from protons on water molecules present in the deuteroacetone solvent. The signal at 3.3 ppm is attributable to the presence of trace amounts of methanol in the sample (127). Since the NMR spectrum of this sample is identical with that of peak 1 in the region containing signals from methylene and methyl protons, it can be inferred that the ring portion of the molecule is the same for both compounds and that methyl groups at carbons 1, 5, 9 and 13 are not substituted.

The vinyl region of the NMR spectrum between 5.4 and 7.3 ppm is expanded in the upper part of Figure 33 while a LAOCN3 generated spectrum produced by peak matching is drawn in the lower portion. The limited quantity of peak 2 did not allow for good resolution of this region. Peaks with a cross were found to be contaminants from the solvent since they were present in the NMR spectrum of a sample of deuteroacetone. This portion of the NMR spectrum shows a remarkable similarity to that of the vinyl region of the NMR spectrum of peak 1 (Figure 28) and it could be inferred that the side chain of the two molecules are similar, with <u>trans</u> double bonds between carbons 7 and 8, 10 and 11, 12 and 13.

Signals at 5.68, 6.33, 6.40, 6.84 and 7.06 ppm were attributed to protons on carbons 8, 7, 10, 11 and 12 respectively. Chemical shifts for protons on carbons 7, 11 and 12 varied slightly compared with those for peak 1. Differences were found to be 6 Hz for H_7, 4 Hz for H_{11} and 3 Hz for H_{12} and could be accounted for by the greater amount of contaminating water present in peak 2 or by differences in temperature when the samples were run. The signals on carbons 8 and 10 are shifted upfield compared with those for peak 1. Differences are on the order

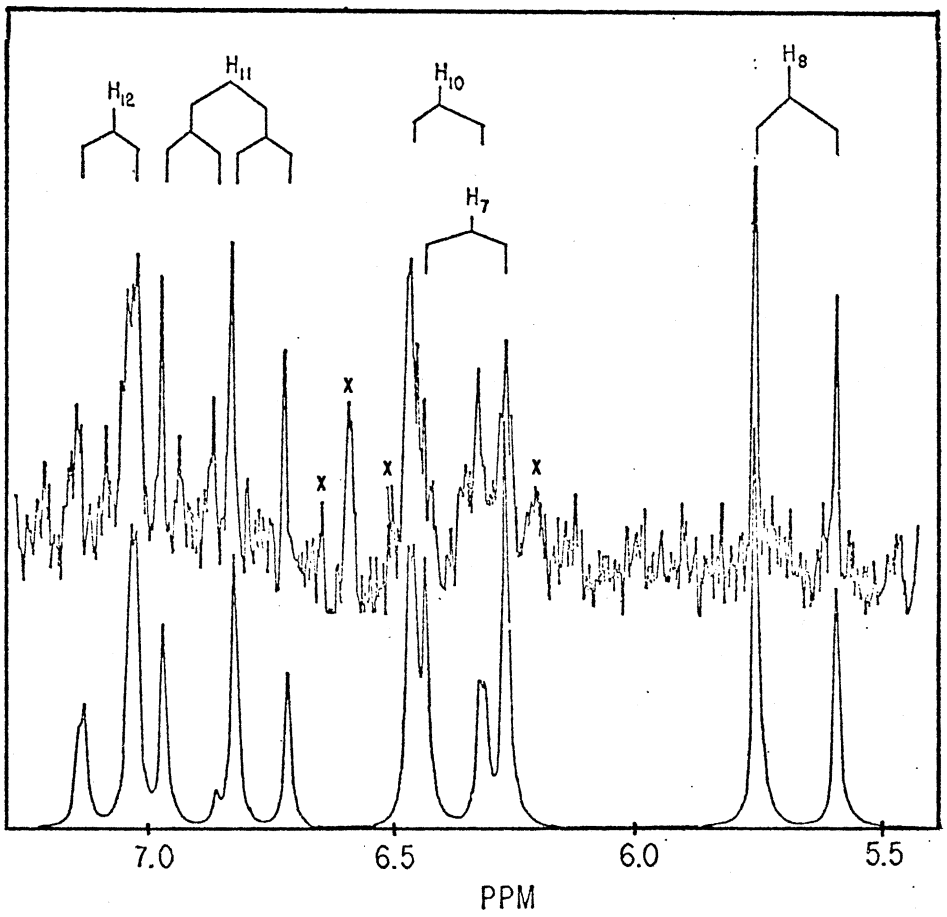

Figure 33. Vinyl Region of NMR Spectrum of the Retinoid from Peak 2

of 17 Hz for H_8 and 10 Hz for H_{10}. These are probably related to the identity of group X on carbon 9, whose presence is necessary to account for the conjugation in the side chain suggested by the NMR data.

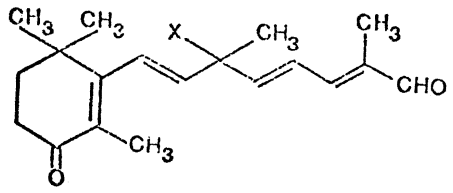

The coupling constant of 16.6 Hz between protons on carbons 7 and 8 and 15.4 Hz between protons on carbons 10 and 11 were indicative of trans double bonds. An 11 Hz coupling constant between protons on carbons 11 and 12 confirmed the presence of a single bond (113, 124).

The identity of group X could not be definitively ascertained, based on the data presently available. The infrared spectra obtained were not helpful due to the small quantities of compound remaining when the scans were performed. The absorption maximum of 280 nm obtained for both peaks 1 and 2 indicated similar amounts of conjugation in accord with the NMR data. The mass spectra data were difficult to reconcile with the NMR data. The molecular ion of 316 is consistent with the formula $C_{19}H_{24}O_4$ which could not be reconciled with the structure of the side chain reflected by the vinyl region of the NMR spectrum. Based on the mass spectral data, the formation of a five-membered endo-peroxide ring was suggested in order to account for the molecular formula. This could involve carbons 9, 10 and 11 or 7, 8 and 9. An endoperoxide ring involving carbon 13 was discounted since the NMR signal for the aldehyde proton clearly indicated the presence of a trans-α-methyl substituted conjugated aldehyde. The presence of an

endoperoxide linkage anywhere in the ring portion was also discounted since the upfield region of the NMR spectrum of peak 2 is clearly identical with that of peak 1. Based on the mass spectral data therefore, structures such as those shown in Figure 34 (top, bottom) were suggested for the compound in peak 2.

The structure suggested based on the NMR data is shown in Figure 34 (middle) and is a 4-oxo-C_{19}-aldehyde with a peroxy group on the side chain, specifically 8-(2,6,6-trimethyl-3-oxo-cyclohex-1-enyl)-2,6-dimethyl-6-peroxy-2,4,7-E-octatrienal. This would lead to a molecular ion of 318. The existence of a hydroperoxy group and of an endoperoxide has been shown in the synthesis of prostaglandins (128). Lipid hydroperoxides have also been prepared and purified from arachidonic acid and γ-linolenic acid (129). The structure suggested based on the NMR data was preferred since it would be a more stable compound than the endoperoxide (128).

Purification of Peaks 4 and 5

Fractions 4 and 5 (Figure 20) were purified separately on Partisil 10-ODS columns at 0.5 ml per min. In Figure 35-A, the HPLC profile of peak 4 is shown. Peak 4 was chromatographed at 55% methanol and 45% water and collected between 60 and 70 min after injection on the column. The peak at 90 minutes corresponded to a gradient of increasing methanol concentration which was initiated at 80 min. It had a λ_{max} of 350 nm as well as 280 nm (Figure 35-B). The extinction coefficient at 350 nm was 60,000 ± 1%. Incubations performed in the presence of retinoic acid labeled with tritium at C_{11} and C_{12} and with ^{14}C at C_{15} (^{3}H:^{14}C = 1) led to the isolation of peak 4 with a ratio of ^{3}H to ^{14}C

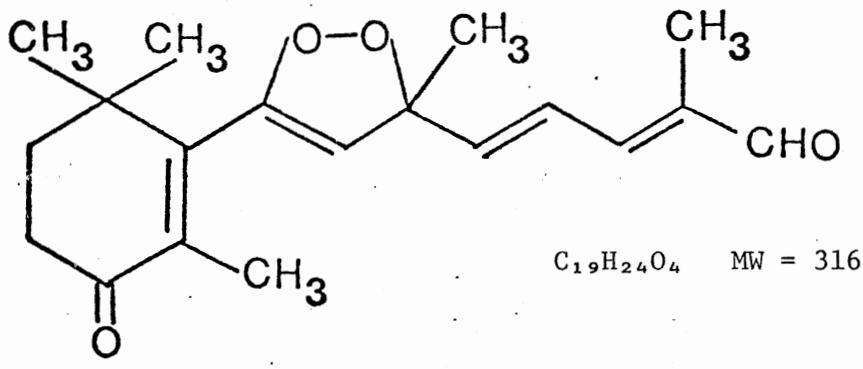

$C_{19}H_{24}O_4$ MW = 316

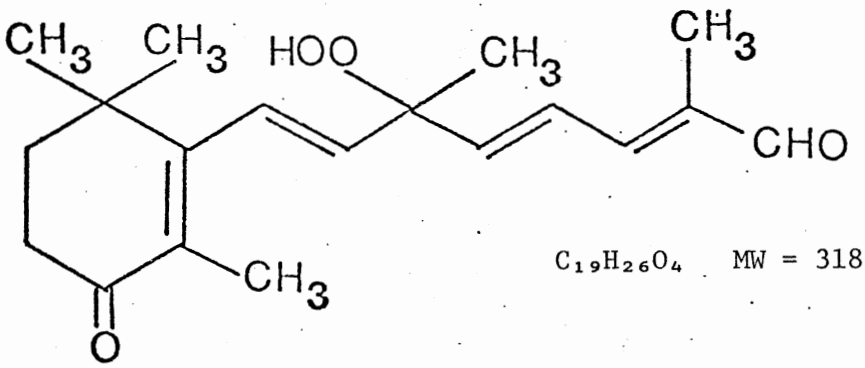

$C_{19}H_{26}O_4$ MW = 318

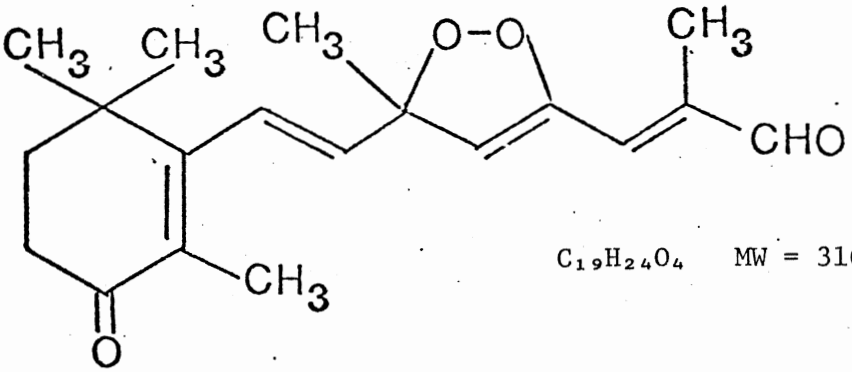

$C_{19}H_{24}O_4$ MW = 316

Figure 34. Proposed Structures for the Retinoid Isolated from Peak 2

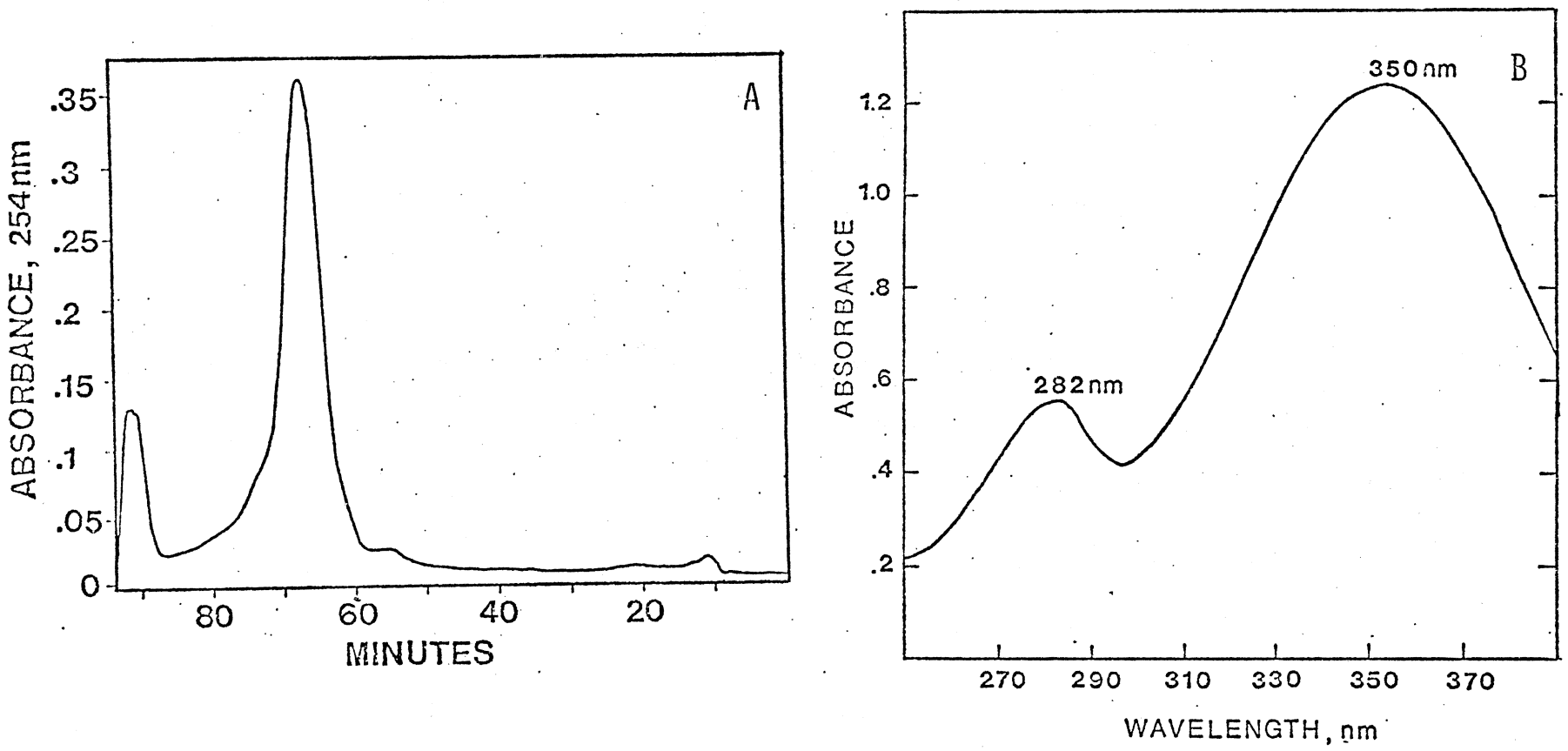

Figure 35. HPLC Profile (A) and Absorption Spectrum (B) of the Retinoid Isolated from Peak 4. Chromatography was performed with two Partisil 10-ODS columns in series, in 55% methanol, 45% water at 0.5 ml per minute.

of 0.65. This indicates the loss of ^{3}H in the formation of this compound. A total of approximately 19 µg of peak 4 was obtained from 100 incubations containing 100 mg of substrate. This amount was too small to obtain useful NMR or IR data but a mass spectrum (Figure 36) revealed a mass ion of 300 and a base peak of 43.

Peak 5 was purified at 60% methanol and 40% water (Figure 37-A), eluting between 37 to 55 minutes. Approximately 150 µg of compound were obtained from 100 incubations. The ^{3}H to ^{14}C ratio was identical with that of the starting material indicating no loss of label from the starting material in the formation of peak 5. The absorption spectrum had a λ_{max} of 300 nm and the extinction coefficient was 30,000 ± 3% (Figure 37-B). As in the case of peak 4, the mass spectrum revealed a mass ion of 300 (Figure 38).

Purification and Identification of Peak 6

Fraction 6 in Figure 20 was eluted when 100% methanol was injected on the column. It contained only one peak when chromatographed in 70% methanol and 30% water at 0.8 ml per min (Figure 39-A). The mass spectrum of this peak was identical with that of the starting material, all-trans-retinoic acid (Figure 40). The λ_{max} of the compound was found to be 337 nm (Figure 39-B). However, in the presence of trace amounts of HCl, the maximum was shifted to 350 nm, as reported by Robeson et al. (130) for all-trans-retinoic acid.

Discussion

The oxidative decarboxylation of retinoic acid was investigated utilizing a model system consisting of all-trans-retinoic acid, H_2O_2

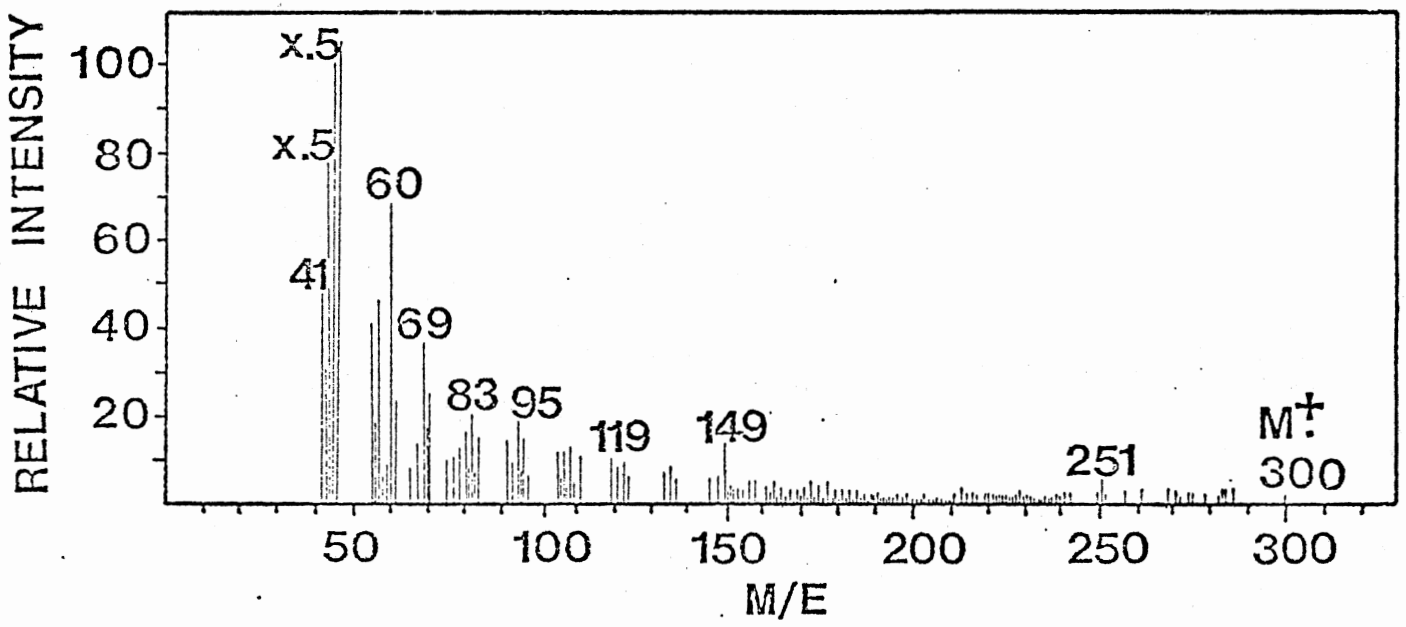

Figure 36. Mass Spectrum of the Retinoid from Peak 4

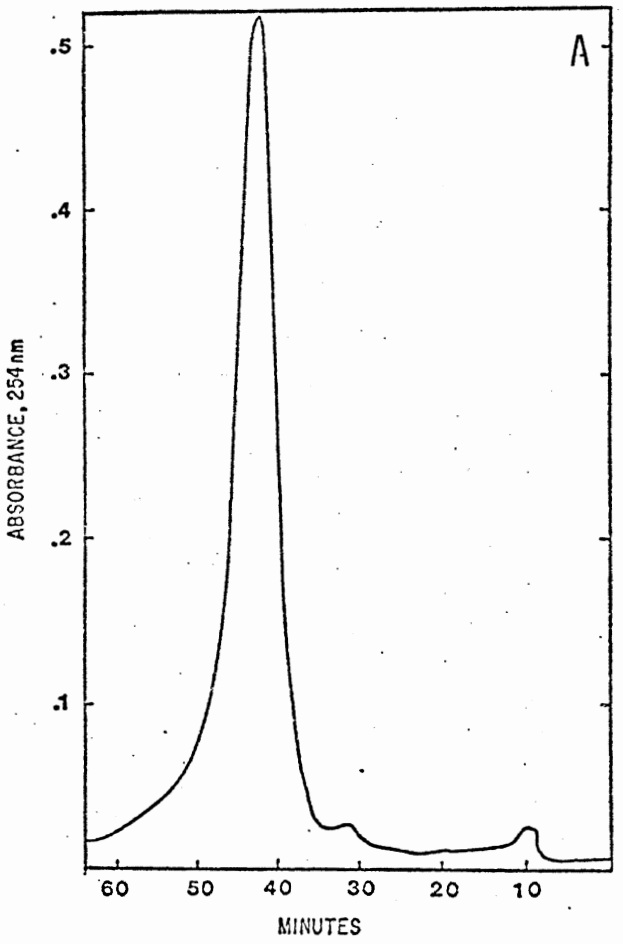

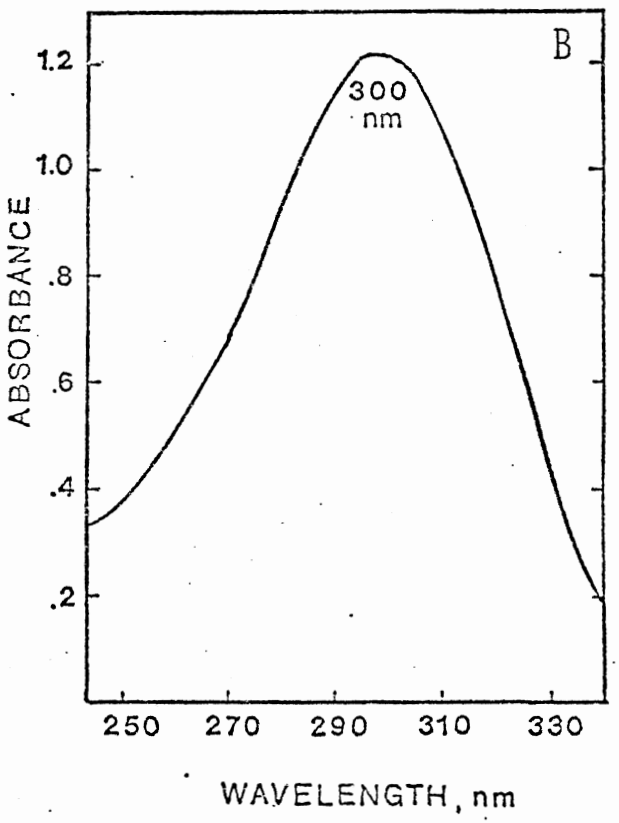

Figure 37. HPLC Profile (A) and Absorption Spectrum (B) of the Retinoid from Peak 5. Chromatography was performed with two Partisil 10-ODS columns in series, in 60% methanol, 40% water at 0.5 ml per minute.

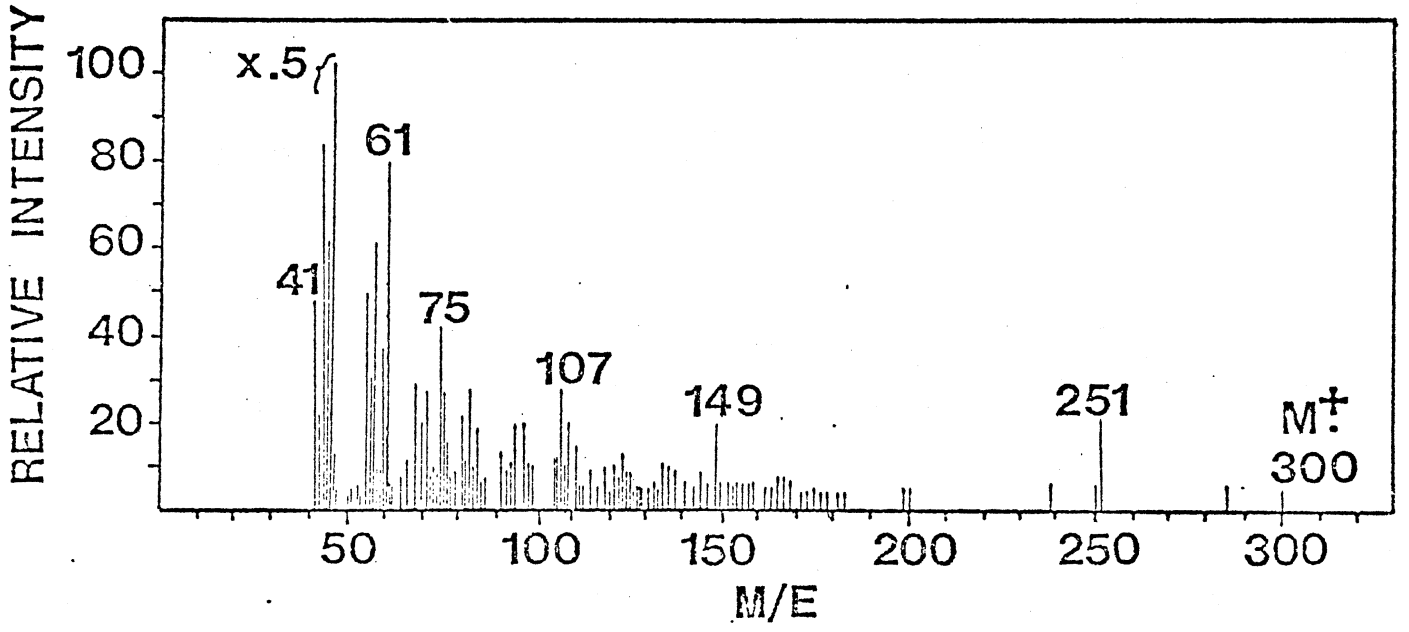

Figure 38. Mass Spectrum of the Retinoid from Peak 5

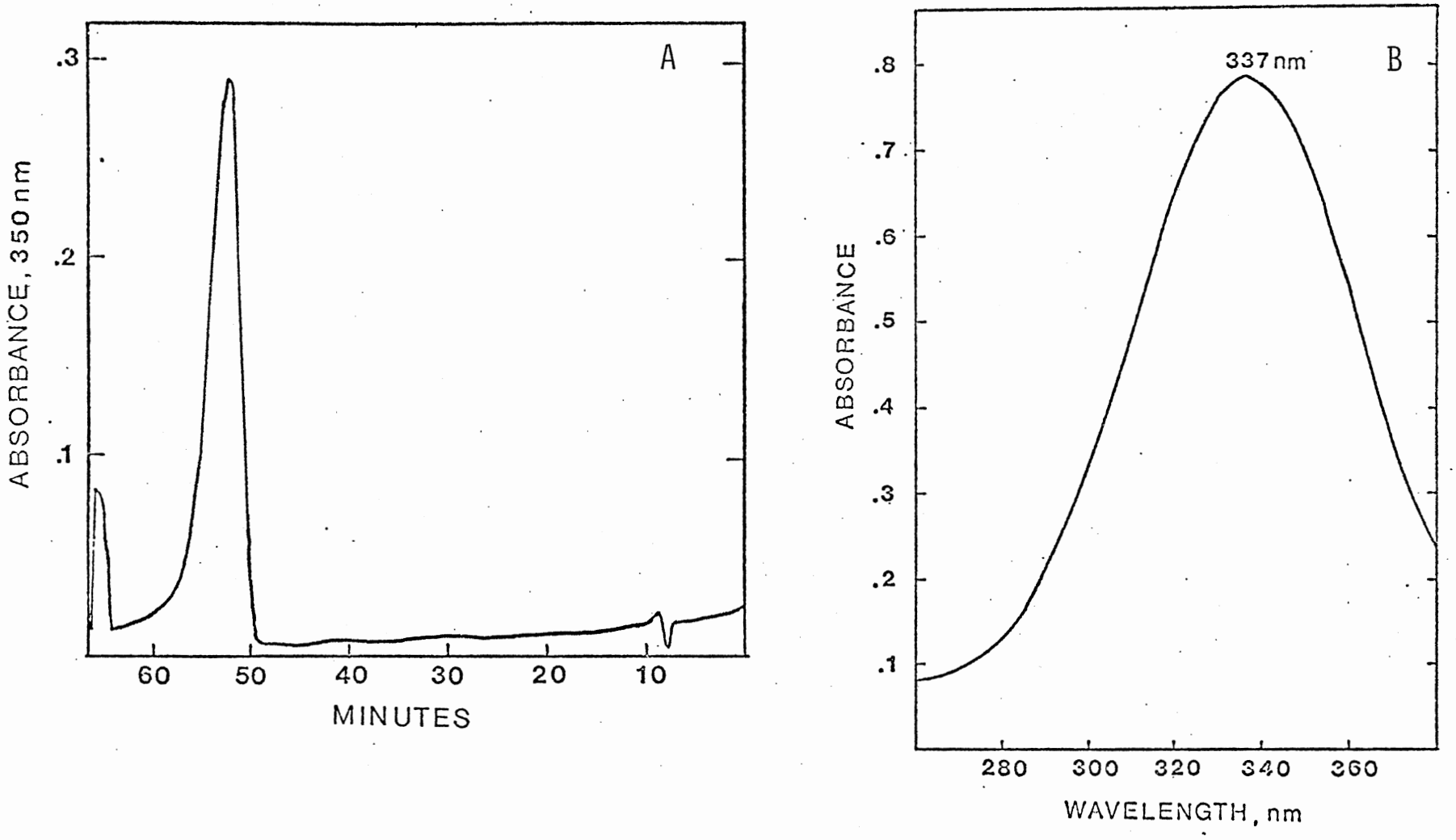

Figure 39. HPLC Profile (A) and Absorption Spectrum (B) of the Retinoid from Peak 6. Chromatography was performed with two Partisil 10-ODS columns in series, in 70% methanol, 30% water at 0.8 ml per minute.

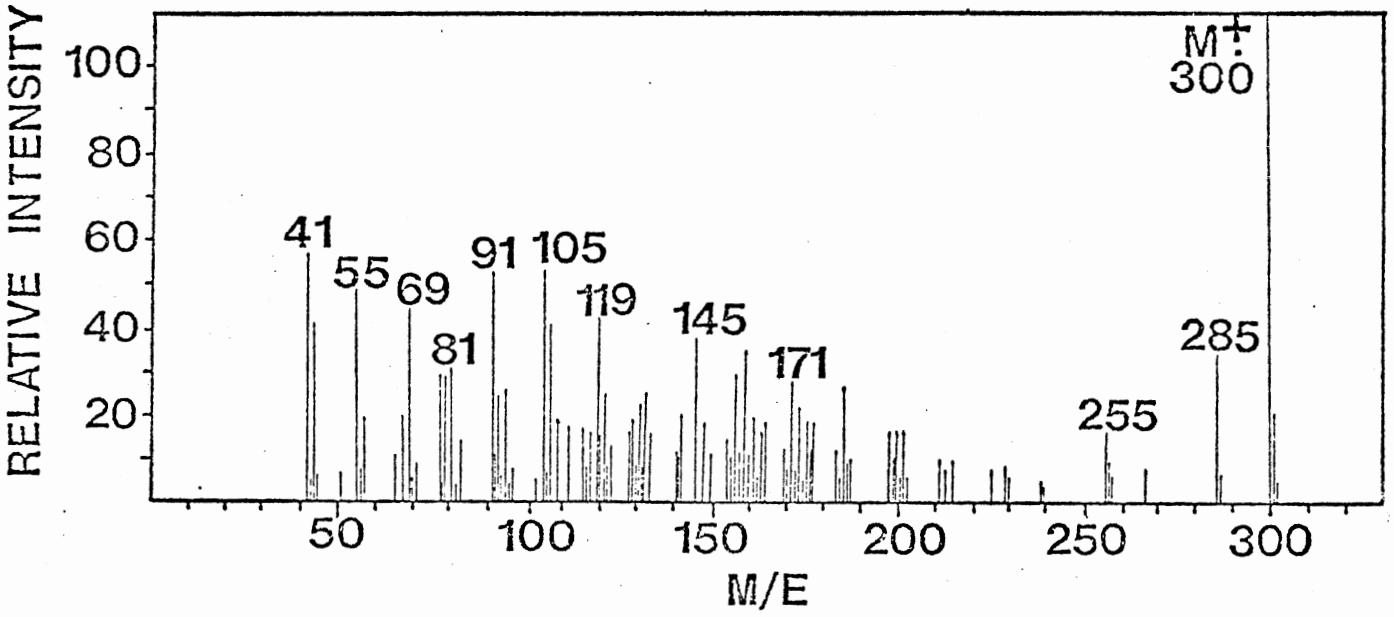

Figure 40. Mass Spectrum of the Retinoid from Peak 6

and horseradish peroxidase, as described in Chapter II. The decarboxylation products were purified by high performance liquid chromatography on bonded, octadecylsilane columns. Based on mass spectral, NMR, UV and FT-IR analyses, the major decarboxylation product or peak 1 was identified as a 4-oxo-C_{19}-aldehyde with the hydroxyl group on the side chain at C_9, specifically 8-(2,6,6-trimethyl-3-oxocyclohex-1-enyl)-2,6-dimethyl-6-hydroxy-2,4,7-E-octatrienal.

The oxidation of retinoic acid on the side chain and at C_4 in the ring has been observed by other investigators. For example, 4-oxo-retinoic acid has been identified as a metabolite of retinoic acid incubated with hamster liver or trachea (93) and it has been hypothesized that the major pathway of retinoic acid metabolism in hamster liver microsomes follows the scheme retinoic acid → 4-hydroxyretinoic acid → 4-oxoretinoic acid → more polar metabolites. The presence of several oxidized metabolites, including 4-oxoretinoic acid and several metabolites hydroxylated at various positions, has been detected in rat urine and feces (86, 87). 5,8-Epoxyretinoic acid has been reported as a metabolite of retinoic acid (91), although it has also been identified as a major impurity of samples of ^{3}H- and ^{14}C-labeled all-trans-retinoic acid (92). Retinoic acid is also thought to be metabolized to a hydroxylated derivative which becomes phosphorylated, linked with mannose, and subsequently leads to the formation of a mannoglycoprotein (51).

A possible mechanism in the production of the major decarboxylation product of retinoic acid is shown in Figure 41. Oxidation at carbon 14 would lead to decarboxylation followed by the addition of a proton from the medium. Tautomerization would then occur followed by oxidation at

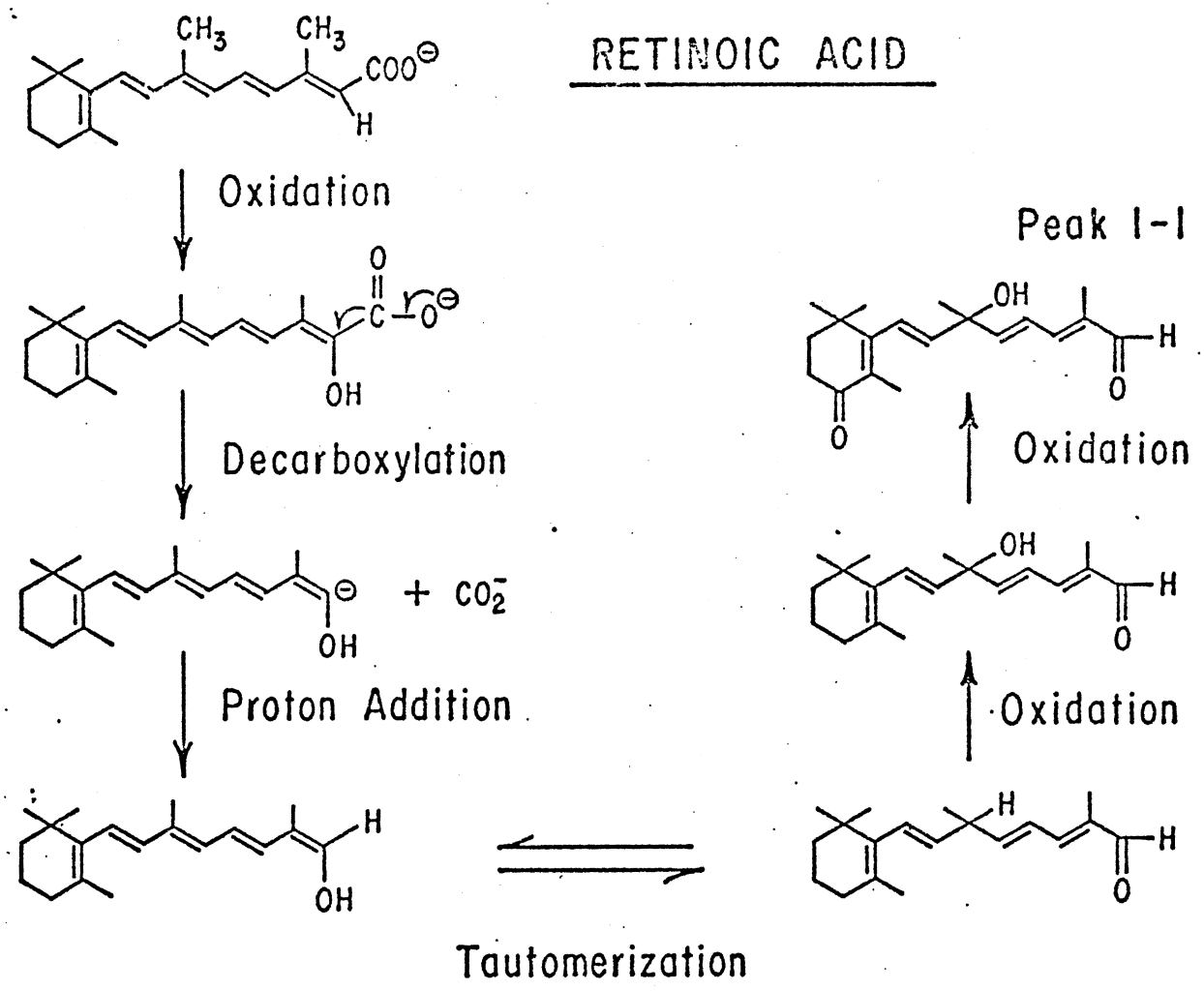

Figure 41. Postulated Pathway for the Formation of the Major Oxidative Decarboxylation Product

carbon 9 and at carbon 4 in the ring. It is also possible that this compound is first oxidized at C_4 on the ring, and subsequently decarboxylated. This would be consistent with a scheme previously suggested (93). Unless intermediates in the reaction are isolated and identified, the mechanism in Figure 41 can only remain a hypothesis.

Tentative structures were suggested for another decarboxylated product, peak 2. This compound was produced in much smaller quantities than peak 1 (one tenth) and was more difficult to identify. A definitive identification will be obtained only with the production of much higher quantities of peak 2.

Peaks 4 and 5 were not decarboxylated products of retinoic acid, as determined by labeling studies. Both of these compounds retained the ^{14}C label on the carboxyl terminal. As in the case of peak 2, the elucidation of the structures of these minor products can only be accomplished by the successful production of larger quantities of material. In spite of the fact that they have the same molecular weight, these compounds are not cis-trans isomers of retinoic acid. The high performance liquid chromatography profiles indicate that they are more polar than the retinoic acid isomers and the mass spectral patterns indicate that they are not fragmented in the same way as retinoic acid and its isomers.

Peak 6 was found to be identical with the starting material all-trans-retinoic acid.

A summary of the Abs_{max}, mass ion, $^{3}H/^{14}C$ and extinction coefficient data peaks 1, 2, 4 and 5 are given in Table V.

TABLE V

SUMMARY OF ABS_{MAX}, MASS ION, $^{3}H/^{14}C$ RATIO AND EXTINCTION COEFFICIENT DATA OF OXIDATION AND DECARBOXYLATION PRODUCTS ISOLATED FROM PEAKS 1, 2, 4, 5

Peak	Abs_{max}	Mass Ion	$^{3}H/^{14}C$	ε
1	280	302	∞	37,000 ± 4%
2	280	316	∞	27,000 ± 5%
4	350	300	0.65	60,000 ± 1%
5	300	300	1.0	30,000 ± 3%

CHAPTER IV

INFRARED SPECTROSCOPY OF RETINOIDS

Although the metabolism of retinoic acid has been under investigation for the last two decades, this search has revealed only a few compounds. Furthermore the physiological importance and mode of production of these compounds *in vivo* remain to be ascertained (25, 82-87, 90, 91, 93, 97). Along with mass spectrometry, ultraviolet absorbance and nuclear magnetic resonance spectroscopy, infrared spectroscopy is an important tool for the identification of metabolites of retinoic acid.

Infrared analyses have been reported for some of the vitamins A. Spectra for 9-*cis*-, 13-*cis*-, 9,13-*dicis*-retinol (130) and for all-*trans*-retinol (130-132) were the earliest to appear in the literature. Infrared data also were reported for all-*trans*- (132, 133), 9-*cis*-, 13-*cis*-, 9,13-*dicis*- (133) and 11-*cis*- (134) retinal, as well as for all-*trans*- (132, 135), 9-*cis*-, 11-*cis*-, 13-*cis*- and 11,13-*dicis*-vitamin A_2 alcohols (135). Vitamin A esters have also been analyzed by infrared spectroscopy, including retinyl acetate (131) and retinyl palmitate (136). More recently, McKenzie et al. (112) compared the IR spectra of seven of the isomers of methyl retinoate. Oxidation of the vitamins A by manganese dioxide has led to the synthesis of several oxo-derivatives whose structures were resolved by various spectroscopic methods including infrared. 4-Oxoretinol and 4-oxoretinal were prepared from retinol

and retinal respectively by Henbest et al. (137) while 4-oxoretinoic acid was prepared from methyl retinoate by Surekha Rao (125). The 5,6- and 5,8-epoxy derivatives of retinol, retinyl acetate and retinal were synthesized by Jungalwala and Cama (138) while methyl 5,6-epoxyretinoate was prepared by Morgan and Thompson (139). 11,12-Epoxyretinol and 11,12-epoxyretinal were prepared by Ogata et al. (140, 141). The structures of these epoxy compounds were confirmed by infrared analysis.

No previous attempt has been made to correlate the infrared data available on the vitamins A and to indicate trends in the frequencies of the absorbances of these compounds. In this chapter we attempt such a correlation in the hope that this will simplify the task of identifying metabolites of retinoic acid. The Fourier transform infrared spectra of all-trans-retinoic acid, 4-oxoretinoic acid, 5,6-epoxyretinoic acid, 5,8-epoxyretinoic acid, retinal, 9-cis-retinal, 13-cis-retinal, C_{19}-aldehyde and 4-oxo-9-hydroxy-C_{19}-aldehyde (peak 1 isolated in Chapter III) are reported and compared. The use of Fourier transform infrared spectroscopy allows for short measurement times and for high resolution spectra from small amounts (ng) of sample to be obtained.

Experimental

Materials

Retinoids. All-trans-retinoic acid, 4-oxoretinoic acid (RO-12-4824/701), 5,6-epoxyretinoic acid (RO-08-3249/701), 5,8-epoxyretinoic acid (RO-08-3250/000) and C_{19}-aldehyde (RO-1-8340) were obtained as gifts from Dr. W. E. Scott, Hoffmann-La Roche Inc. (Nutley, NJ). Retinal (R-2500, type XVI), 9-cis-retinal (R-2250, type XIII) and 13-cis-

retinal (R-2375, type XV) were purchased from Sigma Chemical Co. (St. Louis, MO). 4-Oxo-9-hydroxy-C_{19}-aldehyde (peak 1) was purified from incubations of retinoic acid, horseradish peroxidase and hydrogen peroxide, as described in Chapter III.

Solvents. Glass distilled residue-free solvents (Burdick and Jackson) were used for high performance liquid chromatography and for infrared analyses. The water used for chromatography was deionized and redistilled in glass.

Methods

Purification of Retinoids by High Performance Liquid Chromatography. All retinoids were purified prior to infrared analysis by high performance liquid chromatography (HPLC) on reverse phase columns. The integrity of the sample was also checked by HPLC following the IR scans. Either a Partisil PXS 10/25 ODS-2 column (Whatman, Clifton, NJ) or a μBondapak C_{18} column (Waters, Milford, MA) was used for the purification. The Waters column was operated through the Isco pump and DuPont gradient-elution accessory described in Chapter II, while the Whatman column was operated by a Waters pumping system. This consisted of a Model 660 solvent programmer, a Model 440 absorbance detector, Model M 6000A pumps, a Model U6K injector and a Sargent-Welch Model XKR recorder (Sargent-Welch Scientific, Dallas, TX). Solvents used were methanol and water, or methanol and 0.01 M acetic acid in water.

Infrared Analyses. The infrared (IR) spectra were obtained on a Digilab FTS-2DC interfaced to a Data General Nova 3/12 (Digilab Inc.,

Cambridge, MA). Two hundred scans of each sample were collected except for C_{19}-aldehyde and 4-oxoretinoic acid (250 scans) and 13-cis-retinal (1000 scans). The resolution for all analyses was 4 cm^{-1}. The sample in the solvent was applied on a NaCl or a KBr window (32 x 3 mm, 7000-451 or 7000-452 from Barnes Engineering Co., Stanford, Conn). The solvent used, chloroform or carbon tetrachloride, was then allowed to evaporate to dryness before the window was inserted into the cell holder and introduced into the instrument. A background spectrum of a window without sample was routinely ratioed with that of the sample to obtain transmission spectra. Since the concentration of each sample was not determined prior to IR analysis, no extinction coefficients are reported.

Results and Discussion

Purification of Retinoids by High Performance Liquid Chromatography

All compounds (shown in Figure 42) were chromatographed by HPLC in order to ensure their purity both before and after infrared analyses. Retinal and 9-cis-retinal were purified on the Whatman column (70% methanol, 30% water, at a flow rate of 1 ml per min) and eluted at 39 min and 20 min, respectively. The same column was used to elute 5,6-epoxyretinoic acid and 5,8-epoxyretinoic acid, both at 56 min (80% methanol, 20% 0.01 M acetic acid, at 0.5 ml per min). In order to ensure that each epoxy compound did not contain contaminants of the other, both compounds were scanned in methanol by ultraviolet absorbance and found to have only one λ_{max}, at 326 nm for 5,6-epoxyretinoic acid

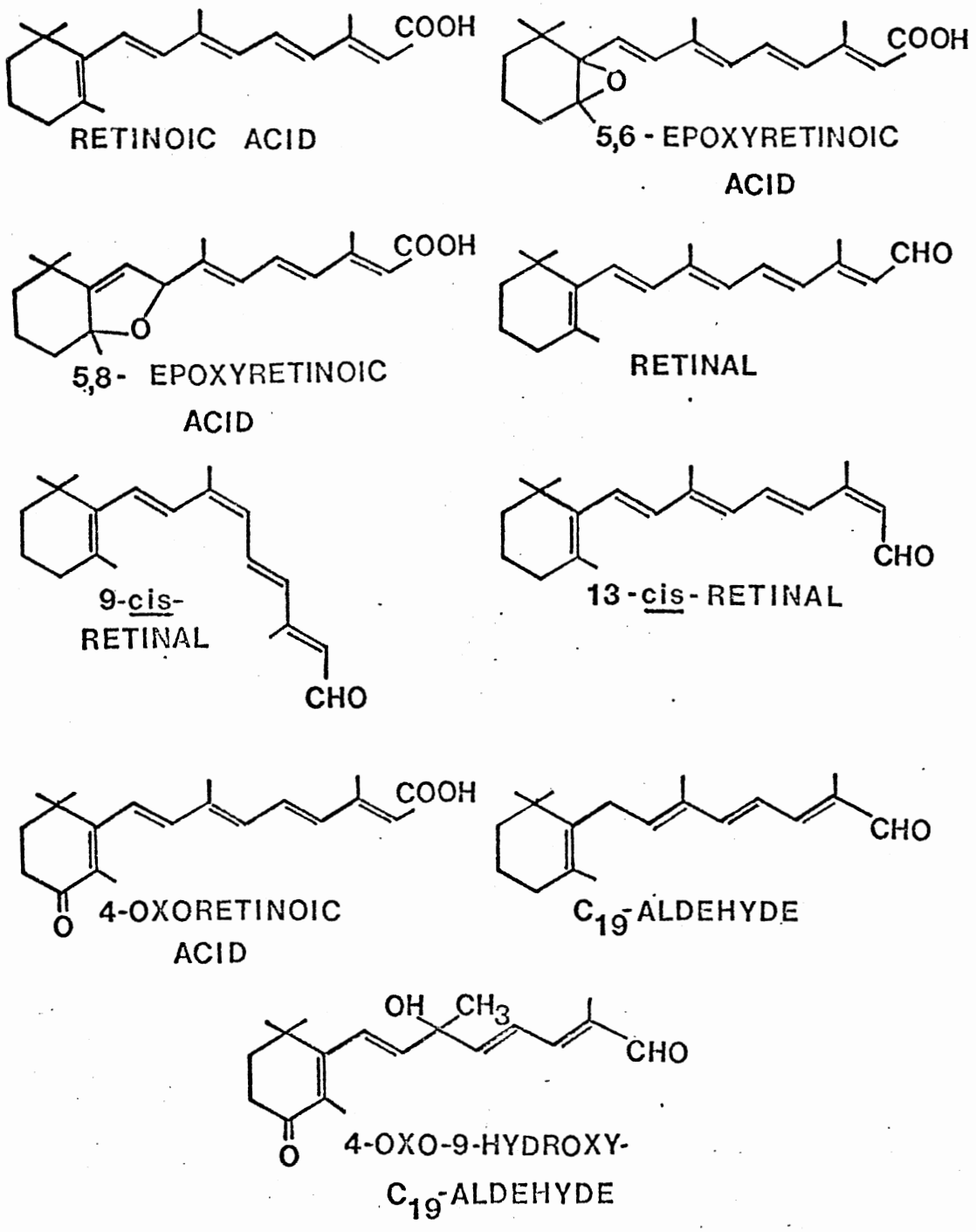

Figure 42. Structures of Nine Retinoids

and at 296 nm for 5,8-epoxyretinoic acid.

The Waters column was used to purify 13-cis-retinal (85% methanol, 15% 0.01 M acetic acid, at 0.6 ml per min), which eluted at 54 minutes. The C_{19}-aldehyde eluted from the column at 33 min (90% methanol, 10% 0.01 M acetic acid, 0.65 ml per min), while 4-oxoretinoic acid was collected at 50 min (75% methanol, 25% 0.01 M acetic acid, at 0.6 ml per min). All-trans-retinoic acid and 4-oxo-9-hydroxy-C_{19}-aldehyde (peak 1) were purified as described in Chapter I and II, respectively.

Infrared Analyses

The infrared spectra of the nine retinoids are shown in Figures 43-45. The band at 2400-2300 cm^{-1} in the spectra of 13-cis-retinal, 4-oxoretinoic acid and 5,6-epoxyretinoic acid is due to atmospheric CO_2. Since the absorption due to the C-H stretch of methyl and methylene groups (3000-2800 cm^{-1}) remains fairly constant for all the samples considered, only the region from 2000 to 600 cm^{-1} is expanded in Figures 46 to 54. Infrared frequencies are tabulated in Table VI where references to "strong", "medium" and "weak" bands are given only as approximate indications of absorption intensity.

The weak bands which appear at 2720 cm^{-1} in the aldehydic compounds reflect the presence of an aldehyde carbon-hydrogen stretch (127). The presence of broad bands above 3000 cm^{-1} in the spectra of retinoic acid, 4-oxoretinoic acid and 5,8-epoxyretinoic acid is due to the acid hydrogen, and in the spectra of retinal and 13-cis-retinal to atmospheric water. The hydroxyl group in 4-oxo-9-hydroxy-C_{19}-aldehyde absorbs in the same region.

Bands between 1690 and 1650 cm^{-1} are attributed to the C=O

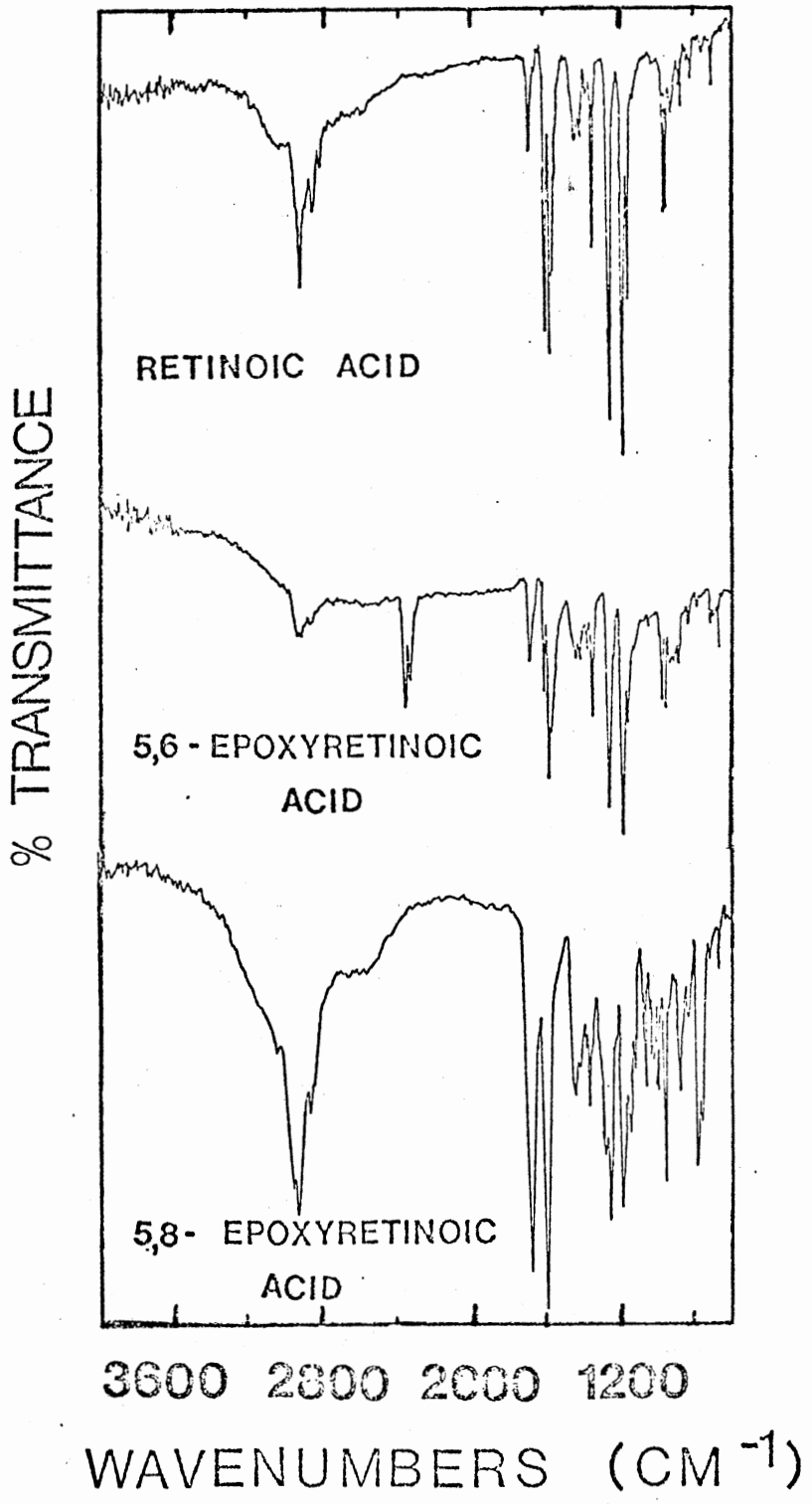

Figure 43. Infrared Spectrum of Retinoid Acid (Top), 5,6-Epoxyretinoic Acid (Middle) and 5,8-Epoxyretinoic Acid (Bottom) from 4000 to 600 cm^{-1}

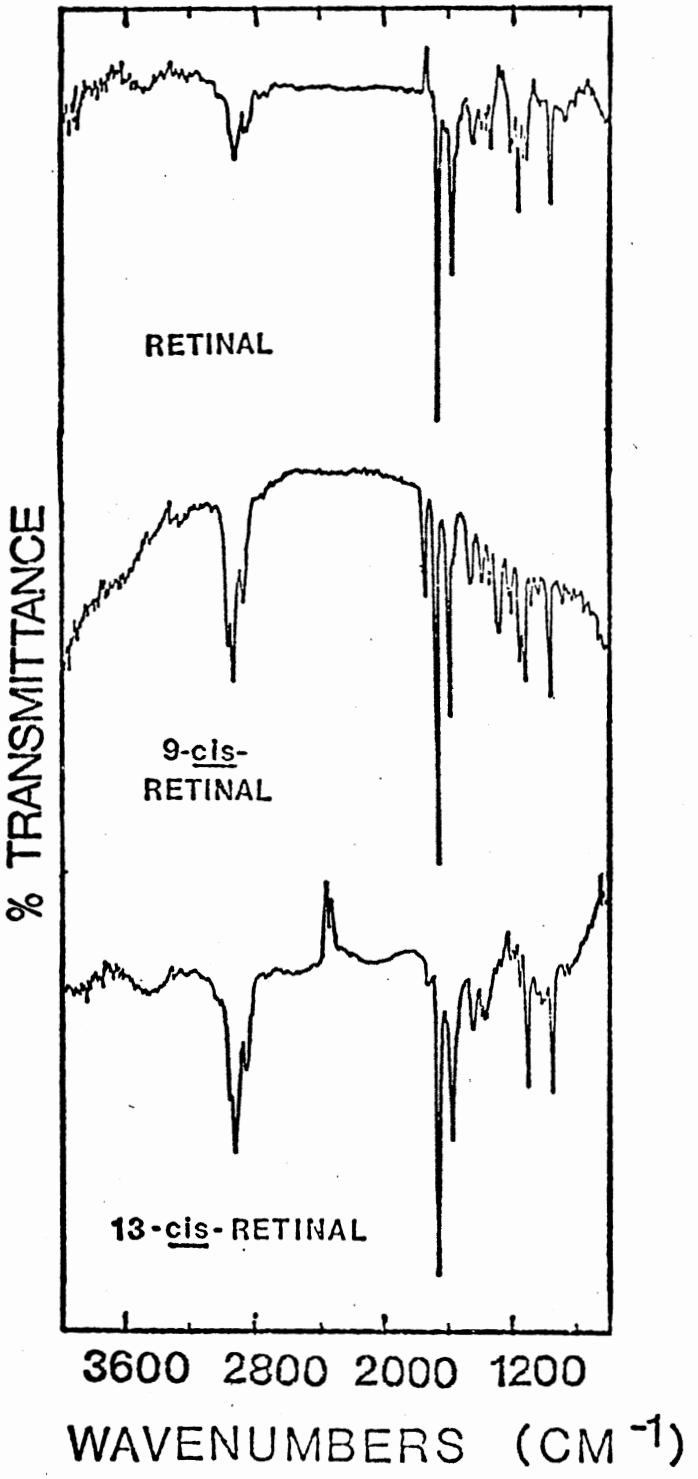

Figure 44. Infrared Spectra of Retinal (Top), 9-cis-Retinal (Middle) and 13-cis-Retinal (Bottom) from 4000 to 600 cm^{-1}

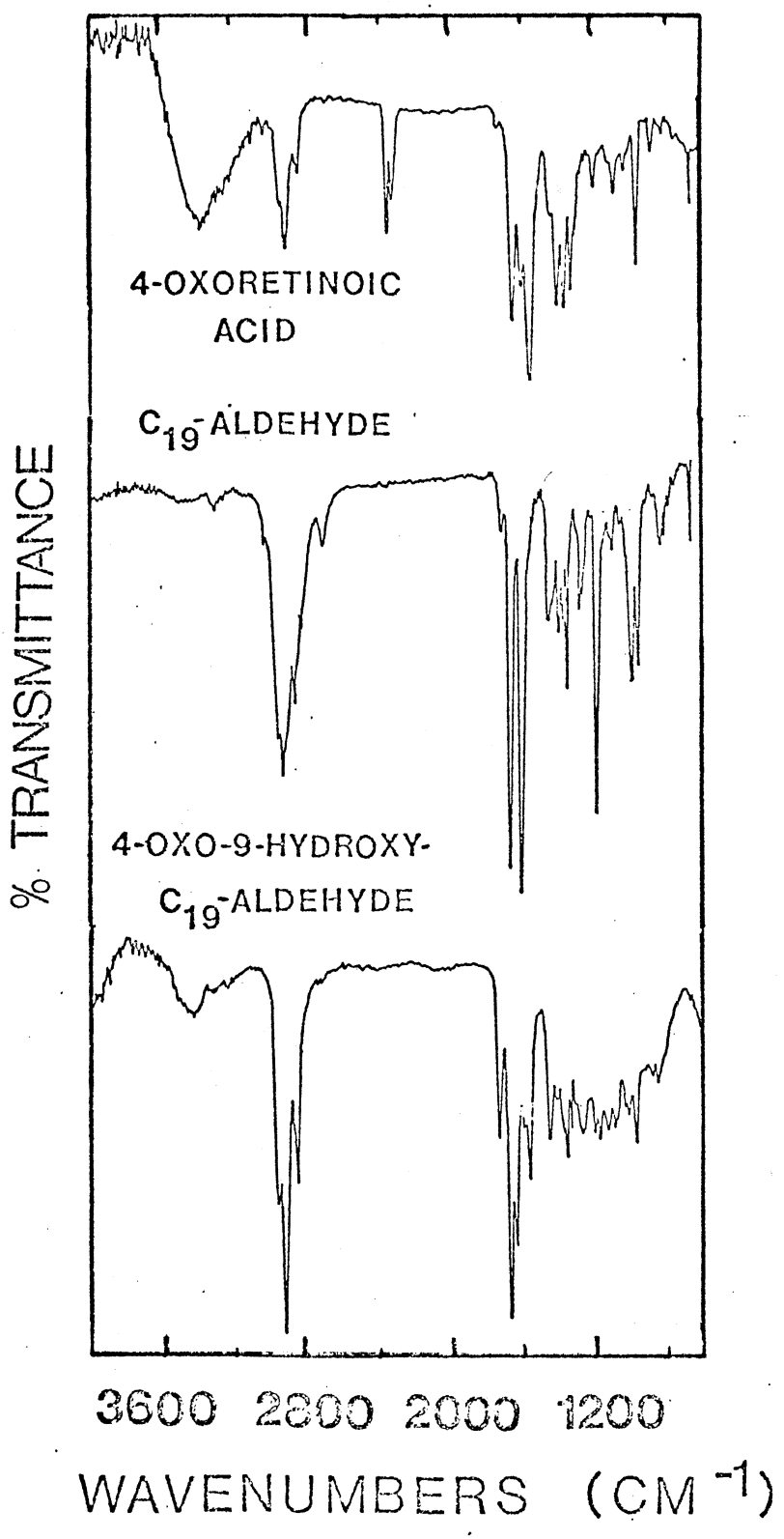

Figure 45. Infrared Spectra of 4-Oxoretinoic Acid (Top), C_{19}-Aldehyde (Middle) and 4-Oxo-9-hydroxy-C_{19}-Aldehyde (Bottom) from 4000 to 600 cm^{-1}

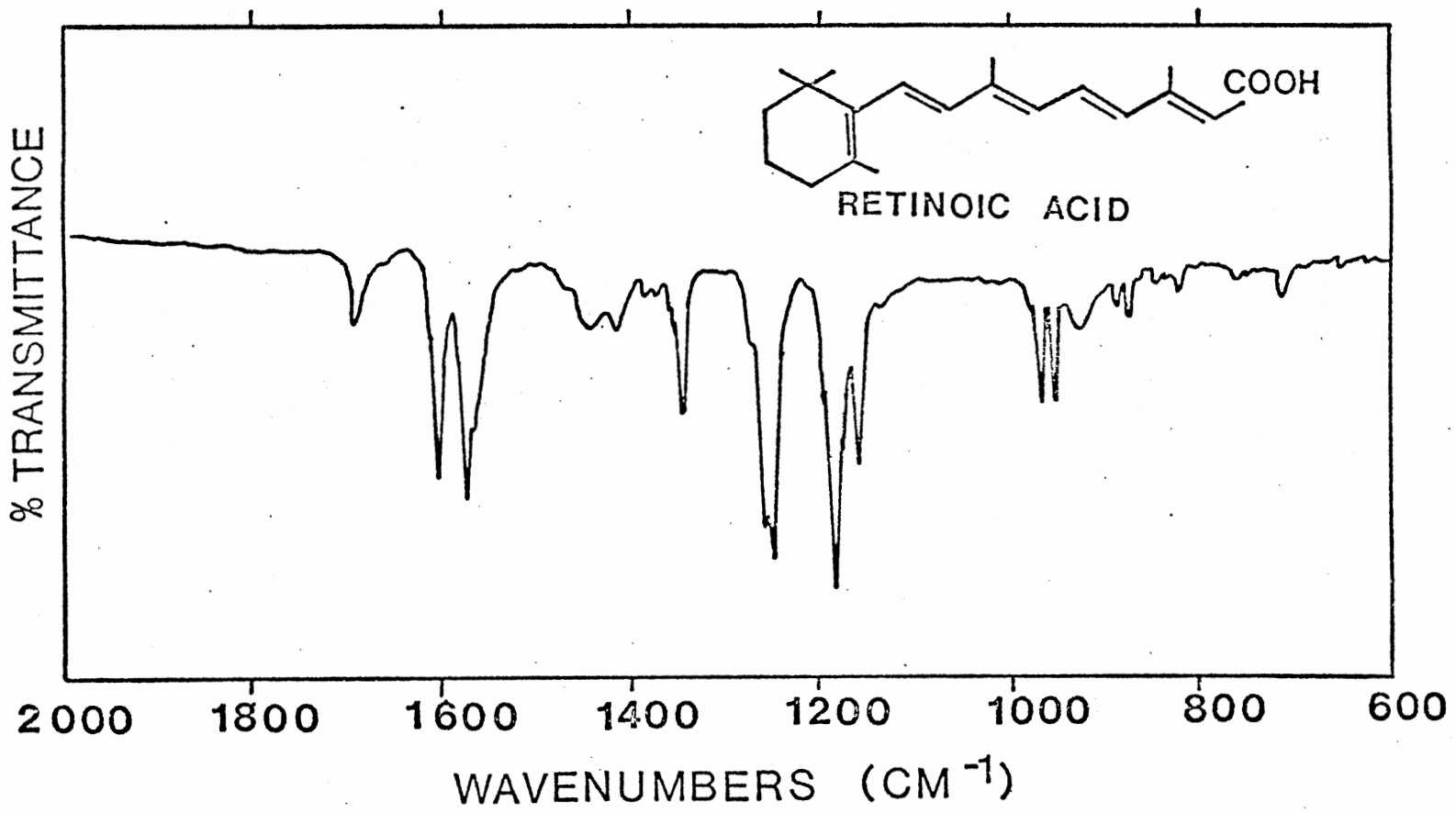

Figure 46. Infrared Spectrum of Retinoic Acid from 2000 to 600 cm^{-1}

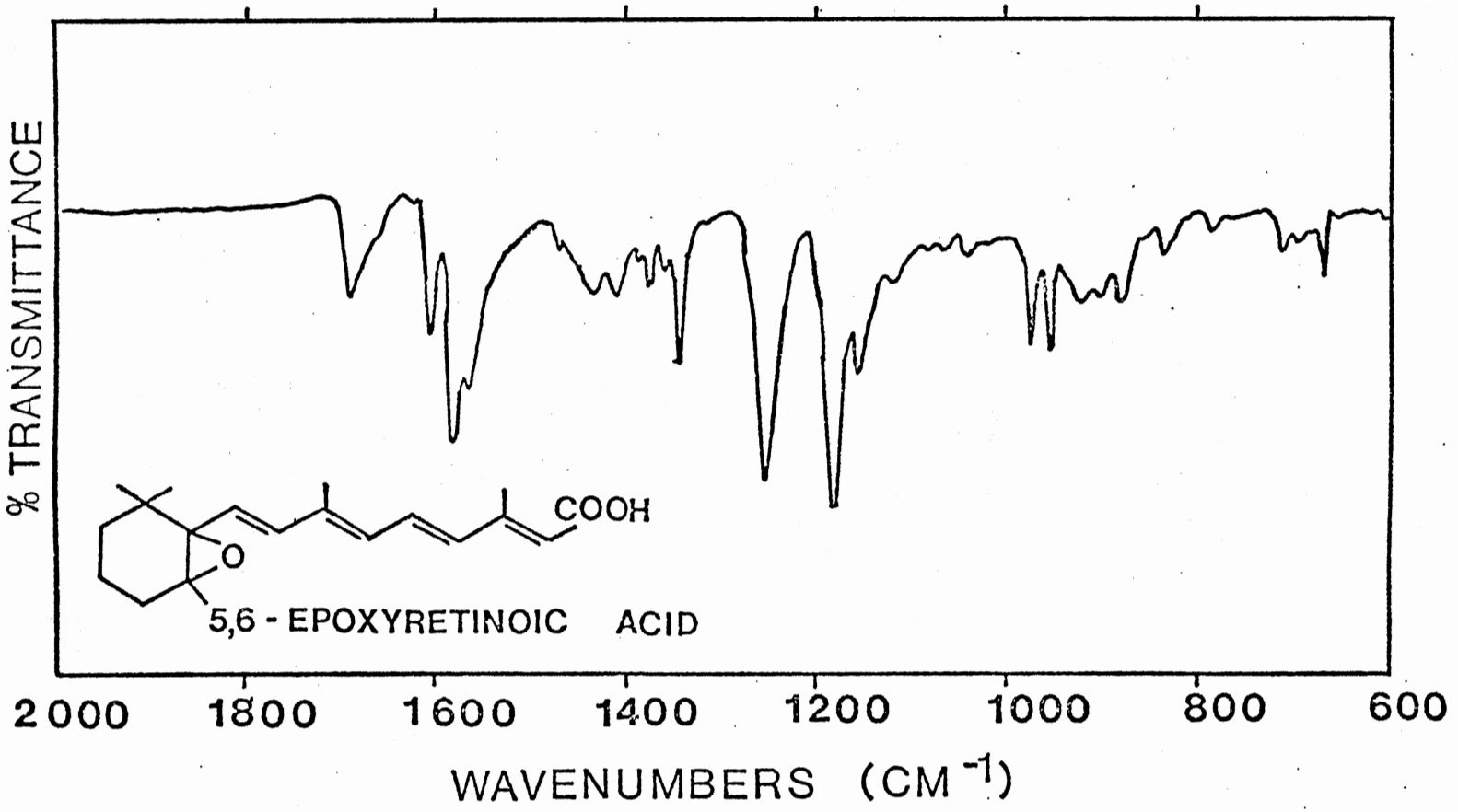

Figure 47. Infrared Spectrum of 5,6-Epoxyretinoic Acid from 2000 to 600 cm^{-1}

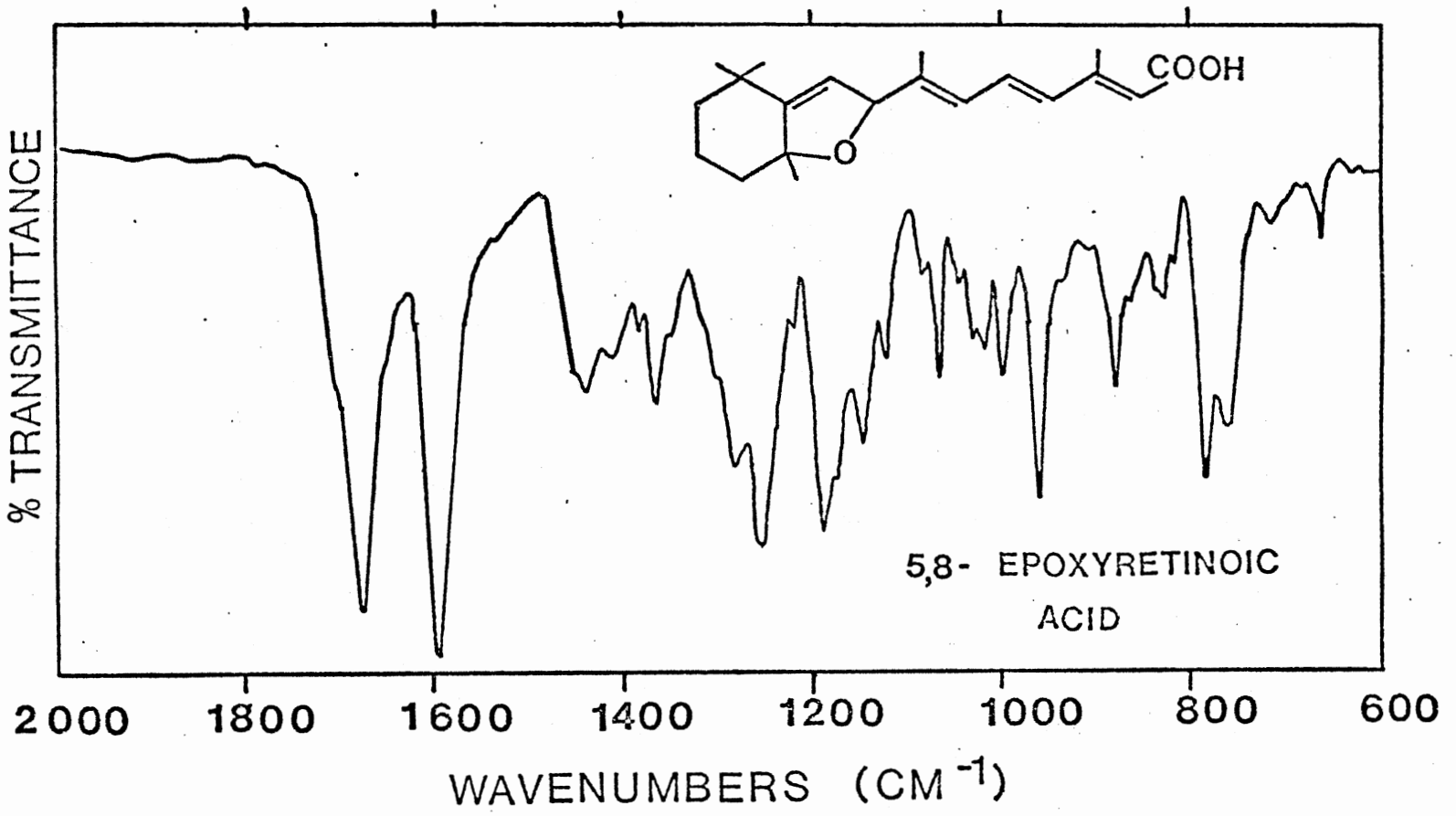

Figure 48. Infrared Spectrum of 5,8-Epoxyretinoic Acid from 2000 to 600 cm^{-1}

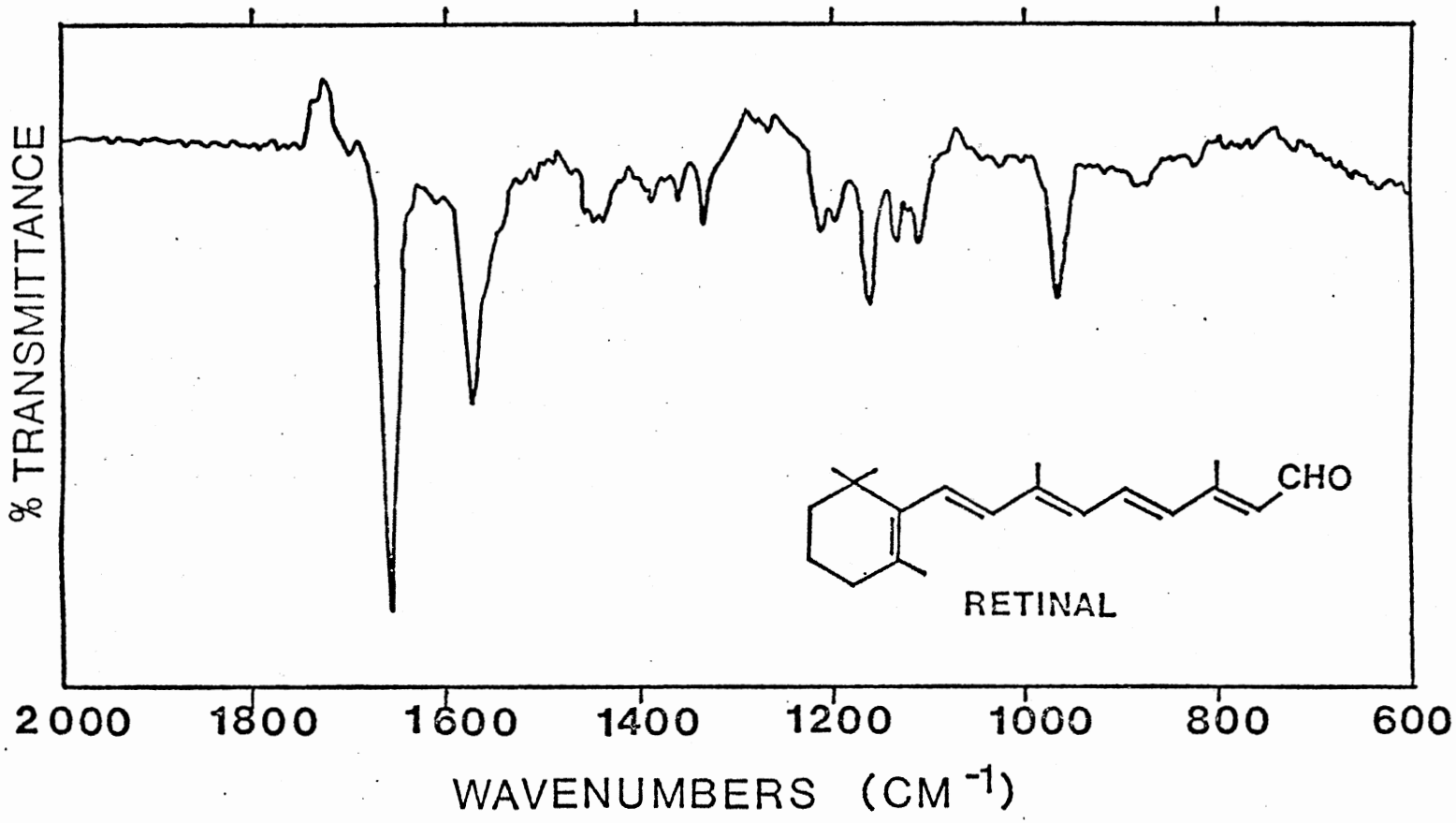

Figure 49. Infrared Spectrum of Retinal from 2000 to 600 cm^{-1}

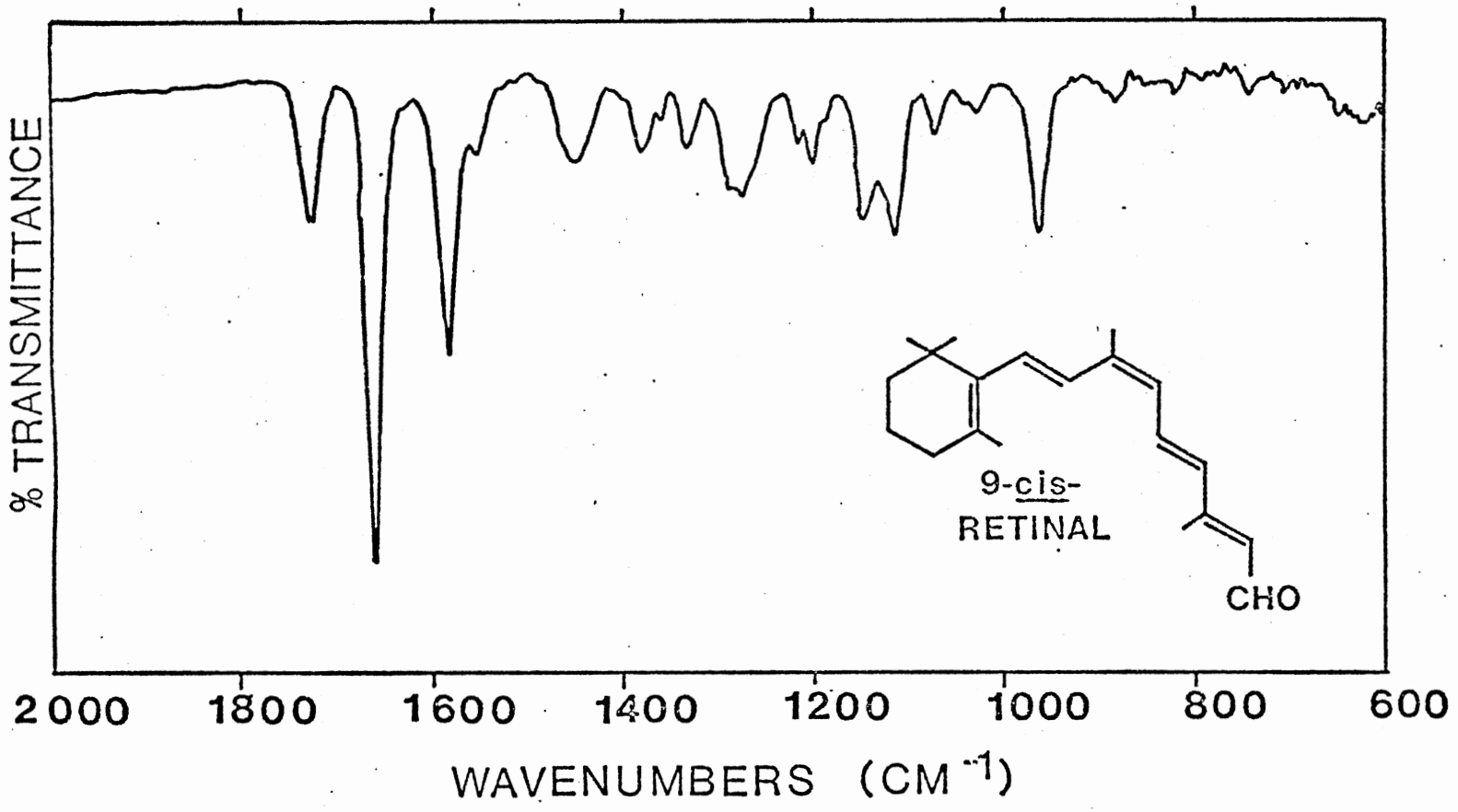

Figure 50. Infrared Spectrum of 9-cis-Retinal from 2000 to 600 cm^{-1}

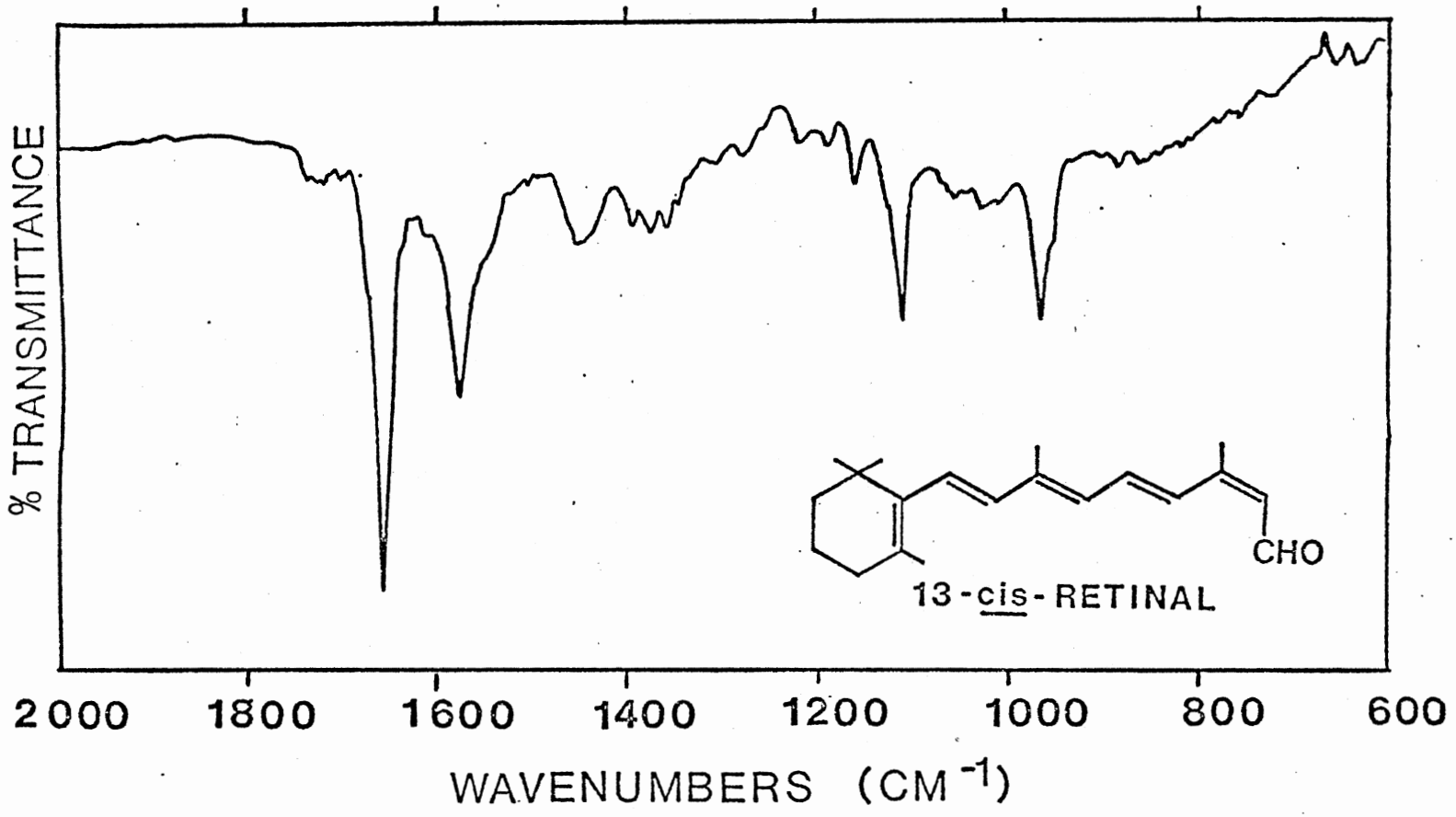

Figure 51. Infrared Spectrum of 13-cis-Retinal from 2000 to 600 cm^{-1}

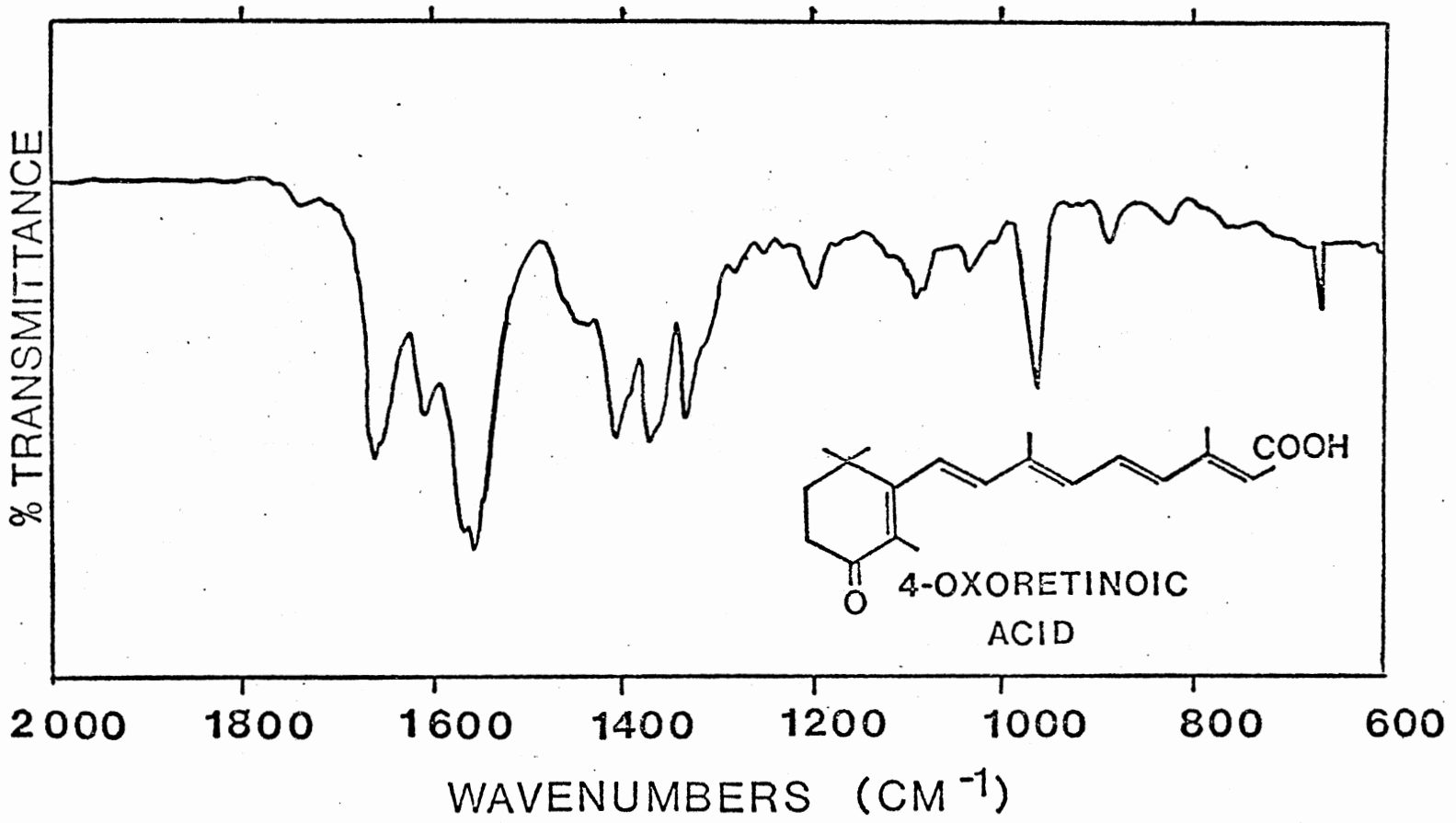

Figure 52. Infrared Spectrum of 4-Oxoretinoic Acid from 2000 to 600 cm^{-1}

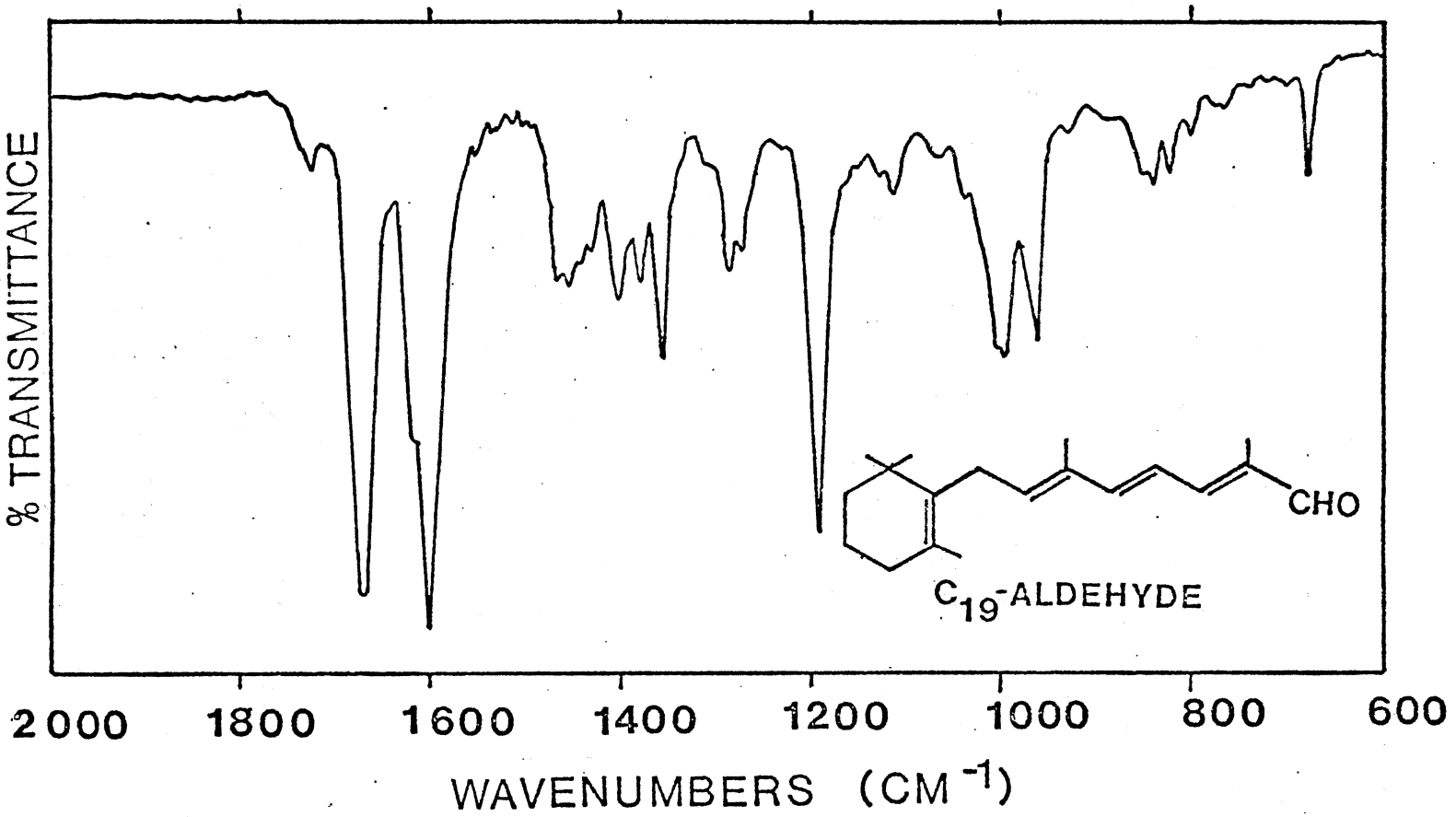

Figure 53. Infrared Spectrum of C_{19}-Aldehyde from 2000 to 600 cm^{-1}

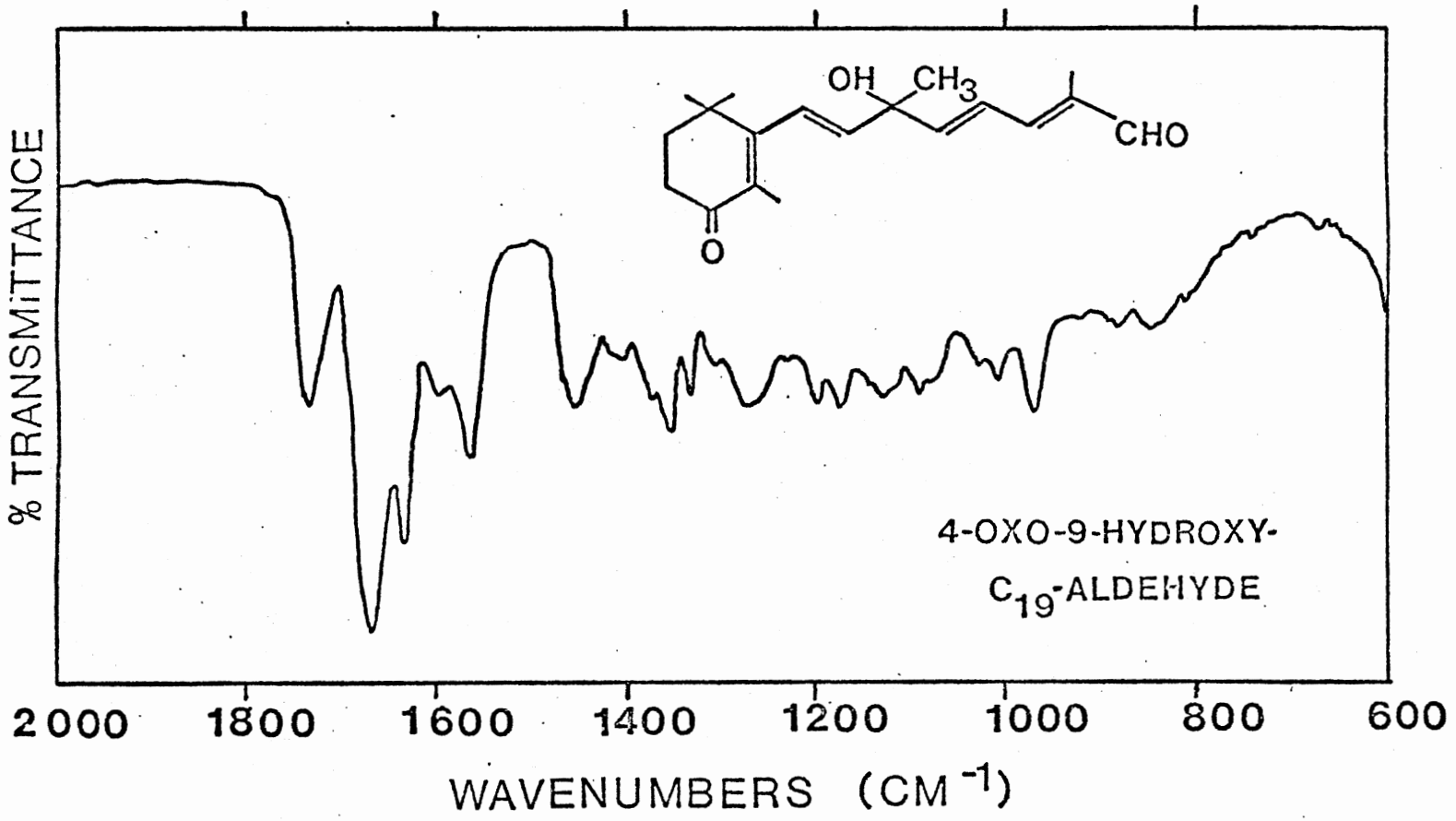

Figure 54. Infrared Spectrum of 4-Oxo-9-Hydroxy-C_{19}-Aldehyde from 2000 to 600 cm^{-1}

TABLE VI

INFRARED FREQUENCIES OF RETINOIDS

Retinoid	C-H Stretch	$RC(=O)-H$ Stretch	C=O Stretch		C=C Stretch
Retinoic Acid	2930_s, 2860_m, 2820_w	-	-	1690_m	1605_s, 1578_s
5,6-Epoxyretinoic Acid	2940_m, 2920_m, 2860_w	-	-	1690_m	1605_m, 1580_s
5,8-Epoxyretinoic Acid	2960_m, 2925_s, 2860_m	-	1710_w	1680_s	1650_m, 1600_s
Retinal	2950_m, 2920_s, 2850_m	2720_w	-	1660_s	1578_s, 1560_m
9-cis-Retinal	2960_m, 2930_s, 2860_m	2720_w	1730_m	1664_s	1585_s, 1555_m
13-cis-Retinal	2950_m, 2920_s, 2850_m	2720_w	1730_w	1660_s	1580_s, 1560_m
4-oxoretinoic Acid	2940_m, 2930_s, 2850_m	-	1730_w	1660_s, 1650_s	1605_m, 1555_s
C_{19} Aldehyde	2945_m, 2930_s, 2860_m	2720_m	1725_w	1670_s	1620_m, 1600_s
4-Oxo-9-hydroxy-C_{19} Aldehyde	2960_m, 2930_s, 2855_m	2720_w	1730_m	1672_s	1640_s, 1565_m

Retinoid	H-C-H Bending	CH_3 on cis Double Bond	H-C-H Bending	1300-1100 cm^{-1}	H Bending of $RC(H)=C(H)R'$ trans, unsubstituted
Retinoic Acid	1445_w	-	1350_m	1260_s, 1255_s, 1190_s, 1160_m	970_m, 955_m
5,6-Epoxyretinoic Acid	1445_w	-	1345_m	1258_s, 1182_s, 1158_m, 1120_w	975_m, 955_m
5,8-Epoxyretinoic Acid	1445_m	-	1365_w	1280_m, 1252_s, 1190_s, 1145_m, 1120_m	960_m
Retinal	1450_w	-	1335_w	1200_w, 1162_m, 1134_w, 1110_w	968_m
9-cis-Retinal	1450_m	1380_w	1335_w	1270_w, 1200_w, 1145_m, 1110_m	962_m
13-cis-Retinal	1450_w	1378_w	1390_w	1160_w, 1110_m	964_m
4-Oxoretinoic Acid	1450_w	-	1370_m, 1340_m	1200_w	968_m
C_{19}-Aldehyde	1450_w	-	1360_m	1290_m, 1270_m, 1190_s, 1115_w	962_m
4-Oxo-9-hydroxy-C_{19}-Aldehyde	1455_m	-	1355_w	1270_w, 1200_w, 1180_w, 1130_w	970_m

s = strong; m = medium; w = weak

stretch of ketones, aldehydes and acids. Frequencies for the non-conjugated C=O stretch generally are higher than for the conjugated bond and usually are between 1730 and 1710 cm^{-1} (142). Unsaturation in conjugation with the C=O group leads to delocalization of the π electrons of the C=O, causing a decrease in the frequency of absorption of this group (127, 142-144). The introduction of the first C=C double bond results in a 30 cm^{-1} shift to lower frequency while the introduction of the second results in an additional shift of 15 cm^{-1} (142). The position of the band is essentially constant for C=O containing compounds with more than two unsaturations (144). Since all the compounds studied had at least two C=C bonds conjugated with the C=O, the frequencies are all within the same range.

A band around 1730 cm^{-1} also appears in some of the spectra. This band could be due to the presence of two different conformations (cis and trans) around the terminal carbon. If the carbonyl is cis to the conjugated system, the frequency will be much higher than if it is trans (127).

The carbon-carbon double bond stretch frequency is affected in the same way as the C=O by unsaturation (127, 142). Conjugation with another C=C or C=O leads to a shift to a lower frequency of approximately 40 to 60 cm^{-1} with a substantial increase in intensity (144). The highest frequencies are found for the 4-oxo-9-hydroxy-C_{19}-aldehyde (1640 and 1600 cm^{-1}) with two C=C in conjugation with each carbonyl, C_{19}-aldehyde (1620 and 1600 cm^{-1}) and 5,8-epoxyretinoic acid (1650 and 1600 cm^{-1}) with three C=C conjugated with the C=O. The remaining compounds all have 5 or 6 conjugated double bonds and the C=C stretch bands therefore has a lower frequency (between 1605

and 1555 cm^{-1}).

The region between 1455 and 1445 cm^{-1} is similar in the spectra of the nine retinoids and is due to the non-symmetrical HCH bending of methyl groups and the HCH bending (scissoring) of methylene groups (144, 145). The presence of a cis double bond in the 9-cis- and 13-cis-retinals is confirmed by the absorption at 1380 and 1378 cm^{-1} respectively, due to the deformation vibration of the methyl group attached to a cis double bond (146). The absorption due to the symmetrical HCH bending of methyl groups is found between 1370 and 1335 cm^{-1} in all spectra (127). The most helpful information in terms of retinoid structural identification comes from band splitting due to the presence of gem dimethyl groups at C_1. Only the most prominent band is listed in the table.

The 1300 to 1100 cm^{-1} region, also known as the fingerprint region, has several bands but is not very useful as an aid for identification of unknown compounds due to the large number of vibrations which contribute to it. These include the C-O stretch of a carboxylic acid at 1320 to 1210 cm^{-1} (127), the C-C stretch of geminal dimethyl groups which produce bands at 1195 and at 1125 cm^{-1} (142), and the bending deformations (twisting and wagging) of the methylene groups at 1350 to 1180 cm^{-1} (142).

The strong absorbances at 1258 cm^{-1} in the spectrum of 5,6-epoxyretinoic acid and at 1252 cm^{-1} in that of 5,8-epoxyretinoic acid are attributable to symmetrical stretching of the epoxide ring (140, 127). The presence of bands at 1065, 1083 and 1175 cm^{-1} confirms the furan structure in the 5,8-epoxyretinoic acid (138).

An out-of-plane hydrogen bending vibration of a trans -CH=CH- or

"unsubstituted trans" bond leads to the absorbances at 975 to 955 cm^{-1} present in all the spectra (143, 145, 147, 148). The intensity of the bands increases with the number of such bonds in a conjugated system.

The only strong bands in the 800 to 700 cm^{-1} range appear at 880 cm^{-1} (m), 792 cm^{-1} (s) and 760 cm^{-1} (m) in the spectrum of 5,8-epoxyretinoic acid. They reflect the presence of unsymmetrical stretching of an epoxy ring in which the C-C bond is stretching during contraction of the C-O bond (127, 140). These bands also appear in the spectrum of 5,6-epoxyretinoic acid at 880 cm^{-1}, 840 cm^{-1} and at 780 cm^{-1} but are much weaker (139).

In summary, retinoids which have C=O groups (aldehydes, acids or 4-oxocompounds) will have a band between 1690 and 1650 cm^{-1} if they are conjugated. Compounds with 3 to 4 conjugated unsaturations will have a C=C stretch between 1650 and 1600 cm^{-1} while more unsaturations will lead to bands between 1610 and 1555 cm^{-1} and to an increase in intensity. The presence of cis double bonds with a methyl group attached is indicated by an absorption at 1380 cm^{-1} while an epoxy ring leads to bands around 1250, 880 and 790 cm^{-1}. A furan structure is confirmed by bands at 1065, 1083 and 1175 cm^{-1}. Unsubstituted trans C=C bonds, present in most retinoids are detectable by absorbances at 975 to 955 cm^{-1}, with an increased intensity as the number of these bonds becomes larger.

The presence of some of these absorption bands in the infrared spectrum of an unknown metabolite of vitamin A should be helpful in the determination of the structure of unknown compounds and, as

discussed in Chapter III, prove definitive in the identification of oxidation products of retinoic acid.

CHAPTER V

SUMMARY

The objective of this study was to characterize products of retinoic acid produced in vitro. Isomerically and radiochemically pure all-trans-[15-^{14}C]- and [11,12-$^{3}H_2$]retinoic acid, H_2O_2 or $FeCl_2$ and horseradish peroxidase were incubated for 2 hours at 37°C and $^{14}CO_2$ was collected. The nature of the heme catalyst, the type and pH of the buffer, the concentrations of retinoic acid, H_2O_2 or $FeCl_2$, and horseradish peroxidase were optimized for the production of the greatest amount of oxidized and decarboxylated products. Products of retinoic acid were extracted from the H_2O_2 reaction with chloroform, purified by high performance liquid chromatography and identified by infrared, nuclear magnetic resonance, ultraviolet and mass spectroscopy.

The Fourier transform infrared spectra of all-trans-retinoic acid, 5,6-epoxyretinoic acid, 5,8-epoxyretinoic acid, retinal, 9-cis-retinal, 13-cis-retinal, 4-oxoretinoic acid, C_{19}-aldehyde and 4-oxo-9-hydroxy-C_{19}-aldehyde were obtained as an aid in the identification of metabolites of retinoic acid.

Optimum concentrations which generated the highest levels of oxidation and decarboxylation products were 133 μM retinoic acid, 4 μM horseradish peroxidase and 1 mM H_2O_2 or 2 mM $FeCl_2$. The H_2O_2 reaction decarboxylated retinoic acid in a pH range of 6.4 to 8.0 regardless of the type of buffer. The $FeCl_2$ reaction, however, required oxygen and

and phosphate, Tris or TES as buffer. The only heme catalyst which successfully decarboxylated retinoic acid in the Fe^{+2} reaction was horseradish peroxidase. In the presence of H_2O_2, the decarboxylation reaction was heme catalyzed. Cytochrome c, hemoglobin or hemin could be substituted for horseradish peroxidase. The mechanisms of these reactions seemed to involve oxidation as well as decarboxylation of retinoic acid. The high performance liquid chromatography elution profile for the H_2O_2 and horseradish peroxidase catalyzed reaction was identical to that obtained when retinoic acid was incubated with hemoglobin and H_2O_2 or with Fe^{+2}, oxygen and horseradish peroxidase. When extracts from incubations containing retinoic acid and chick liver microsomal fraction were chromatographed by high performance liquid chromatography, the product profiles were similar to those generated from heme containing incubations. In both types of incubation, the decarboxylation products eluted from the column in the polar fractions.

Products of retinoic acid were isolated from the H_2O_2 reaction and purified by high performance liquid chromatography. The major decarboxylation product was subjected to mass spectral analysis and yielded a molecular ion of 302. The extinction coefficient at 280 nm (λ_{max}) was 37,000 ± 4%. Based on the mass spectral fragmentation pattern, on peak matching of the nuclear magnetic resonance spectrum by the LAOCN3 computer program and on the infrared spectrum, this product was identified as a 4-oxo-C_{19}-aldehyde with a hydroxyl group on the side chain at C_9, specifically 8-(2,6,6-trimethyl-3-oxo-cyclohex-1-enyl)-2,6-dimethyl-6-hydroxy-2,4,7-E-octatrienal. Another decarboxylated product of retinoic acid was isolated and tentatively identified by nuclear magnetic resonance spectroscopy as a 4-oxo-C_{19}

aldehyde with a peroxy group on the side chain at C_9, specifically 8-(2,6,6-trimethyl-3-oxo-cyclohex-1-enyl)-2,6-dimethyl-6-peroxy-2,4,7-E-octatrienal. Several oxidized nondecarboxylated products were also isolated from the incubations.

The Fourier transform infrared spectra of 9 purified retinoids were compared. Retinoids could be identified by the presence of a band between 1650 and 1600 cm^{-1} due to C=C stretching where 3 to 4 conjugated C=O and C=C bonds were present or between 1610 and 1555 cm^{-1} where more conjugated unsaturations were present. The intensity of this band increased with the number of unsaturations. The presence of cis double bonds was confirmed by a band at 1380 cm^{-1} while unsubstituted trans double bonds led to absorbances at 975 to 955 cm^{-1} with an increased intensity as the number of such bonds increased. Epoxy rings present in some retinoids led to bands at 1250, 880 and 790 cm^{-1} while a furan structure was confirmed by bands at 1065, 1083 and 1175 cm^{-1}. Retinoids with conjugated C=O groups revealed the presence of a band between 1690 and 1650 cm^{-1}.

BIBLIOGRAPHY

(1) McCollum, E. V., and Davis, M. (1913) J. Biol. Chem. 15, 167-175.

(2) McCollum, E. V., and Davis, M. (1913) J. Biol. Chem. 19, 245-250.

(3) Osborne, T. B., and Mendel, L. B. (1915) J. Biol. Chem. 20, 379-385.

(4) Karrer, P., Morf, R., and Schopp, K. (1930) Helv. Chim. Acta 14, 1036-1046; 1431-1436.

(5) Karrer, P., and Eugster, C. H. (1950) Helv. Chim. Acta 33, 1172-1174.

(6) Sporn, M. B., Dunlop, N. M., Newton, D. L., and Smith, J. M. (1976) Fed. Proc. 35, 1332-1338.

(7) De Luca, L. M. (1978) in The Fat-Soluble Vitamins, H. F. DeLuca, ed., pp. 1-67. Plenum Press, New York.

(8) Wasserman, R. H., and Corradino, R. A. (1971) Ann. Rev. Biochem. 40, 501-532.

(9) Roels, O. A. (1970) J. A. M. A. 214, 1097-1102.

(10) Olson, J. A. (1969) Fed. Proc. 28, 1670-1677.

(11) Olson, J. A. (1972) Keratomalacia 8, 1170-1178.

(12) Olson, J. A. (1967) Pharmacol. Rev. 19, 559-596.

(13) Wald, G. (1935) J. Gen. Physiol. 19, 351.

(14) Arens, J. F., and Van Dorp, D. A. (1946) Nature 157, 190-191.

(15) Van Dorp, D. A., and Arens, J. F. (1946) Nature 158, 60.

(16) Arens, J. F., and Van Dorp, D. A. (1946) Nature 158, 622.

(17) Dowling, J. E., and Wald, G. (1960) Vitamins and Hormones 18, 515-541.

(18) Dowling, J. E., and Wald, G. (1960) Proc. Nat. Acad. Sci. 46, 587-608.

(19) Thompson, J. N., Howell, J. M., and Pitt, G. A. J. (1961) Biochem. J. 80, 25.

(20) Thompson, J. N., Howell, J. M., and Pitt, G. A. J. (1961) Biochem. J. 80, 16.

(21) Malathi, P., Subba Rao, K., Seshadri Sashy, P., and Ganguly, J. (1963) Biochem. J. 87, 305-311.

(22) Krishnamurthy, S., Bieri, J. G., and Andrews, E. L. (1963) J. Nutr. 79, 503-510.

(23) Nelson, E. C., Dehority, B. A., Teague, H. S., Grifo, A. P., and Sanger, V. L. (1964) J. Nutr. 82, 263-268.

(24) Nelson, E. C., Dehority, B. A., and Teague, H. S. (1965) Anal. Biochem. 11, 418-429.

(25) Dunagin, P. E., Zachman, R. D., and Olson, J. A. (1964) Biochim. Biophys. Acta 90, 432-434.

(26) Dunagin, P. E., Zachman, E. D., and Olson, J. A. (1966) Biochim. Biophys. Acta 124, 71-85.

(27) Crain, F. D., Lotspeich, F. J., and Krause, R. F. (1967) J. Lipid Res. 8, 249-254.

(28) Emerick, R. J., Zile, M., and DeLuca, H. F. (1967) Biochem. J. 102, 606-611.

(29) Kleiner-Bossaler, A., and DeLuca, H. F. (1971) Arch. Biochem. Biophys. 142, 371-377.

(30) Ito, Y. L., Zile, M., Ahrens, H., and DeLuca, H. F. (1974) J. Lipid Res. 15, 517-524.

(31) Ito, Y., Zile, M., DeLuca, H. F., and Ahrens, H. M. (1974) Biochim. Biophys. Acta 369, 338-350.

(32) Smith, J. E., Milch, P. O., Muto, Y., and Goodman, D. S. (1973) Biochem. J. 132, 821-827.

(33) Lehman, E. D., Spivey, H. O., Thayer, R. H., and Nelson, E. C. (1972) Fed. Proc. Fed. Amer. Soc. Exp. Biol. 31, 672.

(34) Sani, B. P., Titus, B. C., and Banerjee, C. K. (1978) Biochem. J. 171, 711-717.

(35) Ong, D. E., and Chytil, F. (1975) J. Biol. Chem. 250, 6113-6117.

(36) Sani, B. P., and Hill, D. L. (1974) Biochem. Biophys. Res. Comm. 61, 1276-1282.

(37) Futterman, S., Saari, J. C., and Swanson, D. E. (1976) Exp. Eye Res. 22, 419-424.

(38) Chytil, F., Page, D. L., and Ong, D. E. (1975) Internat. J. Vit. Nutr. Res. 45, 293-298.

(39) Ong, D. E., Tsai, C. H., and Chytil, F. (1976) J. Nutr. 106, 204-211.

(40) Sani, B. P., and Corbett, T. H. (1977) Cancer Res. 37, 209-213.

(41) Sani, B. P. (1977) Biochem. Biophys. Res. Comm. 75, 7-12.

(42) Sani, B. P., and Donovan, M. K. (1979) Cancer Res. 39, 2492-2496.

(43) Wiggert, B., Russell, P., Lewis, M., and Chader, G. (1977) Biochem. Biophys. Res. Comm. 79, 218-225.

(44) Ong, D. E., and Chytil, F. (1976) Proc. Natl. Acad. Sci. USA 73, 3976-3978.

(45) Ong, D. E., and Chytil, F. (1978) J. Biol. Chem. 253, 4551-4554.

(46) Sani, B. P., and Banerjee, C. K. (1978) Biochem. J. 173, 643-649.

(47) Sani, B. P., and Hill, D. L. (1976) Cancer Res. 36, 409-413.

(48) Chytil, F., and Ong, D. E. (1976) Nature 260, 49-51.

(49) Wilkoff, L. J., Peckham, J. C., Dulmadge, E. A., Mowry, R. W., and Chopra, D. P. (1976) Cancer Res. 36, 964-972.

(50) Moore, T. (1967) in The Vitamins, Second Edition Vol. I, Sebrell, W. H., and Harris, R. S., eds., pp. 245-266. Academic Press, New York.

(51) De Luca, L. M. (1977) Vitamins and Hormones 35, 1-57.

(52) De Luca, L., Maestri, N., Boranni, F., and Nelson, D. (1972) Cancer 30, 1326-1331.

(53) De Luca, L., and Wolf, G. (1972) Agric. Food Chem. 20, 474-476.

(54) Clamon, G. H., Sporn, M. B., Smith, J. M., and Saffiotti, U. (1974) Nature 250, 64-66.

(55) Sporn, M. B., Clamon, G. H., Dunlop, N. M., Newton, D. L., Smith, J. M., and Saffiotti, U. (1975) Nature 253, 47-50.

(56) Chopra, D. P., and Wilkoff, L. J. (1977) J. Natl. Cancer Inst. 58, 923-930.

(57) Chopra, D. P., and Wilkoff, L. J. (1976) J. Natl. Cancer Inst. 56,

583-589.

(58) Lasnitzki, I., and Goodman, D. S. (1974) Cancer Res. 34, 1564-1571.

(59) Rogers, A. E., Herndon, B. J., and Newberne, P. M. (1973) Cancer Res. 33, 1003-1009.

(60) Newberne, P. M., and Rogers, A. E. (1973) J. Natl. Cancer Inst. 50, 439-448.

(61) Sporn, M. B. (1977) Nutr. Rev. 35, 65-69.

(62) Saffiotti, U., Montesano, R., Sellakumar, A. R., and Borg, S. A. (1967) Cancer 20, 857-864.

(63) Bollag, W. (1970) Internat. J. Vit. Nutr. Res. 40, 299-314.

(64) Bollag, W. (1971) Experientia 27, 90-92.

(65) Bollag, W. (1972) Europ. J. Cancer 8, 689-693.

(66) Rettura, G., Schittek, A., Hardy, M., Levenson, S. M., Demetriou, A., and Seifter, E. (1975) J. Natl. Cancer Inst. 54, 1489-1491.

(67) Moon, R. C., Grubbs, C. J., and Sporn, M. B. (1976) Cancer Res. 36, 2626-2630.

(68) Bollag, W. (1974) Experientia 30, 1198-1200.

(69) Sporn, M. B., Newton, D. L., Smith, J. M., Acton, N., Jacobson, A. E., and Brossi, A. (1979) in Carcinogens: Identification and Mechanisms of Action, A. C. Griffin and C. R. Shaw, eds., pp. 441-453. Raven Press, New York.

(70) Sporn, M. B., Dunlop, N. M., Ndwton, D. L., and Henderson, W. R. (1976) Nature 263, 110-113.

(71) Newton, D. L., Frolik, C. A., Roberts, A. B., Smith, J. M., Sporn, M. B., Nürrenbach, A., and Paust, J. (1978) Cancer Res. 38, 1734-1738.

(72) Bollag, W. (1974) Europ. J. Cancer 10, 731-737.

(73) Bollag, W. (1975) Chemotherapy 21, 236-247.

(74) Bollag, W. (1975) Europ. J. Cancer 11, 721-724.

(75) Grubbs, C. J., Moon, R. C., Sporn, M. B., and Newton, D. L. (1977) Cancer Res. 37, 599-602.

(76) Grubbs, C. J., Moon, R. C., and Sporn, M. B. (1976) Proc. Am.

Assoc. Cancer Res. 17, 68.

(77) Moon, R. C., Thompson, H. J., Becci, P. J., Grubbs, C. J., Gander, R. J., Newton, D. L., Smith, J. M., Phillips, S. L., Henderson, W. R., Mullen, L. T., Brown, C. C., and Sporn, M. B. (1979) Cancer Res. 39, 1339-1346.

(78) Port, C. D., Sporn, M. B., and Kaufman, D. G. (1975) Proc. Am. Assoc. Cancer Res. 16, 21.

(79) Sporn, M. B., Squire, R. A., Brown, C. C., Smith, J. M., Wenk, M. L., and Springer, S. (1977) Science 195, 487-489.

(80) Grubbs, C. J., Moon, R. C., Squire, R. A., Farrow, G. M., Stinson, S. F., Goodman, D. G., Brown, C. C., and Sporn, M. B. (1977) Science 198, 743-744.

(81) Becci, P. J., Thompson, H. J., Grubbs, C. J., Brown, C. C., and Moon, R. C. (1979) Cancer Res. 39, 3141-3144.

(82) Dunagin, P. E., Meadows, E. H., and Olson, J. A. (1965) Science 148, 86-87.

(83) Sundaresan, P. R., and Bhagavan, H. N. (1971) Biochem. J. 122, 1-4.

(84) Sundaresan, P. R., and Sundaresan, G. M. (1973) Internat. J. Vit. Nutr. Res. 43, 61-69.

(85) Rietz, P., Wiss, O., and Weber, F. (1974) Vitamins and Hormones 32, 237-249.

(86) Hanni, R., Bigler, F., Meister, W., and Englert, G. (1976) Helv. Chim. Acta 59, 2221-2227.

(87) Hanni, R., and Bigler, F. (1977) Helv. Chim. Acta 60, 881-887.

(88) Lippel, K., and Olson, J. A. (1968) J. Lipid Res. 9, 168-175.

(89) Lippel, K., and Olson, J. A. (1968) J. Lipid Res. 9, 580-586.

(90) Zile, M. H., Emerick, R. J., and DeLuca, H. F. (1967) Biochim. Biophys. Acta 141, 639-641.

(91) Napoli, J. L., McCormick, A. M., Schnoes, H. K., and DeLuca, H. F. (1978) Proc. Natl. Acad. Sci. 75, 2603-2605.

(92) McKenzie, R. M., McGregor, M. L., and Nelson, E. C. (1977) J. Label. Compounds Radiopharm. 15, 265-277.

(93) Roberts, A. B., Lamb, L. C., and Sporn, M. B. (1979) Fed. Proc. 38, 761.

(94) Roberts, A. B., Nichols, M. D., Newton, D. L., and Sporn, M. B. (1979) J. Biol. Chem. 254, 6296-6302.

(95) Roberts, A. B., Frolik, C. A., Nichols, M. D., and Sporn, M. B. (1979) J. Biol. Chem. 254, 6303-6309.

(96) Frolik, C. A., Travela, T. E., Newton, D. L., and Sporn, M. B. (1978) J. Biol. Chem. 253, 7319-7324.

(97) Frolik, C. A., Roberts, A. B., Travela, T. E., Roller, P. P., Newton, D. L., and Sporn, M. B. (1979) Fed. Proc. 38, 761.

(98) Chen, C. C., and Heller, J. (1977) J. Biol. Chem. 252, 5216-5221.

(99) Yagishita, K., Sundaresan, P. R., and Wolf, G. (1964) Nature 203, 410-412.

(100) Roberts, A. B., and DeLuca, H. F. (1967) Biochem. J. 102, 600-605.

(101) Sundaresan, P. R., and Therriault, D. G. (1968) Biochim. Biophys. Acta 158, 92-97.

(102) Lin, R. L. (1969) in Metabolism of Retinoic Acid, Ph.D. Dissertation, OSU.

(103) Roberts, A. B., and DeLuca, H. F. (1968) Arch. Biochem. Biophys. 123, 279-285.

(104) Roberts, A. B., and DeLuca, H. F. (1968) J. Lipid Res. 9, 501-508.

(105) Roberts, A. B., and DeLuca, H. F. (1969) Arch. Biochem. Biophys. 129, 290-295.

(106) Nelson, E. C., Mayberry, M., Reid, R., and John, K. V. (1971) Biochem. J. 121, 731-733.

(107) McKenzie, R. M., and Nelson, E. C. (1979) Biochem. Biophys. Acta 574, 1-7.

(108) Reid, R. R. (1972) in Mass Spectral Analyses and Metabolism of Analogs of Vitamin A, M.S. Dissertation, OSU.

(109) Schlenk, H., and Gellerman, J. L. (1960) Anal. Chem. 32, 1412-1414.

(110) Schneider, W. C., and Hogeboom, G. H. (1950) J. Biol. Chem. 183, 123.

(111) Good, N. E., Winget, G. D., Winter, W., Connolly, T. N., Izawa, S., and Singh, R. M. M. (1966) Biochem. 5, 467-477.

(112) McKenzie, R. M., Hellwege, D. M., McGregor, M. L., Rockley, N. L., Riquetti, P. J., and Nelson, E. C. (1978) J. Chromatogr. 155, 379-387.

(113) Halley, B. A., and Nelson, E. C. (1979) J. Chromatogr. 175, 113-123.

(114) Waller, G. R. (1968) Proc. Okla. Acad. Sci. 47, 271-292.

(115) Diehl, P., Kallerhals, H., and Lustig, E. (1972) in NMR Basic Principles and Progress, P. Diehl, E. Fluck, and R. Kosfeld, eds., Vol. 6, p. 1 Springer-Verlag, New York.

(116) Castellano, S., and Bothner-By, A. A. (1964) J. Chem. Phys. 41, 3863-3869.

(117) Reid, R., Nelsen, E. C., Mitchell, E. D., McGregor, M. L., Waller, G. R., and John, K. V. (1973) Lipids 8, 558-565.

(118) Lin, R. L., Waller, G. R., Mitchell, E. D., Yang, K. S., and Nelson, E. C. (1970) Anal. Biochem. 35, 435-441.

(119) Thomas, A. F., and Willhalm, B. (1967) Tetrahedron 50, 5129-5132.

(120) Enzell, C. R., and Francis, G. W. (1969) Acta Chemica Scandinavica 23, 727-750.

(121) Heyns, K., Stute, R., and Scharmann, H. (1966) Tetrahedron 22, 2223-2235.

(122) DeJongh, D. C., and Shrader, S. R. (1966) J. Am. Chem. Soc. 88, 3881-3882.

(123) Biemann, K. (1962) in Mass Spectrometry, Organic Chemical Applications, p. 102. McGraw-Hill, New York.

(124) Schwieter, U., Englert, G., Rigassi, N., and Vetter, W. (1969) Pure Appl. Chem. 20, 365-420.

(125) Surekha Rao, M. S., John, J., and Cama, H. R. (1972) Internat. J. Vit. Nutr. Res. 42, 368-378.

(126) McKenzie, R. M., Hellwege, D. M., McGregor, M. L., and Nelson, E. C. (1979) Lipids 14, 714-717.

(127) Silverstein, R. M., and Bassler, G. C. (1967) in Spectrometric Identification of Organic Compounds, 2nd edition. John Wiley and Sons, New York.

(128) Samuelsson, B., Granström, E., Green, K., Hamberg, M., and Hammarström, S. (1975) Ann. Rev. Biochem. 44, 669-695.

(129) Funk, M. O., Isaac, R., and Porter, N. A. (1976) Lipids 11, 113-

117.

(130) Robeson, C. D., Cawley, J. D., Weisler, L., Stern, M. H., Eddinger, C. C., and Chechak, A. J. (1955) J. Am. Chem. Soc. 77, 4111-4119.

(131) Rosenkrantz, H. (1957) in Methods of Biochemical Analysis, Vol. 5, pp. 407-416.

(132) Farrar, K. R., Hamlet, J. C., Henbest, H. B., and Jones, E. R. H. (1952) J. Chem. Soc., 2657-2668.

(133) Robeson, C. D., Blum, W. P., Dieterle, J. M., Cawley, J. D., and Baxter, J. G. (1955) J. Am. Chem. Soc. 77, 4120-4125.

(134) Oroshnik, W. (1956) J. Am. Chem. Soc. 78, 2651-2652.

(135) von Planta, C., Schwieter, U., Chopard-dit-Jean, L., Rüegg, R., Kofler, M., and Isler, O. (1962) Helv. Chim. Acta 45, 548-561.

(136) Chapman, D., and Taylor, R. J. (1954) Nature 174, 1011-1012.

(137) Henbest, H. B., Jones, E. R. H., and Owen, T. C. (1957) J. Chem. Soc., 4909-4912.

(138) Jungalwala, F. B., and Cama, H. R. (1965) Biochem. J. 95, 17-26.

(139) Morgan, B., and Thompson, J. N. (1966) Biochem. J. 101, 835-842.

(140) Ogata, Y., Yosugi, Y., and Tomizawa, K. (1970) Tetrahedron 26, 5939-5944.

(141) Ogata, Y., Tomizawa, K., and Takagi, K. (1973) Tetrahedron 29, 47-50.

(142) Pasto, D. J., and Johnson, C. R. (1969) in Organic Structure Determination, p. 109-137. Prentice Hall Inc., Englewood Cliffs, New Jersey.

(143) Krauss, W., Rückert, P., Scheidel, F., and Wagner-Bartak, C. (1968) Ber. Bunsenges. Physik. Chem. 72, 415-418.

(144) Blout, E. R., Fields, M., and Karplus, R. (1948) J. Am. Chem. Soc. 70, 194-198.

(145) Rasmussen, R. S., and Brattain, R. (1947) J. Chem. Physics 15, 120-130.

(146) Lunde, K., and Zechmeister, L. (1955) J. Am. Chem. Soc. 77, 1647-1653.

(147) Sheppard, N., and Sutherland, G. B. B. M. (1949) Proc. Roy.

Soc. (London) A196, 195-216.

(148) Jackson, J. E., Paschke, R. F., Tolberg, W., Boyd, H. M., and Wheeler, D. H. (1952) J. Am. Oil Chem. Soc. 29, 229-234.

VITA

Natalie Larsen Rockley

Candidate for the Degree of

Doctor of Philosophy

Thesis: OXIDATIVE DECARBOXYLATION OF RETINOIC ACID IN VITRO

Major Field: Biochemistry

Biographical:

Personal Data: Born in Kabul, Afghanistan, July 19, 1951, the daughter of Mr. and Mrs. H. Larsen. Married to Dr. Mark G. Rockley of New Plymouth, New Zealand, on August 1, 1974.

Education: Attended grade school in Meudon-Bellevue, France and high school in Sèvres, France; graduated from Clarendon School, Abergele, North Wales, United Kingdom, in July, 1968, with Cambridge Advanced levels in History, French and English, and General Certificate in Mathematics and Spanish; received the Bachelor of Arts degree in chemistry from Hope College, Holland, Michigan, in June, 1971; received the Master of Public Health degree in Nutrition from the University of Minnesota, Minneapolis, Minnesota, in July, 1974; completed the requirements for the Doctor of Philosophy degree in December, 1979, at Oklahoma State University.

Professional Experience: Graduate Research Assistant, Biochemistry Department, University of Minnesota, September 1971 to August 1973; Graduate Research Assistant, School of Public Health, University of Minnesota, September 1973 to July 1974; Graduate Research Assistant, Biochemistry Department, Oklahoma State University, January 1976 to December 1979.